The role of Wolframin in the pathogenesis of Wolfram or Didmoad syndrome

Thesis

UNRESTRICTED

INSTITUT FÜR DIABETESFORSCHUNG MÜNCHEN

THE ROLE OF WOLFRAMIN IN THE PATHOGENESIS OF WOLFRAM OR DIDMOAD SYNDROME

Christine Marie Philbrook
Bachelor of Science in Biochemistry

submission of thesis for the degree of

Doctor of Philosophy in Biology

to the Open University

date of submission: January 29, 2003

Abstract

The Wolfram Syndrome (WS) is an autosomal recessive neurodegenerative disorder characterised by insulin-dependent diabetes mellitus (IDDM) and bilateral progressive optic atrophy. Manifestations in neural and neuroendocrine tissues generally arise, but are not a requirement for diagnosis. A novel gene was identified in 1998 on chromosome 4p16.1 (WFS1 or Wolframin) that contains loss-of-function mutations in a majority of Wolfram patients. This gene encodes for a putative hydrophobic transmembrane protein of 890aa and its predicted molecular weight is 100.29 kDa based on the amino acid sequence. This thesis was intended to study the localisation and function of this gene product in order to gain insight into its role in the pathogenesis of diabetes mellitus and neurodegeneration.

In order to study the role of the Wolframin gene in diabetes, its mRNA expression was analysed during the development of diabetes in the Nonobese Diabetic (NOD) mouse model. This showed a decrease in Wolframin expression in the pancreas of NOD mice 9 days after induction for diabetes, indicating a possible involvement of Wolframin in the survival of β-cells.

Fibroblast cells and blood samples from Wolfram patients were obtained and analysed for their mutations. One patient was compound heterozygotic for two separate mutations and one patient was homozygotic for a single insertion leading to an early stop codon. RT-PCR of these cells showed no significant difference in mRNA expression as compared to either fibroblasts from first-grade relatives or control cells. These cells were used in various functional assays. First of all, microarray analysis was used to identify genes that are affected when the Wolframin gene is non-functional. These results lead to the investigation of the role of Wolframin in

senescence using the markers of growth rate and radiation. No difference was found between fibroblasts from a Wolfram patient and her sibling, not supporting a role for Wolframin in senescence.

Since the mouse homologue is 83% identical to the human variant on an amino acid level it is likely that there is also functional homology. Therefore, in order to study the pathomechanisms acting in human disease, a knock-out mouse construct was produced thus overcoming the limitation to obtain human material. Two constructs were electroporated into embryonic stem cells and so far a total of 1080 colonies were screened, however, no positive clones were obtained.

In order to investigate this gene on a protein level, antibodies were raised against the N- and C- terminus. The respective protein was found to be expressed in many tissues and cell lines with the highest expression in brain, pancreas, heart and insulinoma β-cell lines. Using sub-cellular fractionation techniques, the protein was found exclusively in microsomal fractions. Immunofluorescence on transfected cos-7 cells showed intracellular localisation to the endoplasmic reticulum. Incubating mouse pancreas slices with the Wolframin antibody showed exclusive staining in the β-cells and co-localisation to insulin. Immunofluorescence analysis also showed immunoreactivity to structures of the limbic system in the mouse brain. These results give the first clues towards a possible function in processing or trafficking of proteins involved in the survival of neuronal and endocrine cells.

Table of Contents

Chapter 1. Introduction

Diabetes mellitus is a common feature in over 40 different inherited syndromic diseases. Most of these diabetic syndromes are likely caused by a monogenetic defect. The genes responsible for these syndromes can be found on many different chromosomes and most are inherited in an autosomal recessive manner. These "diabetic syndromes" are characterised by diabetes accompanied by a variety of neurodegenerative symptoms, with deafness and optical abnormalities among the most common. Understanding the molecular mechanisms behind these syndromes is important to the understanding of the relationship between diabetes and the subsequent neurodegenerative symptoms found in these diseases. Some of the genes responsible for these syndromes are either located on mitochondrial DNA and therefore directly affect energy metabolism, or are located on nuclear DNA but affect mitochondrial functions by encoding for a mitochondrial-localised protein.

Mitochondrial DNA (mtDNA) is important because it encodes 13 of the genes for oxidative phosphorylation (OXPHOS), which is important for energy production and cellular respiration (Chinnery, Howell et al. 1999). When OXPHOS is stimulated in the mitochondria, ATP is produced. An increase in ATP causes closure of the ATP-dependent potassium channels, which in turn results in an opening of calcium channels in pancreatic β-cells. This increase in calcium levels triggers insulin secretion in insulin producing β-cells. Mutations in mtDNA which affect OXPHOS proteins and subsequent ATP production could thus be one cause of diabetes mellitus by reducing insulin secretion (Gerbitz, Gempel et al. 1996). Two important syndromes in which the underlying genetic defect has been identified as being based on mitochondrial

functions are the maternally inherited diabetes-deafness syndrome, and Friedreich's ataxia.

The diabetes-deafness syndrome is caused by a point mutation at mtDNA nucleotide pair 3243 (Reardon, Ross et al. 1992). The diabetes here is a mild form of adult onset type 2 diabetes thought to be due to β-cell failure (Kadowaki, Kadowaki et al. 1994). In addition to being susceptible to diabetic retinopathy, many of these patients also have pigmentary retinal dystrophy (Smith, Bain et al. 1999). Diabetic retinopathy is a condition common to type 2 diabetics, where prolonged diabetes damages tiny blood vessels in the retina, which in turn causes bleeding and clouds vision. Pigmentary retinal dystrophy, on the other hand, is caused by pigmentary degeneration of the retina.

FRDA1 (Friedreich's ataxia) is a mitochondrial disease where diabetes mellitus is present in 20 – 30% of all cases. Normal symptoms are cerebral ataxia, peripheral neuropathy and hypertrophic cardiomyopathy (OMIM 229300). Based on studies with the yeast homologue, Frataxin, the affected gene, appears to be involved in mitochondrial iron transport. Mutations in Frataxin cause iron accumulation, COX deficiency and mtDNA instability (Wong, Yang et al. 1999).

A variety of other diseases have been described which are based on mitochondrial malfunctions where neurodegeneration plays a leading role. For instance, LHON (Leber Hereditary optic neuropathy) is characterised by bilateral optical atrophy and central vision loss and is caused by one or more of three single mtDNA mutations, where only one mutation is required for LHON (Wallace, Singh et al. 1988). Other missense mutations can be found at a higher frequency in LHON patients and can influence the severity of the symptoms. For example, a base exchange at nucleotide base pair 14459 (np14459) in the ND6 gene causes LHON in association with

Dystonia. This indicates a variability of symptoms associated with missense mutations (Lamminen, Huoponen et al. 1997).

Leigh Syndrome (LS) is a severe neurodegenerative disorder characterised by dysfunction of the brain stem and basal ganglia (Leigh, 1951). Magnetic resonance imaging (MRI) of affected infants shows lesions in the brain stem, thalamus and posterior columns of the spinal cord (Manzi, Hager et al. 1990). LS is genetically heterogeneous and can be caused by mtDNA mutations, autosomal recessive defects of a nuclear gene and can even be inherited as an X-linked trait (OMIM: 208800, 252011, 220110, 252010). In all cases, however, the terminal oxidative metabolism is affected. The neurodegeneration is therefore most likely caused by a failure of energy production in the developing brain (Filiano, Goldenthal et al. 2002).

The Mohr-Tranebjaerg Syndrome (MTS) is an X-linked form of syndromic sensorineural deafness. Symptoms are: progressive sensorineural deafness, cortical blindness, dystonia and mental deterioration (Jin, 1996). The responsible gene in humans, DDP1 is a mitochondrial protein that resembles the small yeast Tim proteins, Tim9, Tim10 and Tim12, which are located in the intermitochondrial space and are responsible for the import of certain proteins into the mitochondrial inner membrane (Bauer, Rothbauer et al. 1999). Thus, it has been hypothesised that a defect in the import of mitochondrial proteins might cause this disease (Bauer, Rothbauer et al. 1999).

In a few cases, the responsible gene has no connection to mitochondrial function. For example, the gene responsible for Wolcott-Rallison syndrome, a disease distinguished by permanent neonatal diabetes (Wolcott and Rallison 1972), was found to be located on chromosome 2p12. This gene, EIF2AK3, encoding translation initiation factor 2-α kinase 3, regulates protein translation and is highly expressed in pancreatic islets

(Delepine, Nicolino et al. 2000). No individual with the Wolcott-Rallison syndrome has been reported to live beyond the teenage years.

The thiamine-responsive megaloblastic anaemia syndrome is characterised by megaloblastic anaemia, childhood-onset non-autoimmune diabetes mellitus and sensorineural deafness. Some patients show abnormalities of the retina and optic nerve, including optic atrophy (Randall, Scheithauer et al. 1985; Rindi, Patrini et al. 1994). A gene has been mapped to chromosome Iq23.3 that contains mutations in affected individuals (Diaz, Banikazemi et al. 1999; Fleming, Tartaglini et al. 1999; Labay, Raz et al. 1999). This gene is a vitamin transporter gene, SLC19A2 and encodes for a transmembrane protein, THTR-1. THTR-1 is thought to be a high-affinity thiamine transporter as these patients show reduced activity of thiamine-dependent enzymes (Fleming, Tartaglini et al. 1999).

The analysis of such characterised diabetes related disorders provides a strong indication that the phenotype of diabetic patients with sensorineural deafness and unrelated neurological features is due to underlying mitochondrial defects. Another of these diabetic syndromes with similar symptoms in which the responsible gene has been recently identified is the so-called Wolfram syndrome.

The Wolfram Syndrome (WS) was first described in 1938 by DJ Wolfram and HP Wagner, who observed four siblings out of eight presenting both diabetes mellitus and bilateral progressive primary optic atrophy (Wolfram and Wagener 1938). Non-autoimmune, juvenile onset diabetes mellitus and bilateral progressive optic atrophy are the two obligatory features of the Wolfram Syndrome, where diabetes mellitus normally occurs in the first decade and the latter occurs in the second decade of life. The acronym DIDMOAD arose after the discovery of additional clinical features and comprises the four most commonly seen: Diabetes Insipidus, Diabetes Mellitus, Optic

Atrophy and Deafness (Fraser and Gunn 1977; Richardson and Hamilton 1977). Wolfram syndrome is a progressive neurodegenerative disorder affecting the central and peripheral nervous systems as well as the neuroendocrine system. Predisposition to psychiatric illness such as depression and psychotic behaviour has also been associated with Wolfram syndrome patients (Evans, Lawson et al. 2000). Inheritance occurs in an autosomal recessive manner with approximately 25% of patients being consanguineous. The prevalence is very low at 1 in 100,000 in a US study and 1 in 770,000 based on investigations in the UK (Barrett, Bundey et al. 1995; Kinsley, Swift et al. 1995). Accordingly, the carrier frequency could be calculated to be 1 in 175 to 350 (Barrett, Bundey et al. 1995).

1.1 Clinical features of the Wolfram syndrome

1.1.1 Overview

There are two major types of diabetes mellitus: the so-called type 1 and type 2 diabetes. Type 1 diabetes or insulin dependent diabetes mellitus (IDDM) is normally juvenile onset and is due to an autoimmune response where autoantibodies attack insulin-producing β-cells, thus resulting in drastically reduced insulin production (Soeldner and Slone 1965). Insulin is required for the uptake of glucose from the blood stream into the cell. Type 2 diabetes or non-insulin dependent diabetes mellitus (NIDDM) is usually late onset and generally preceded by insulin resistance (Bogardus, Lillioja et al. 1989; Warram, Martin et al. 1990; Martin, Warram et al. 1992). Obesity and nutrition have been shown to play a large role in the occurrence of this disorder. Unlike type 1 diabetics, type 2 diabetics do produce insulin, however the insulin cannot function properly to cause transport of glucose from the blood system into cells.

Type 1 diabetics need to regulate their glucose early on with insulin injections. In later stages of type 2 diabetes, insulin production exhausts and finally also many of these patients need to be treated with insulin.

The diabetes in WS usually begins within the 1st decade of life and rapidly becomes insulin-dependent (Barrett and Bundey 1997). In contrast to type 1 diabetes, the diabetes in Wolfram syndrome is non-autoimmune. In particular, autoantibodies against islet cells and GAD65, an enzyme that catalyzes the synthesis of γ-aminobutyric acid in the β-cell, are negative (Baekkeskov, Aanstoot et al. 1990). The HLA (human leukocyte antigen) class 2 molecule is responsible for the presentation of CD4+ T-cell antigens in the immune system and is the gene area most associated with type 1 diabetes. HLA -typing in WS patients revealed no significant difference to non-diabetic controls (Bertrams, Wendel et al. 1983; Monson and Boucher 1983). In comparison, 90% of type 1 diabetics carry specific histocompatibility haplotypes. The lack of autoimmune markers and selective absence of β-cells suggest that the diabetes in WS is due to a genetically programmed selective loss of β-cells and therefore a decrease in production of insulin (Karasik, O'Hara et al. 1989).

The optic atrophy is a bilateral degeneration of the optic nerve and usually manifests after onset of diabetes (Barrett, Bundey et al. 1997). It presents with reduced colour vision and visual acuity leading to blindness in most of the patients. Abnormal retinal pigmentation is usually absent. Visual evoked potentials showed abnormalities, which are typical for optic nerve disease. Therefore, loss of vision in these patients is not a result of diabetic retinopathy (Barrett, Bundey et al. 1997), a condition that can arise after prolonged diabetes.

Diabetes insipidus is caused by a malfunction of or lack of the antidiuretic hormone, vasopressin (VP). Vasopressin is made by the cells of the hypothalamus and is stored and secreted by the posterior pituitary gland. This hormone gets released into the bloodstream where it causes tubules within the kidney to reabsorb water and thus concentrates urine. Therefore, such patients must urinate frequently and replenish with plenty of fluids. The diabetes insipidus in DIDMOAD is cranial and can be partial or complete (Peden, Gay et al. 1986). It begins at the hypothalamo-pituitary level and can be sufficiently treated by nasal application of an antidiuretic hormone and is therefore non-nephrogenic in origin (Thompson, Charlton et al. 1989). Immunostaining shows no reactivity for processed vasopressin in the supraoptic and paraventricular nuclei of WS patients, although the precursor is present. This suggests a possible defect in VP precursor processing (Gabreels, Swaab et al. 1998).

The deafness in WS results from a progressive sensorineural hearing loss on both sides affecting the high frequencies (Young, Ives et al. 2001). Often hearing aids are required. Such hearing loss is relatively common in the general population and is based on a diverse genetic background. DIDMOAD patients show a loss of nerve fibres in the cochlear nerves and mild gliosis in the auditory brainstem (Genis, Davalos et al. 1997).

Additional, but less frequent features are caused by disturbances of the neuroendocrine system and by renal tract and neurological abnormalities. The irregularities of the urinary tract include: bladder atony, incontinence and recurrent infections and are based on a dilated renal outflow tract, likely due to degeneration of the nerves leading to the ureters and urinary bladder (Chu, Staff et al. 1986).

The most common neurological features are; ataxia, nystagmus, peripheral neuropathy and depression (Barrett, Bundey et al. 1995). Pituitary-gonadal malfunctions such as:

hypogonadism, menstrual irregularities and sexual retardation are less common and normal pregnancy in patients and partners of patients is possible (Peden, Gay et al. 1986).

1.1.2 Prevalence of the various clinical features and their age of onset

Diabetes mellitus usually manifests itself as the first symptom before the age of ten. It is followed by optic atrophy, which occurs at a median age of around 11 years (Barrett, Bundey et al. 1997). All additional features, however, develop later during the course of the disease. In particular, diabetes insipidus and deafness usually appear in the second decade, the renal tract abnormalities early in the third decade and neurological complications develop late with a median onset in the fourth decade (Barrett and Bundey 1997). The prevalence of the additional features range between 50% and 75%. However, in the individual patient, the obligatory symptoms are associated with a variable spectrum of additional features.

In general, Wolfram syndrome leads to a premature death at a median age of 30 (25-40) years (Barrett, Bundey et al. 1995). Central respiratory failure is presumably due to brain-stem atrophy and commonly causes premature death in these patients (Barrett and Bundey 1997).

1.2 Brain atrophy

In general, the neurological symptoms found in WS reflect local degeneration and atrophies of distinct brain regions. This can best be seen in an example of magnetic resonance imaging in comparison to a normal control (Rando, Horton et al. 1992; Saiz, Vila et al. 1995; Galluzzi, Filosomi et al. 1999). Figure 1.1 shows one such example. The abnormalities that can be seen include: brain atrophy of the cerebral cortex and

brain stem and severe atrophy of the cerebellum. In addition, atrophies of the pons and medulla can be seen which might cause respiratory failure, thereby determining the fate of many of these patients. Atrophy of the hypothalamus, the region that produces vasopressin, can also be seen. In some cases, specific alteration of the pituitary gland and reduced signals or shrinkage of the optic nerve can be seen (Galluzzi, Filosomi et al. 1999).

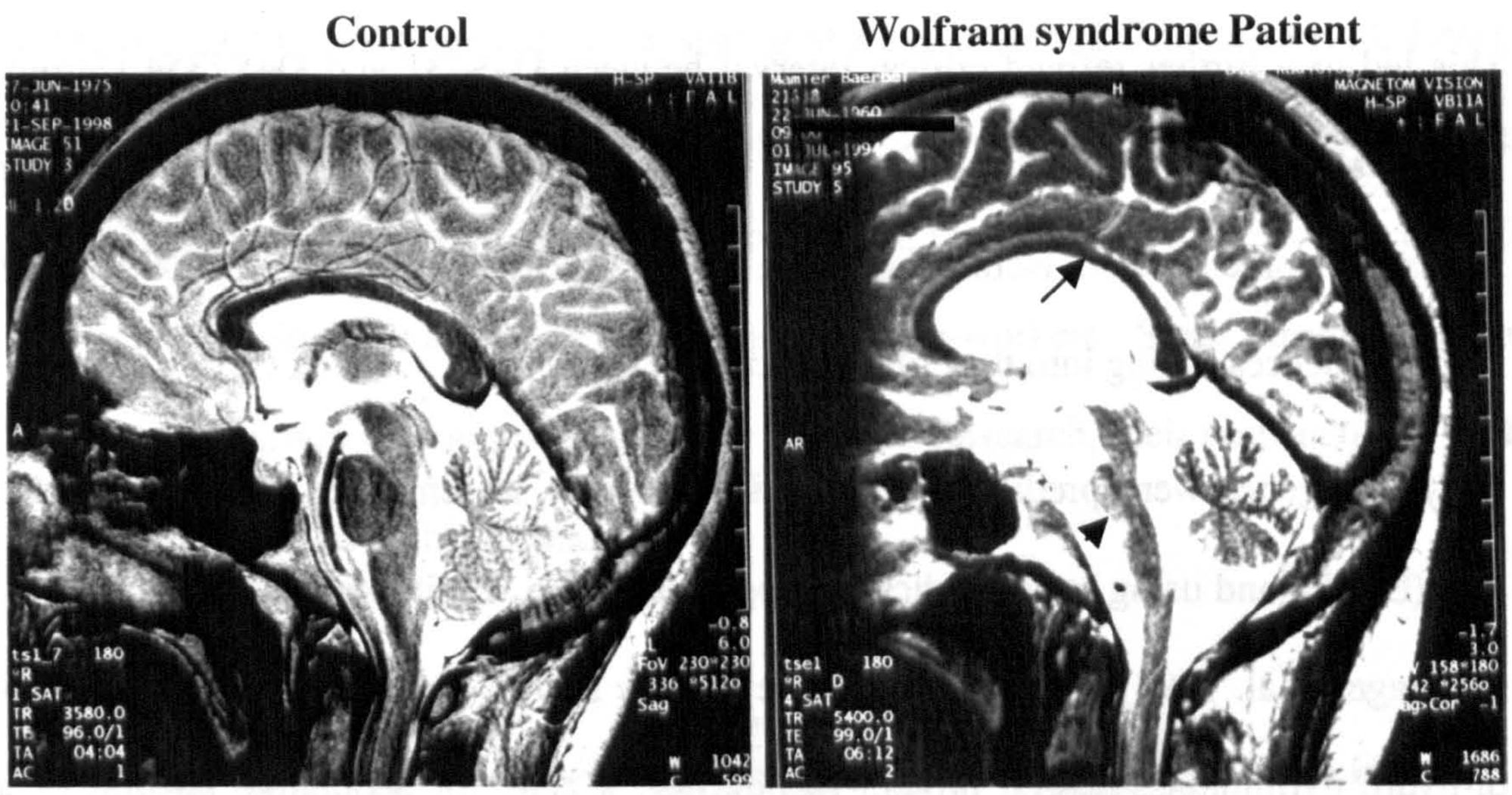

Figure 1.1 MRI of a control person and a Wolfram patient. In the patient sample, a generalized brain atrophy, pronounced atrophy of the cerebellum (arrow) and atrophy of the brain stem (arrow head) can be seen. Also of note are an absence or reduced signal in structures of the limbic system.

1.3 The Wolfram Disease Gene

1.3.1 Linkage analysis

Although Wolfram patients have been characterised extensively on a clinical level, the defective gene and the underlying pathomechanism of this disorder are only beginning to be unravelled. In 1994, the Wolfram disease gene was mapped using microsatellite repeat polymorphisms reported in the Genethon map of the human genome

(Polymeropoulos, Swift et al. 1994). Based on a linkage analysis of 11 families, the gene was found to be linked to markers on the short arm of chromosome 4. The location of the gene was refined in 1996 to the interval between D4S432 and D4S431 by the lab of Sarah Bundey. This provided the first piece of evidence that WS was not a mitochondrial DNA disease (Collier, Barrett et al. 1996) .

Assuming that the disease locus was linked to this interval, Strom et al. (1998) screened for single recombination events in DNA from available Wolfram families. This led to a further refined critical interval between D4S431 and D4S2354 (Strom, Hortnagel et al. 1998). This region was sequenced and available early during the Human Genome Project. Both Strom et al. (1998) and Inoue et al. (1998) analysed the DNA sequences falling into the critical interval at 4p16.1.

Only five genes were predicted within this region by screening expressed sequence tags (EST's) and using exon prediction programs (Inoue, Tanizawa et al. 1998; Strom, Hortnagel et al. 1998). Two of them were already known genes: DRP-1 the gene for di-hydro-pyrminidase-related protein-1 and BRg, a gene for a putative subunit of a human protein phosphatase. WM1 and WM3 were novel authentic genes, partially covered by EST's. WM4 appeared not to be a true gene since no expressed sequences could be found in EST databases. Thus, the candidate genes for Wolfram syndrome were: WM1, WM3, DRP-1 and BRg.

Based on this information, mutational analysis of all four genes in various patients was performed. All exons from these four genes were amplified and screened by single-strand conformation polymorphism (SSCP) analysis. For SSCP analysis, DNA fragments were amplified and subjected to non-denaturing polyacrylamide gel electrophoresis. Since single stranded nucleic acids form secondary structures in solution that can be altered by only a single nucleotide substitution, mutations in the

DNA can be seen as a mobility shift. Polymorphic fragments where mobility gel shifts were seen were directly sequenced from the PCR product. Sequencing revealed mutations in only the WM1 gene in a majority of the cases tested (Inoue, Tanizawa et al. 1998; Strom, Hortnagel et al. 1998). The lack of mutations in WM1 in some of these patients could be accounted for by the fact that intron-exon boundaries and the non-coding exon 1 were not included in this analysis. Also, due to its high phenotypic heterogeneity, it could be possible that another locus plays a role in this disorder. WM1 is a 33.4 kb spanning region consisting of 8 exons (Inoue, Tanizawa et al. 1998). The coding region includes exons 2 to 8, where exon 8 encodes more than 50% of the entire protein. The structure of WM1 can be seen in Figure 1.2. This gene was named Wolframin by Strom et al. and WFS1 by Inoue and co-workers. Since Strom et al. is a collaborating group here at the Institute for Diabetes Research, their nomenclature will consistently be used in this thesis.

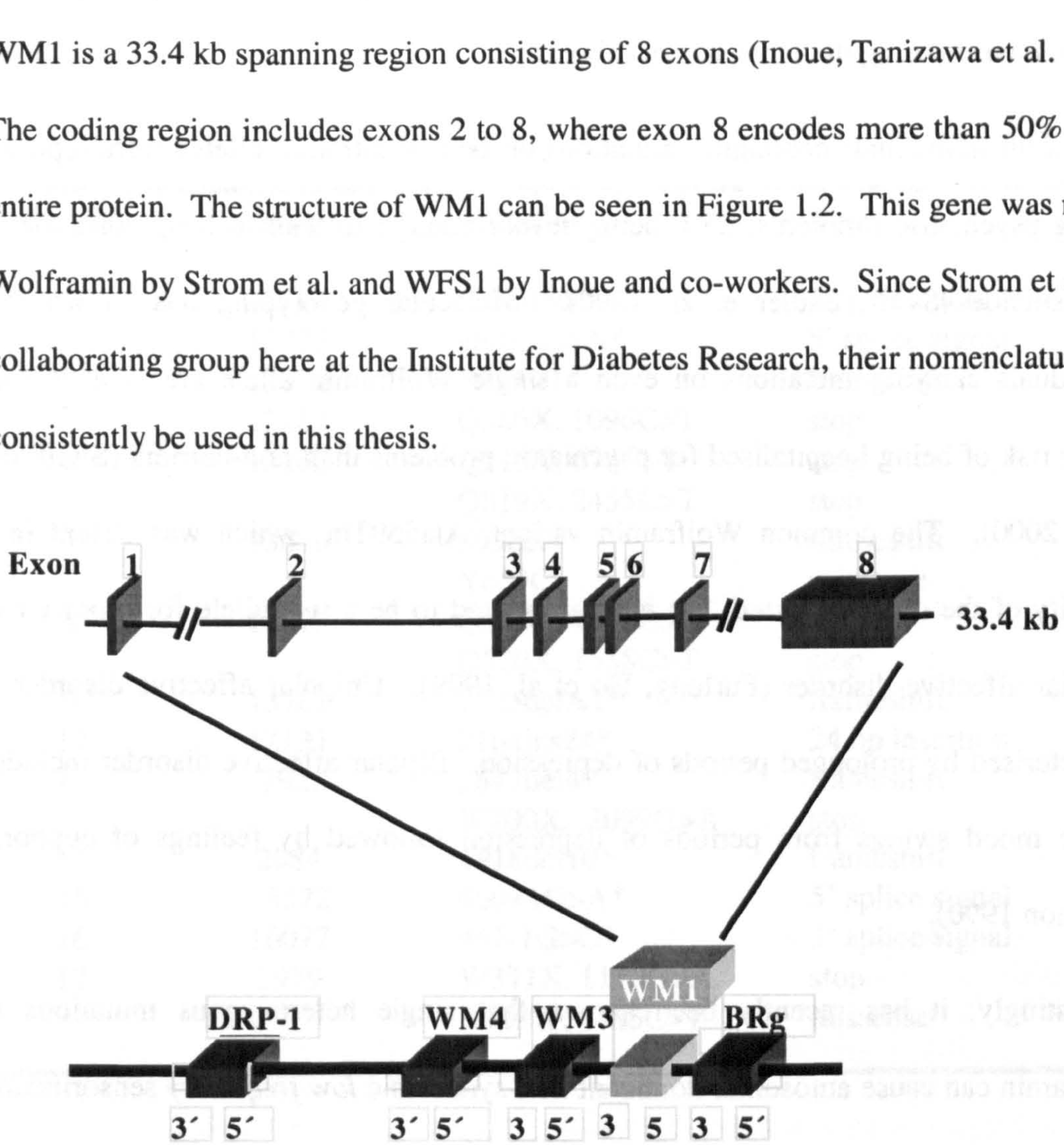

Strom et al. Human Molecular Genetics (1998)

Figure 1.2 Structure of the Wolframin gene. The coding region contains 8 exons, indicated here with boxes. The last exon, exon 8, is by far the largest. The total genomic sequence consists of 33.4 kb of information

1.3.2 Mutation Analysis

The mutations found on the Wolframin gene included; nonsense, frameshift, missense, deletions and insertions (Strom, Hortnagel et al. 1998). Most patients are either homozygous for a single mutation on both alleles or compound heterozygous for two different mutations on two separate alleles. Therefore, loss-of-function mutations of the Wolframin gene are responsible for the phenotype found in DIDMOAD. Most of the causative mutations are located in exon 8 (Hardy, Khanim et al. 1999). This seems plausible considering the large size of this exon.

60% of all individuals containing mutations on both Wolframin alleles were reported having psychiatric problems, 25% being severe enough to lead to hospitalisation or even suicide (Swift, Sadler et al. 1990). Molecular genotyping has shown that individuals carrying mutations on even a single Wolframin allele are at a 26-fold higher risk of being hospitalised for psychiatric problems than non-carriers (Swift and Swift 2000). The common Wolframin variant, Ala559Thr, which was absent in a majority of the controls tested, has been suggested to be a risk allele for bipolar and unipolar affective disorder (Furlong, Ho et al. 1999). Unipolar affective disorder is characterised by prolonged periods of depression. Bipolar affective disorder includes drastic mood swings from periods of depression followed by feelings of euphoria (Gershon 1990).

Interestingly, it has recently been shown that single heterozygous mutations in Wolframin can cause autosomal dominant non-syndromic *low frequency* sensorineural hearing loss (LFSNHL) (Bespalova, Van Camp et al. 2001; Young, Ives et al. 2001). This means, certain mutations in the gene responsible for WS are able to cause a separate disease. Even though hearing loss is a frequent symptom of Wolfram patients, it is normally restricted to the high frequencies and not to the low frequencies

as in LFSNHL. This phenomenon is not completely understood, however, the progressive nature of LFSNHL suggests a role for Wolframin in sound transduction rather than in development of cochlear cells (Young, Ives et al. 2001). The mutations in LFSNHL have all been found in the portion of exon 8 that encodes for the C-terminal domain. No mutations have yet been found in the N-terminal or transmembrane domains, suggesting these mutations are dominant-negative by interfering with the specific function of the C-terminal domain (Bespalova, Van Camp et al. 2001).

Family	Patient	Mutation	Type	Exon
1	5519	1380del9*	9 bp deletion	8
2	13775	460+1G>A*	5' splice signal	4
4	13070	599delT*	frameshift	5
5	13885	Q366X, 1096C>T	stop	8
6	13062	Q226X, 676C>T	stop	6
		Q819X, 2455C>T	stop	8
7	13076	599delT	frameshift	5
		Y669C	missense	8
8	13073	Q366X, 1096C>T	stop	8
		Q520X, 1558C>T	stop	8
9	13781	1523delAT*	frameshift	8
12	12131	2164ins24*	24 bp insertion	8
13	2922	2647del4*	frameshift	8
		W700X, 2099G>A	stop	8
14	2984	1918del10*	frameshift	5
15	15572	460+1G>A*	5' splice signal	6
16	16077	461-1G>C*	3' splice signal	8
17	2979	W371X, 1112G>A	stop	8
		R629W, 1885C>T	missense	8

Strom et al. Human Molecular Genetics (1998)
Inoue et al. Nature Genetics (1998)

Figure 1.3 Screening results of two independent experiments. * indicates homozygous mutations.

Various groups have tried to analyse mutations in the Wolframin gene for correlation to phenotype. Hardy and co-workers screened 30 patients from 19 families for mutations in the coding region of the Wolframin gene. Results of this study and others show that a majority of the patients are compound heterozygotes for two mutations leading to loss-of-function of the gene. For example, 28 of Hardy's 30 patients contain mutations on both alleles. Since intron boundary regions were not tested, these could account for the missing mutations. Figure 1.3 summarises the screening results from three independent studies (Barrett, Bundey et al. 1995; Inoue, Tanizawa et al. 1998; Strom, Hortnagel et al. 1998). It turns out that direct loss-of-function mutations resulting in an altered stop codon are the predominant cause of the Wolfram syndrome. These comprise about 80% of the mutations, whereas missense mutations are present in only roughly 20% of all cases. Most mutations can be found in the last exon and 47% of all mutations resulted in loss of the carboxy terminal tail, indicating that the carboxy terminus most likely plays an important role in protein function (Hardy, Khanim et al. 1999). In all additional patients studied so far, including the studies of Inoue and Hardy, no common mutations have been identified. No phenotype-genotype correlation has been observed based on the comparison of mutation location with severity of symptoms, clinical course or age of onset.

1.3.3 Additional Locus

Mutational analysis has provided evidence that the Wolframin gene contains loss-of-function mutations in a majority of patients. Although there is no indication that specific mutations cause certain phenotypes, the symptoms of this disease are so diverse that patients can be categorised into severity and prevalence of one symptom over another. For example, locus heterogeneity was suspected when a family with a

variable phenotype (optical atrophy presented one decade before diabetes mellitus) showed no linkage to Wolframin (Collier, Barrett et al. 1996). In another study, 16 patients were investigated who showed no sign of having or obtaining diabetes insipidus (El-Shanti, Lidral et al. 2000). In these families, linkage was found to a second locus on 4q22-24 instead of on markers for 4p16. This region includes 22 genes and needs to be narrowed down further by positional cloning. Genetic heterogeneity in DIDMOAD is not surprising considering the multitude of symptoms seen in these patients. In addition, the main symptom, diabetes mellitus, is correlated with mutations in many diverse genes and located in many different positions within the genome. In fact, type 1 diabetes itself is a result of many genes working together, where even environmental factors may play a large role (Füchtenbusch 1995).

1.4 Expressional analysis

Northern blot analysis revealed that the Wolframin gene is expressed in RNA from all tissue homogenates investigated so far (Inoue, Tanizawa et al. 1998; Strom, Hortnagel et al. 1998). Higher mRNA steady state levels were detected in heart, brain, placenta, lung and pancreas. A more detailed expression analysis by Inoue and co-workers (1998) revealed that the expression in pancreatic tissue is restricted to the pancreatic islets, while expression in the exocrine pancreas is very low (figure 1.4). The high expression in pancreatic islet cells might explain that the earliest manifestation of Wolfram syndrome is IDDM. These observations led to the speculation that the Wolframin gene product might function in the survival of islet β-cells and neuronal cells (Inoue, Tanizawa et al. 1998).

The exact function of the Wolframin gene product is yet to be elucidated. In particular, no information could be derived from sequence searches in available DNA and protein databases. A Wolframin homologue was identified in mouse, which shows 83%

sequence similarity at the nucleotide level and 87% at the amino acid level (Strom, Hortnagel et al. 1998). A putative Wolframin homologue in Drosophila and *C. elegans* was also identified, however, lower eukaryotes like the yeast *S. cerevisiae* that can easily be manipulated on the genetic level, seem to lack Wolframin-like gene

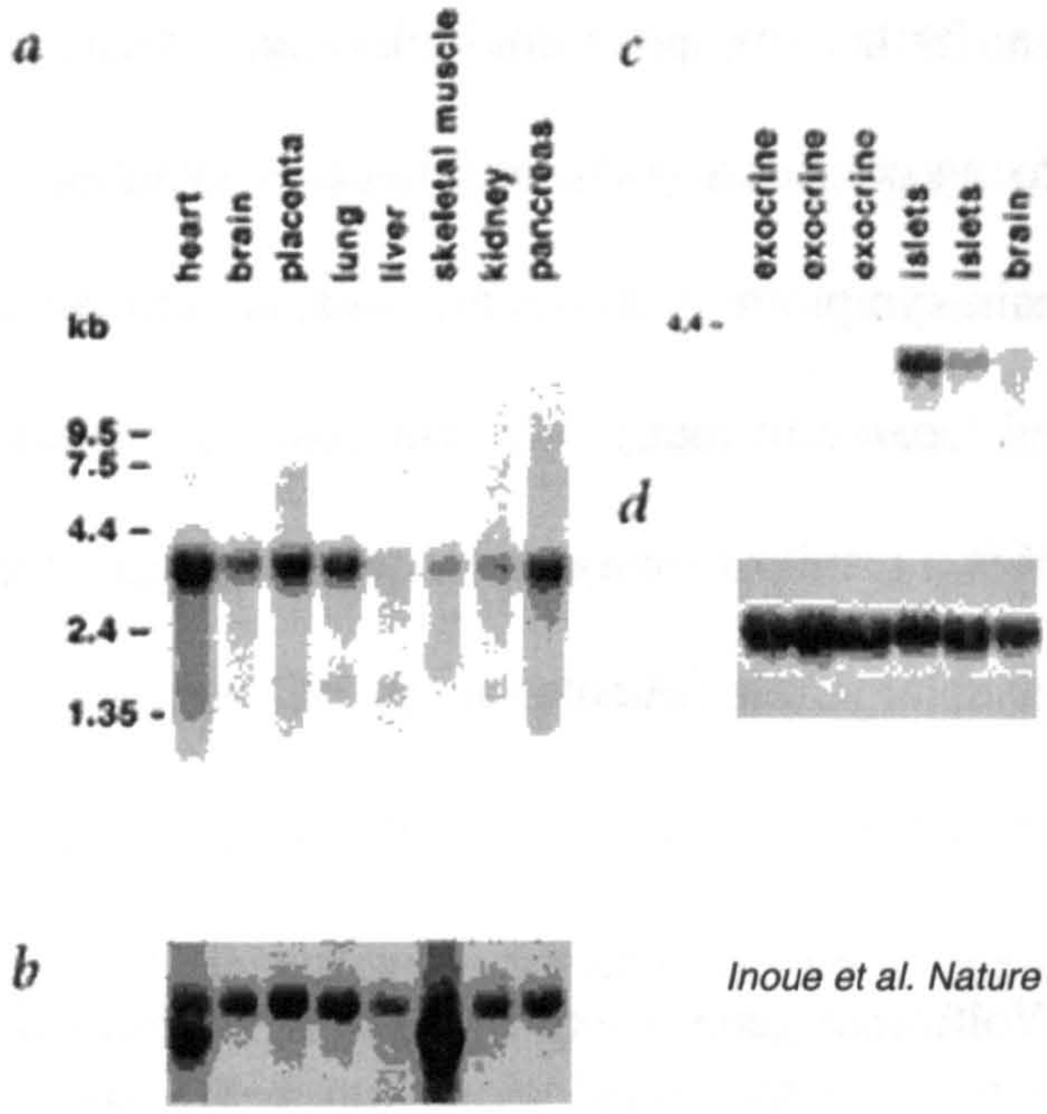

products (Strom, Hortnagel et al. 1998).

Figure 1.4 mRNA expression pattern of Wolframin. A and C show Wolframin expression on various tissues, including isolated exocrine and islet fractions from pancreas. B and D show the respective β-actin expression.

1.5 Hydropathy plot

Secondary structure prediction programs (Rost, Casadio et al. 1995) suggest that Wolframin is a membrane spanning protein of 100.29 kDa consisting of a central hydrophobic portion flanked by two large hydrophilic domains, each of which comprises 300 to 350 amino acid residues. Predictions also suggest 9 transmembrane segments with an N-out/C-in topology. The functional role of the hydrophilic domains

is not yet known. However, the C-terminus appears to exhibit an important function as even the truncation of the last 8 amino acids appears to disrupt the protein function and result in a full-blown disease-phenotype (Hardy, Khanim et al. 1999). The majority of loss-of-function mutations are found on exon 8. Since this last exon also contains all of the transmembrane regions, disruptions here would most likely be important to the protein's stability.

Five possible Asn-glycoslylation sites exist at positions 28, 335, 500, 661 and 746. No known leader sequences targeting this protein to a particular function have been found based on amino acid information. For example, the dilysine (KK)/ diarginine (RR) and KDEL motifs which sort proteins into the ER are absent. There is no indication of a mitochondrial import signal or any other sequences targeting this protein to a specific sub-cellular localisation or function.

1.6 Objective of this work

The Wolfram syndrome is a syndromic form of diabetes in which the gene product had not yet been characterised. This syndrome is especially interesting because it is a monogenic form of diabetes, presenting with a diverse array of neurodegenerative symptoms. The diabetes in DIDMOAD patients is non-autoimmune and is directly due to loss-of-function mutations in the Wolframin gene. The heterogeneity of mutations and varying levels of severity of the symptoms in these patients has shown no relationship to one another. Understanding the pathomechanisms behind the Wolfram syndrome will allow important insights into the molecular mechanisms involved in cell death and neurodegeneration.

As a first step in understanding the function of the Wolframin gene, I set out to make antibodies to the respective protein. Antibodies enable one to determine the localisation of the encoded protein and are a valuable tool for determining how the protein itself interacts and its possible interaction with other proteins. Important to understanding a novel protein, is determining its cellular and sub-cellular localisation. Expression studies in the pancreas, will clarify if the Wolframin protein is expressed in the β-cells. This will help explain if Wolframin is part of a pathway leading to the selective loss of β-cells or if it has a function in β-cells themselves. Determining the cellular localisation in the brain will show in which regions this protein is expressed and provide insight into how such diverse effects could be caused. Information from sub-cellular localisation studies can give important information on the possible function in the cell and finally answer the question, whether or not this really is a mitochondrial protein.

DIDMOAD is a very rare disease and adequate material to study the role of the Wolframin gene in its pathogenicity is difficult to obtain. It was, however, possible to obtain skin fibroblasts and blood from three Wolfram patients and other family members. Expression of the protein in these cells was observed and Wolframin positive and negative cells were used for various functional assays.

The mouse homologue is 83% similar to the human and modelling diseases in mice is a good way to study underlying molecular mechanisms. Therefore, one of the approaches to determining the function of the Wolframin protein was to create a Wolframin knock-out mouse. Knock-out mice allow one to study a more rapid development of symptoms, examine molecular or physical changes at any stage and even effects of intervention.

Chapter 2. Materials and Methods

2.1 Materials

2.1.1 Chemicals:

Chemicals were purchased from Roth, Merck or Sigma, unless otherwise stated. All locations refer to German cities unless otherwise stated. Restriction enzymes were bought from MBI Fermentas, Gibco and Promega. [alpha-^{32}P] dCTP was purchased from Amersham Biosciences, Freiburg, Germany.

pQE40 expression vector was purchased from Qiagen. AdvanTAge PCR cloning kit, pIRES and pIRES2EGFP were from Clontech.

2.1.2 Materials supplied by others:

ploxpneo-1 vector was kindly provided by Dr. Rolf Sprengel, Max Planck Institute for Medical Research, Heidelberg, Germany. Mitotracker Red mitochondrial selective dye was purchased by Molecular Probes, USA

2.1.3 Primary antibodies

PC2: polyclonal rabbit anti-Prohormone Convertase 2	Chemicon International, CA, USA
Penta-HIS: monoclonal mouse anti-6xHIStag	Qiagen, Hilden
β-actin: monoclonal mouse anti- β-actin	Sigma, München
PDI: monoclonal mouse anti- ER	StressGen Biotechnologies, Canada
Golgi: monoclonal mouse anti-Golgi, 58 K	Sigma, München
TIM23: monoclonal mouse anti-mitochondria	BD Biosciences, Heidelberg
Glucagon: monoclonal mouse anti-Glucagon	Sigma, München

Insulin: monoclonal guinea pig anti-Insulin	Sigma, München

2.1.4 Secondary antibodies

goat anti-mouse IgG FITC conjugate	Sigma, München
goat anti-mouse IgG TRITC conjugate	Sigma, München
rabbit anti-guinea pig IgG TRITC conjugate	Sigma, München
goat anti-rabbit IgG FITC conjugate	Sigma, München
goat anti-rabbit IgG TRITC conjugate	Sigma, München
anti-mouse IgG peroxidase conjugate	Sigma, München
anti-rabbit IgG peroxidase conjugate	Sigma, München

2.2 Solutions

PBS: 137 mM NaCl, 2.7 mM KCl, 4.3 mM Na_2HPO_4, 1.4 mM KH_2PO_4.

6x DNA loading buffer: 25% sucrose, 0.1 M EDTA, 0.05% (w/v) bromophenol blue.

5x RNA loading buffer: 1 mM EDTA, pH 8.0, 0.25% (w/v) bromophenol blue, 50% glycerol.

20x SSC: 3M NaCl, 0.3M Na-citrate.

TE: 10 mM Tris-Cl, pH 8.0, 1 mM EDTA

Church buffer: 1 mM EDTA, 0.25% phosphate buffer, 7% SDS.

20x MOPS buffer: 400 mM morpholinopropanesulfonic acid (MOPS), 100 mM Na-acetate, 20 mM EDTA, pH 7.0

Laemmli running buffer: 3.5 mM SDS, 25 mM Tris-acetate, 192 mM glycine.

4x Laemmli loading buffer: 8% SDS, 40% glycerol, 240 mM Tris-Cl pH 6.8, 0.08% (w/v) bromophenol blue, 20% 2-mercaptoethanol.

HEPES lysis buffer: 10 mM HEPES, 250 mM sucrose, 1 mM EDTA.

Western blotting buffer: 20 mM Tris-acetate, 150 mM glycine, 0.02% SDS, 20% methanol.

Tween TBS wash buffer: 10 mM Tris-Cl, 0.9% NaCl, pH 7.4, 0.5% Tween 20.

E. Coli lysis buffer (native): 100 mM NaH_2PO_4, 10 mM Tris-Cl, 6 M guanidine hydrochloride, pH 8.

E. Coli lysis buffer (denaturing): 100 mM NaH_2PO_4, 10 mM Tris-Cl, 8 M urea, pH 8.

50x TAE buffer: 40 mM Tris base, 5.71 % glacial acetic acid, 2 mM Na_2EDTA.

10x TBE: 890 mM Tris base, 890 mM boric acid, 20 mM EDTA.

2.3 Bacterial Culture and Manipulation

2.3.1 Media for bacterial growth. Luria Broth (LB) medium and agar were purchased from Sigma.

2.3.2 Preparation of transformation-competent bacteria. An overnight culture of E. coli bacteria: DH5α or XL-1 blue were inoculated into 100ml LB medium until approximately OD_{550} = 0.3 and centrifuged for 5 minutes at 1500 x g at 4°C. The bacterial pellet was resuspended in 30 ml ice-cold TFBI buffer (100 mM RbCl, 50 mM $MnCl_2$, 30 mM KAc, 10 mM $CaCl_2$, 15% glycerol, pH 5.8), stored on ice for 90 minutes and centrifuged again for 5 minutes at 1500 x g at 4°C. The pellet was resuspended in 4 ml TFBII buffer (10 mM MOPS, 10 mM RbCl, 75 mM $CaCl_2$, 15% glycerol) and aliquots of 200μl each were snap frozen in liquid nitrogen and stored at -80°C. TOP10F' competent bacteria were purchased from Invitrogen.

2.3.3 Transformation of competent bacteria. DNA was added to 200μl of competent bacteria and stored on ice for 20 - 30 minutes and heat-shocked at 42°C for 90 seconds and subsequently placed on ice for 2 minutes. The bacteria were then shaken at 37°C for 1 hour and plated on either LB-ampicillin or LB-kanamycin plates, containing 100 µg/ml antibiotic overnight at 37°C. Colonies were picked on the next day and grown overnight in 3 ml LB medium containing antibiotic with shaking at 37°C. 2 ml of this culture was used for mini-preparation (see section 2.4.2).

2.4 Nucleic Acid Methods

2.4.1 Purification of DNA. DNA was purified using phenol/chloroform extraction in conjunction with ethanol precipitation. DNA was mixed at a 1:1 ratio with a phenol:chloroform:iso-amylalcohol mixture (25:24:1), vortexed and centrifuged for 2 minutes. The upper aqueous phase was pipetted into a fresh tube and mixed with 1 volume of chloroform:isoamylalcohol (24:1). The resulting DNA solution was precipitated by adding 1/10 the volume of Na-Acetate, pH 4.8 and 2.5 times the amount of 100% Ethanol. The mixture was stored at –80°C for 20 – 30 minutes and centrifuged for 10 minutes. The pellet was washed in 70% Ethanol, dried and dissolved in either TE or water.

2.4.2 Plasmid Mini-preparations. 2 ml of an overnight culture were transferred to a 2.0 ml Eppendorf tube and centrifuged at 16,000 x g for 30 seconds. The bacterial pellet was dissolved in 150 μl TE buffer and lysed for 5 minutes at room temperature in 150 μl lysis buffer (2% SDS, 0.4 M NaOH). 500μl neutralization buffer (0.9 M NaOAc, pH 4.9, 0.5 M NaCl) was then added and incubated at –20°C for 5 minutes

before centrifuging for 10 minutes. 750 μl Isopropanol was added to 500μl of the supernatant and centrifuged for another 10 minutes to pellet the DNA. DNA was washed in 70% Ethanol, dried and redissolved in TE buffer containing 10μg RNase A.

2.4.3 Plasmid Maxi-preparations. The preparation was done using the Qiagen maxi kit. 200 ml of an overnight culture was sedimented at 5,000 x g for 10 minutes. The bacterial pellet was resuspended in 10 ml of Buffer B1 (100 μg/ml RNase A, 50 mM Tris-Cl, 10 mM EDTA, pH 8.0) and lysed with 10 ml buffer P2 (200 mM NaOH, 1% SDS). Neutralization was done with 10 ml buffer P3 (2.55 M KAc, pH 4.8) on ice for 15 minutes in order to separate the SDS. This solution was centrifuged at 20,000 x g for 30 minutes, the supernatant was transferred to a fresh tube and centrifuged again for 15 minutes. This new supernatant was loaded onto an equilibrated Qiagen maxi column. The column was washed twice with buffer QC (1 M NaCl, 50 mM MOPS, 15% EtOH, pH 7.0) and eluted with 15 ml QF buffer (1.25 NaCl, 50 mM MOPS, 15% EtOH, pH 8.2) and precipitated with 10.5 ml isopropanol. After centrifugation at 15,000 x g, the DNA pellet was washed in 70% EtOH, dried and resuspended in TE.

2.4.4 Agarose gel electrophoresis. Agarose gels from 0.8% to 2% were poured, depending on the size of DNA fragments to separate. Agarose was dissolved in either TAE or TBE by heating in a microwave oven. Ethidium bromide was added after the gel had cooled down to 60°C to a final concentration of 0.5μg/ml in order for the DNA to be photographed under UV light of 320nm. For quantitative RT-PCR, VistraGreen (Amersham Biosciences) was added to the loading buffer and no ethidium bromide was used. 6x loading buffer was added to the respective DNA before loading. VistraGreen is a chemical that emits fluorescence when it interacts with DNA at a

level that is more indicative to the relative amount of DNA then the intercalation of ethidium bromide. Quantification was done using a Flourescent Image Analyzer 2000 (FLA) (Fujifilm Raytest). The gels were run between 80 and 120V. Running buffer used was used was the same as the buffer to dissolve the agarose.

2.4.5 Isolation of DNA fragments. DNA was loaded onto a 1% Agarose Gel in TAE buffer and the fragment to be isolated was cut out with a scalpel after observation with UV light. DNA was isolated using Amersham's GFX PCR DNA and Gel Band Purification Kit according to the manufacturer's instructions.

2.4.6 Restriction enzyme digestions. Restriction enzyme digests were performed according to the manufacture's instructions with commercially available endonucleases. Buffers were used as directed for single digests. Double digests were done in one suitable buffer for both, otherwise DNA was digested with the lowest ionic strength buffer first and the higher ionic strength buffer was added subsequently.

2.4.7 Sub-cloning and ligations. DNA to be subcloned was either cut from an existing vector or PCR amplified and cloned into the AdvanTAge PCR cloning kit (Clonetech) and cut out using either the two flanking EcoRI sites or using restriction enzymes on either side of the EcoRI sites. Ligation was performed with 1 μl T4 ligase (400,000 units/ml) (New England Biolabs) in a 10 μl reaction at 14°C overnight. Ligated DNA was then used to transform competent bacteria.

2.4.8 DNA Sequencing. The BigDye terminator cycle sequencing kit was used in connection with an ABI PRISM 310 Genetic Analyzer (Perkin Elmer). Either PCR

products or whole plasmids were used as template for the cycle sequencing reaction. The cycle sequence reaction was done for 25 cycles of 10 seconds at 96°C, 5 seconds at 56°C – 59°C and 4 minutes at 60 °C. The DNA was then precipitated at room temperature for 15 minutes. Pellets were dissolved in 13 μl template suppression reagent and heated at 95°C for 5 minutes. Samples were then loaded and run according to manufacturer's instructions.

2.4.9 Southern blotting. 20 – 50μg DNA was digested with a respective restriction enzyme overnight and the DNA was ethanol precipitated to an amount, which can be easily loaded on an agarose gel. A 0.8% gel was poured and run for 4 - 5 hours at 95V until loading buffer had gone 15 cm. The gel was then washed twice for 15 minutes in denaturing buffer (500 mM NaOH, 1.5 M NaCl) and 30 minutes in neutralization buffer (500 mM Tris base, 1.5 M NaCl) and rinsed in 20xSSC. Transfer was performed overnight in 20xSSC by capillary transfer using the Whatman 3MM filter paper wick method (current protocols in molecular biology). After transfer, the gel and Nylon membrane Hybond N^+ were checked by observation under UV light. The membrane was briefly washed in water and dried for 30 minutes at 37°C and subsequently linked in a UV oven at 1200 μjoules x 100. Radioactive labelled probes were hybridised to the blot in church buffer overnight at 65°C in a glass rotating tube. On the next day, the filters were washed at 65°C in 2x SSC/0.1% SDS and then in 1x SSC/0.1% SDS. If this washing was not sufficient, 0.5x SSC/0.1% SDS was used.

2.4.10 Production of radiolabelled probes. DNA probes were made using the Rediprime kit from Amersham. In short, 40 ng DNA was diluted in a total volume of 45 μl TE and denatured for 10 minutes at 95°C. After cooling on ice, the sample was

added to the Rediprime tube (containing the Klenow fragment of DNA polymerase I, nucleotides and buffer). After gentle mixing, α-^{32}P-dCTP was added and incubated for 10 minutes at 37°C. Unbound radioactive nucleotides were filtered over a Sephadex-G50 column. All of the flow-thru was added to the hybridization solution.

2.4.11 Preparation and analysis of RNA. RNA isolation from mouse tissues was performed using a Guanidiniumisothyiocyanate (GTC) denaturing solution (4 M guanidine thiocyanate, 25 mM sodium citrate, 0.5% Sarkosyl and 0.1 M 2-mercaptoethanol) and isolation from cells was done using Trizol Reagent (GIBCO). The desired tissue was homogenized in 2 ml GTC denaturing solution using a glass teflon homogeniser. 0.1 ml of 2 M sodium acetate, pH 4.0 was added and mixed. 0.1 M Phenol was added and mixed again, after which 0.2 ml chloroform was added and mixed by vortexing. The solution was incubated on ice for 15 minutes. The tube was then centrifuged for 20 minutes at 10,000 x g. The aqueous phase was transferred to a clean tube. Adding 1 ml isopropanol and incubating for 30 minutes at –20°C precipitated the RNA. The RNA was pelleted by centrifugation for 10 minutes at 10,000 x g at 4°C and washed in 75% Ethanol for 10 minutes at room temperature to dissolve remaining guanidine. DEPC-treated water was added to the air-dried pellet and dissolved at 56°C. RNA was then stored at –70°C. Cells were washed in PBS and scraped in Trizol reagent. RNA was prepared according to the provided protocol from GIBCO.

2.4.12 Isolation of poly A$^+$ RNA. Oligotex mRNA mini kit from Qiagen was used according to manufacture's directions. Elution was done using 70°C OEB buffer. The first eluate was mixed with 10μl fresh OEB buffer, reheated to 70°C and loaded onto

the column for a second elution. For microarray analysis, the RNA was subsequently precipitated with addition of 5mg/ml glycogen.

2.4.13 Quantitative RT-PCR. Total RNA was prepared from mouse tissues using the GTC method and from cells using Trizol. cDNA was synthesized from total RNA using SUPERSCRIPT II (Gibco). 5 μg of RNA was reverse transcripted with Oligo dT according to the instructions. cDNA was stored at –20°C until use. RT-PCR was initially performed at varying cycles to determine the exponential range. For each sample, β-actin was also amplified at the same time. Quantification of bands was done using VistraGreen and observing on an FLA (refer to section 2.4.4). Band intensity of products was normalized to that of β-actin and this relative amount was then compared between samples. All RT-PCRs were loaded twice to reduce possible inaccuracies due to loading. Reverse transcriptase was repeated three times and a single PCR was performed for each cDNA produced.

2.5 Cell Culture and Manipulation

2.5.1 Tissue culture media. All media and media supplements were purchased from Gibco. A penicillin/streptomycin (P/S) mixture was added to all media at an end concentration of 100 U/ml and 100 μg/ml respectively. Amphotericin B was frequently added at a concentration of 2.5 μg/ml. Trypsin/EDTA and PBS were also purchased from Gibco.

2.5.2 Tissue culture. Human primary fibroblasts and COS-7 cells were grown in Dulbecco's modified Eagle's medium (DMEM) containing Glutamax supplemented

with 10% fetal calf serum (FCS). βTC-tet cells were grown in DMEM plus Glutamax supplemented with 2.5% FCS and 15% horse serum. In-RI-G9 α-cells were grown in RPMI medium supplemented with 10% FCS. Embryonic Stem (ES) cells were grown in DMEM supplemented with 0.1 mM non-essential amino acids, 1 mM Sodium Pyruvate, 10^{-6} M β-mercaptoethanol, 2 mM L-glutamine, 15% FCS, 1% P/S and 1000 U/ml Leukemia Inhibitory Factor (LIF). All cells were incubated at 37°C and 5% CO_2.

Adherent cells were passaged by removing medium, washing in PBS, adding trypsin at 1/3 the volume needed for growth and incubating 3 - 10 minutes at 37°C. An equal volume of medium was added to the detached cells and this mixture was centrifuged for 5 – 10 minutes at 1000 x g. The pellet was resuspended in fresh medium and diluted 1:2 – 1:5 depending on cell type and confluence. Cells were frozen for long-term storage by first trypsinizing and then resuspending in 1 ml per 75 cm^2 flask of freezing solution containing normal growth medium supplemented with 10% dimethysulfoxide (DMSO). This solution was transferred to cryotubes and stored overnight at –80°C before being placed in liquid nitrogen (-196°C) to be stored permanently.

2.5.3 Transfection. 4 x 10^4 cells were seeded per well of a 24-well plate the day before transfection and grown overnight in normal medium without Penicillin/Streptomycin (P/S). For 24-Well plates, other sizes were scaled up or down proportionately to the surface area, 0.8 μg DNA and 2 μl Lipofectamine 2000 (Invitrogen) were each diluted in 50 μl medium containing no serum and no P/S. These two solutions were mixed together within 5 minutes and let to sit at room temperature for 30 minutes, during which the cells were washed in serum-free

medium. After 30 minutes, 150 μl serum-free medium was added, gently mixed and overlaid onto washed cells. After 5 hours of incubation, another 250 μl of medium was added containing twice the normal serum but no P/S. Cells were harvested for western blot or fixed for immunofluorescence after 24 hours. If pIRES2egfp vector was used, cells were observed under a fluorescence microscope for transfection efficiency.

2.6 Recombinant Protein Production

2.6.1 Expression of pQE vectors in E. Coli. pQE40 vectors, containing either N- or C- terminal Wolframin sequences were used to express recombinant protein. Positive clones were inoculated in 30 ml LB-Amp culture overnight. On the next day, the 30 ml culture was over-inoculated into 300 ml LB-Amp medium and grown to an $OD_{600} \approx$ 0.2. At this point, gene expression was induced with 1mM Isopropyl$_{\beta\text{-D-}}$ Thiogalactopyroanoside (IPTG) and grown for an additional 3-4 hours to an $OD_{600} \approx$ 0.6-0.8. Cells were harvested and the pellet dissolved in 4ml of either native or denaturing lysis buffer. The pellet was then frozen overnight at –20 °C or for longer periods of time at –80 °C. Lysozyme was adding after thawing and incubated for one hour on ice. Cells were opened by subjection to ultrasound three times at 30 seconds each with one minute in between. Cell debris was pelleted at 20,000 x g for 20 minutes at 4 °C. Supernatant was transferred to a separate tube and the pellet was dissolved in 4ml of 1x Laemmli buffer. Both the pellet and supernatant were observed on SDS-PAGE gel. If the protein was not over-expressed in the soluble fraction, lysis was attempted in a denaturing buffer.

2.6.2 Ni-NTA column purification. 1 ml of Qiagen Ni-NTA gel was pipetted into a 12 ml tube and centrifuged at 100 x g for two minutes and the ethanol storage solution was discarded. The gel was then washed twice in 1 ml lysis buffer before being resuspended in 1 ml lysis buffer and loaded onto a column. At 4°C, 15 ml of lysis buffer was run over the column before exchanging the buffer with the protein sample. The column was reloaded twice with flow thru to assure maximum binding capacity. Washing was done with 10 ml lysis buffer + 20mM imidazole. Wash buffer was then exchanged with 10 ml of lysis buffer containing 200mM imidazole to elute bound protein. The elutates were collected in 1 ml volumes in Eppendorf tubes and saved for SDS-PAGE gel analysis and western. Eluates, which contained the expressed protein were pooled and used to immunize rabbits.

2.7 Protein Methods

2.7.1 Separation of proteins on SDS-PAGE. Protein separation was done according to the Laemmli method. Protein samples were boiled for 5 –10 minutes in Laemmli loading buffer containing 5% β-mercaptoethanol as reducing agent. Either 10% or 12% polyacrylamide gels plus stacking gel were poured into BioRad mini protean 3 plates and electrophoresed using this system. Electrophoresis was done at 120V for 1.5 hours. Coomassie stained gels were incubated in 0.25% (w/v) Coomassie Brilliant blue R250 (Serva) in 40% methanol and 10% acetic acid overnight at 4°C. Destaining was done in 10% acetic acid and 30% methanol.

2.7.2 Western blot and detection. Those gels to be blotted were placed on 3 layers of 3MM Whatmann paper pre-wetted in blot buffer (20 mM Tris, 150 mM glycine,

0.02% SDS and 20% methanol). Pre-wetted Protran BA 85 cellulose nitrate (Schleicher and Schuell) was placed on the gel followed by an additional 3 layers of pre-wetted Whatmann and blotted in a semi-dry electroblotter (PeqLab) for 1.1 – 1.5 hours at 210 mAmp. Blots were stained in Ponceau solution for 20 minutes and washed in water to observe protein bands. After blots were dry, they were blocked for 30 minutes in 5% non-fat dried milk in tween TBS. Antibody incubation was done at 4°C overnight. The membrane was washed in Tween-TBS three times at 10 minutes each and incubated at room temperature with horse radish peroxidase-conjugated anti-rabbit or anti-mouse IgG, depending on source of primary antibody. The membranes were washed for 4 times at 10 minutes each in Tween-TBS and detected using the ECL system (Roth).

2.7.3 Protein extraction. Protein extracts from tissue culture cells were prepared by dissolving cell pellets at a concentration of 1 x 10^3 cells/μl in 1x Laemmli loading buffer and boiling them before loading 20μl (= 2 x 10^4 cells) on an SDS-PAGE gel. Homogenate protein solutions from mouse tissues were prepared by homogenizing in HES buffer (10 mM HEPES, 250 mM sucrose, 1 mM EDTA, 1 mM PMSF). Protein concentration was determined using Rotiquant solution from Roth, measuring OD 550 nm.

2.7.4 Sub-cellular fractionation. Tissue was extracted and kept in ice-cold HES buffer. The tissue was then weighed and homogenized in 10 ml HES buffer per gram of tissue. Homogenization was done with 6 strokes of a glass/teflon potter and 2 strokes in a glass douncer with a loose fitting and once with a tight fitting. This homogenate was centrifuged at 600 x g for 10 minutes to pellet out cell debris and the

nuclear fraction. The supernatant was centrifuged 3 times at 1,000 x g for 10 minutes each to ensure that no nuclear debris would contaminate the mitochondrial fraction (Mt). Pellets were pooled from the second and third centrifugation at 1,000 x g, washed and used as the nuclear pellet (Nuc). The supernatant was then centrifuged at 8,000 x g for 10 minutes to pellet the mitochondrial fraction. The resulting pellet was then washed in 5 ml HES buffer and centrifuged at 10,000 x g. The Mt pellet was then dissolved in 2 ml HES buffer and purified over a sucrose gradient of 1.2 M and 1.5 M sucrose by ultra centrifugation at 40,000 x g for 25 minutes. The band at the interface was pipetted out into a 1.5 ml tube, centrifuged for 15 minutes at full speed in a table top centrifuge at 4°C and the pellet resuspended in TE buffer and used as the mitochondrial fraction (Mit). The post-mitochondrial supernatant was centrifuged at 100,000 x g for 1 hour to separate the microsomal fraction (Ms) from the cytosol fraction (Cyt). Protein concentration was measured using the Bradford method (Bradford 1976) and an equal amount of each fraction was loaded onto a western blot.

2.8 Histological Techniques

2.8.1 Tissue sections. Tissues were placed in a 10ml tube containing 4% Paraformaldehyde (~2ml) and incubated for 2h at 4°C and then overnight at 4°C in 30% Sucrose in PBS. Tissues were then snap frozen in aluminium foil in liquid nitrogen and stored at -80°C. Sections were sliced at 5 μm on a Cryostat and stored at –20 °C.

2.9 Immunological Methods

2.9.1 Immunohistochemistry. Frozen slides were taken out of -20°C and dried at room temperature for approximately 15 minutes. Dried slides were fixed for 10 minutes in acetone. Fixed slides were dried for 1 hour at room temperature. They were then washed in PBS and blocked for 30 minutes at room temperature in a humid chamber with either goat serum or BSA at a 1:50 dilution in PBS depending on source of primary antibody. After blocking, slides were washed twice for around 5 minutes each time in PBS. Next, the primary antibody was added at varying concentrations in 1:200 blocking serum and incubated overnight in a humid chamber at 4°C. On the next day, the humid chamber was allowed to equilibrate to room temperature for 15 min. The slides were then washed in PBS and the secondary antibody was added and incubated at room temperature for 30 min to 1 hour. Afterwards, the slides were wash in PBS and fixed with Fluoromount-G, Southern Biotechnology Associates, Inc., USA.

2.9.2 Immunofluorescence. Cells were seeded on either 8-Well or 4-Well chamber slides (Nunc) to approximately 80% confluency. Cells were washed in PBS and fixed for 10 minutes at room temperature with 4% Paraformaldehyde in PBS. After washing twice in PBS, permeablization was done with 0.2% Triton X-100 in PBS for 5 minutes and then for an additional three changes over 5 minutes. 50 – 200 μl of primary antibody, diluted in PBS with 3% BSA and 0.2% Triton X-100 was added to the permeablized cells and incubated for either 1 hour at room temperature or overnight at 4°C. Chamber slides were washed again in three changes of 0.2% Triton X-100 in PBS over 5 minutes. Either FITC or TRITC conjugated secondary antibody was added at a dilution of 1:50 for 20 – 30 minutes at room temperature, washed for an additional

5 minutes with 0.2% Triton X-100 in PBS, mounted with fluoromount and observed under a fluorescence microscope (LEICA DM IRB, Leica Microsystems Wetzler GmBh, Germany). The SPOT program version 3.4 (Diagnostic Instruments, Inc.) was used to photograph and analyse all immunofluorescence and immunohistochemistry specimens. Co-localisation was done by merging individual FITC and TRITC pictures of the same region after optimising each using the histogram option.

2.10 Transgenic Techniques

Cloning of the Wolframin mouse knock-out construct. Before genomic sequences were available publicly, the GenomeWalker kit (Clonetech) was used to amplify genomic sequences from the intron between exon 7 and exon 8. The four GenomeWalker libraries containing the adaptor segments were amplified with the given AP1 forward primer, which annealed to the adaptor sequence and a reverse primer in the extreme 5' region of exon 8. A nested PCR was performed with AP2 and a second reverse primer from exon 8. Positive PCR products were isolated and sequenced. The sequences from these products were used to make new reverse primers and the procedure repeated again with the same library DNA. This method was used to sequence 1500 bp of genomic DNA. However, this turned out not to be long enough. Later, sequences available from Celera were used to amplify a 5' segment of 5.3 kb. Amplification was done using the longExpand kit from Boehringer Mannheim. This was cloned into an AdvanTAge PCR cloning vector and cut out with the 2 flanking EcoRI sites. This was subsequently cloned into an EcoRI site located on the ploxpneo1 plasmid 5' from a PGK-1 promoter, neomycin gene and a PGK-1 terminator region. The 3' region from exon 8 was amplified, sequenced and cloned

into pTAdvantage and subcloned in a pBSKII vector at the EcoRI site contained in the multiple cloning site. The 5' region including the neomycin gene was cut out using two flanking XbaI sites and subcloned into the pBSKII vector containing the 3' segment. Orientation was checked by restriction digest.

2.10.1 DNA transfer. 200μg of the Wolframin knock-out mouse construct was digested with XhoI, precipitated and purified over a chromaspin column 1000, exchanging the buffer from TE to PBS. The linearized DNA was electroporated at 240 V, 500 μF into R1-ES cells and the cells transferred to 10 cm dishes containing 0.1% gelatine. Two days after electroporation, medium was exchanged with fresh medium containing 200 μg/ml G418. After 8 – 10 days 600 resistant colonies were picked. 2 – 3 drops of trypsinized cells from each clone were pipetted into individual wells of 96-Well plates containing a layer of mitomycin inactivated feeder cells and the rest was used for DNA preparation.

2.10.2 Screening of ES clones. ES cell clones were pooled at 6 colonies per 1.5 ml tube and DNA isolated by first centrifuging the tubes of ES cells at maximum speed for 45 seconds and washing in 500μl PBS. The pellet was then resuspended in 50μl PCR-grade water and boiled for 10 minutes. Cell debris was digested by incubation in 50 μg of Proteinase K at 55°C for 95 minutes. DNA was denatured by boiling for 10 minutes and was stored at –20°C until used for PCR analysis. Positive pools were screened by nested PCR amplifying with 2 successive forward primers from the neo gene to 2 reverse primers outside of the 3' end of the construct. ES cells from positive pools were propagated from 96-Wells to 24-Wells, pipetting out 50μl for another DNA preparation. The DNA from these individual clones was amplified as before and

positive clones identified. Cells from positive clones were then transferred to a 6-Well and eventually to 10 cm dishes. Cells from a single 10 cm dish were frozen for long-term storage and DNA was isolated for southern analysis from another 10 cm dish.

2.10.3 Isolating DNA from ES cells. Cells were preplated onto gelatine-coated plates for 20 minutes at 37° to remove feeder cells. Feeder cells will attach themselves to the bottom of the plate in this time, but ES cells will not have attached themselves to the feeder cells yet. The plate was then rinsed with its ES cell-containing medium and transferred to another gelatine-coated plate. The preplating was repeated, this time for only 10 minutes. The ES cell-containing medium was then centrifuged and resuspended in 4.4ml TENPK buffer (50 mM TrisCl, 100 mM EDTA, 100 mM NaCl, 100μg/ml Proteinase K) and mixed with a pasteur pipet. 0.6 ml 10% SDS was added and mixed gently by inverting the tube. The DNA was digested for 2 –3 days at 55°C with gently rocking. After this time, DNA was isolated by phenol/chloroform extraction and the precipitated DNA was spooled on a glass rod, washed in 70% Ethanol, resuspended in TE and used for Southern analysis.

Results

Chapter 3. Wolframin expression in the NOD mouse model

Wolframin mRNA expression has been observed in all tissues tested with pancreatic expression being restricted to the endocrine pancreas (Inoue, Tanizawa et al. 1998; Strom, Hortnagel et al. 1998). It is not known why Wolframin mRNA is expressed in so many different tissues, but the functional defect of the Wolframin protein targets primarily neuroendocrine functions. In order to investigate this further, its expression during the progression of diabetes in the well-established nonobese diabetic (NOD) mouse model was studied. 9 female mice of the same age (provided by Dr. Helga Rothe, Institute for Diabetes Research) were used in this experiment. This mouse model was chosen because the main symptom in WS is young onset diabetes mellitus. Even though the NOD mouse model is based on an immune-mediated type 1 diabetes and the diabetes in DIDMOAD is non-autoimmune, both are based on a loss of pancreatic β-cells. This made it reasonable to study whether or not Wolframin expression is changed during a regulated loss of β-cells in cyclophosphamide induced diabetes in NOD mice. It is largely unknown how cyclophosphamide accelerates diabetes, however, it has been postulated that the drug depletes protective T-cells (Yasunami and Bach 1988). Many tissues were examined for a possible effect on Wolframin expression during diabetes. The tissues tested were: brain, heart, kidney, liver, lung, pancreas and spleen. RT-PCR was performed on day 0, day 3 and day 9 after induction of NOD mice for diabetes with cyclophosphamide. Gel bands were quantified using the Advanced Image Data Analyzer (AIDA) program version 1.3. Expression for Wolframin was normalised to quantified β-actin bands. The only tissues that showed any difference between day 0 and day 9 were the brain and

pancreas (figure 3.1). These are also the two tissues affected by WS. Thus, inducing NOD mice for diabetes with cyclophosphamide causes a change in Wolframin mRNA expression in neuroendocrine tissues.

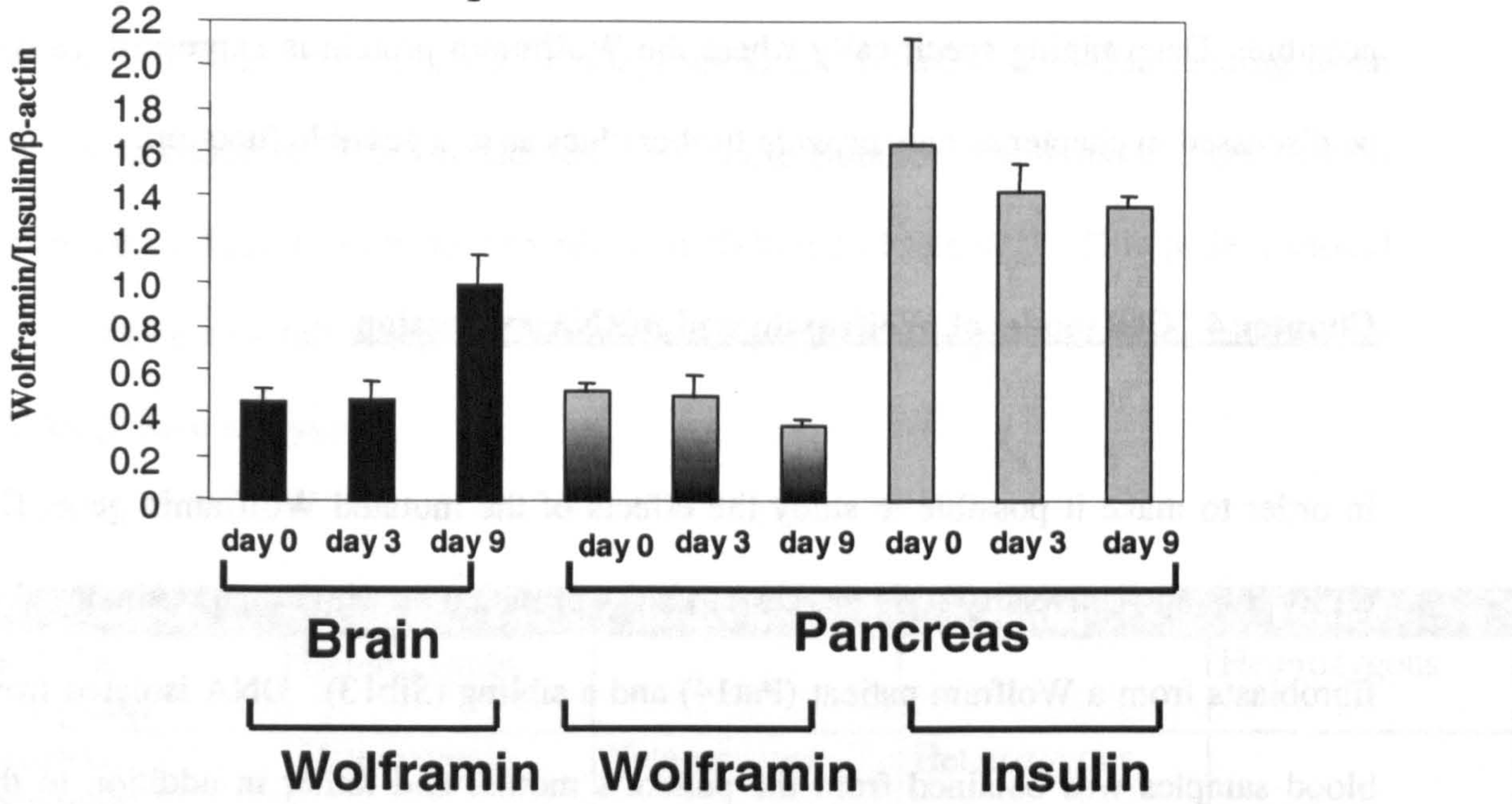

Figure 3.1 RT-PCR of cyclophosphamide treated NOD mice. Expression of either Wolframin or Insulin was normalised to β-actin. Tissues were taken from two separate mice at each time point and three RT-PCR's were performed for each mouse.

To determine if the decrease in the pancreas was due to the destruction of β-cells, insulin expression in the same pancreata was observed. Unfortunately, the decrease in insulin was not as pronounced as the decrease in Wolframin, however, compared to day 0, there was some decrease in expression. 9 days after induction for diabetes, expression in insulin-producing β-cells decreased by 21.5%. Therefore, Wolframin expression decreases with a decrease in β-cells.

Expression in the brain was found to increase by 120% 9 days after induction for diabetes. Considering that the neurodegenerative damage follows the diabetes in WS patients, it is theoretically possible that the neurological symptoms are a consequence of the diabetic conditions in neuronal tissue. However, the expression and modulation of expression of the Wolframin gene in neuronal tissue at least make a direct effect possible. Determining specifically where the Wolframin protein is expressed, as will be discussed in chapter 6, may provide further clues as to a possible function.

Chapter 4. Cell model of Wolframin and mRNA expression

In order to make it possible to study the effects of the mutated Wolframin gene, Dr. Cathy Burson (University of Iowa, USA) kindly provided us with human primary skin fibroblasts from a Wolfram patient (Pat14) and a sibling (Sib13). DNA isolated from blood samples was obtained from the patient's mother and father in addition to the sibling. Fibroblast cells and DNA from another Wolframin patient, PatEC, were also obtained from Michael Ristow (German Institute for Nutrition, Berlin). Blood or cells from relatives of this patient were not available.

4.1 Sequence analysis

Dr. Sabine Hofmann (Institute for Diabetes Research, Munich, Germany) had already sequenced Pat14 DNA for mutations in exons 2 – 8. Two possible disease-causing mutations were found in exon 8. The regions where mutations had already been found in Pat14 were then sequenced in DNA from Sib13 and both parents in order to determine which mutations were enough to cause the WS phenotype. Sequence analysis revealed a typical case of Wolframin mutations: Pat14 is compound

heterozygous for two separate mutations. One allele contains a nonsense mutation leading to an early stop codon at 371aa instead of 890aa and the other allele contains a missense mutation exchanging a Tryptophan for an Arginine (R629W). All other family members were positive for only a single mutation (table 4.1).

DNA from PatEC was sequenced for mutations in the entire exon 8 region. This patient was found to contain a homozygous single insertion at 343aa leading to an early stop codon at 395aa. In addition, a missense mutation was found at 389aa, which exchanges a Histidine for an Aspartic acid (D389H) (Table 4.2). This patient should not produce any full length Wolframin protein and was a good negative control for future protein analyses.

Mutation	Patient 14	Sister 13	Mother	Father
W371X early stop	Heterozygous			Heterozygous
R629W Missense	Heterozygous	Heterozygous	Heterozygous	

Table 4.1 Mutation analysis of a Wolfram patient and parents. Patient 14 is compound heterozygous for two different mutations; one leading in a truncated protein and the other is a missense mutation. Her first grade relatives in comparison are only heterozygous for a single mutation.

Mutation	PatEC
F343 → 395TAA early stop	Homozygous
D389H Missense	Heterozygous

Table 4.2 Mutation analysis of Wolfram patient PatEC. This patient is homozygous for a single base insertion at 343aa, leading to an early stop codon at 395aa. The resulting protein is truncated to only 44% of its normal length.

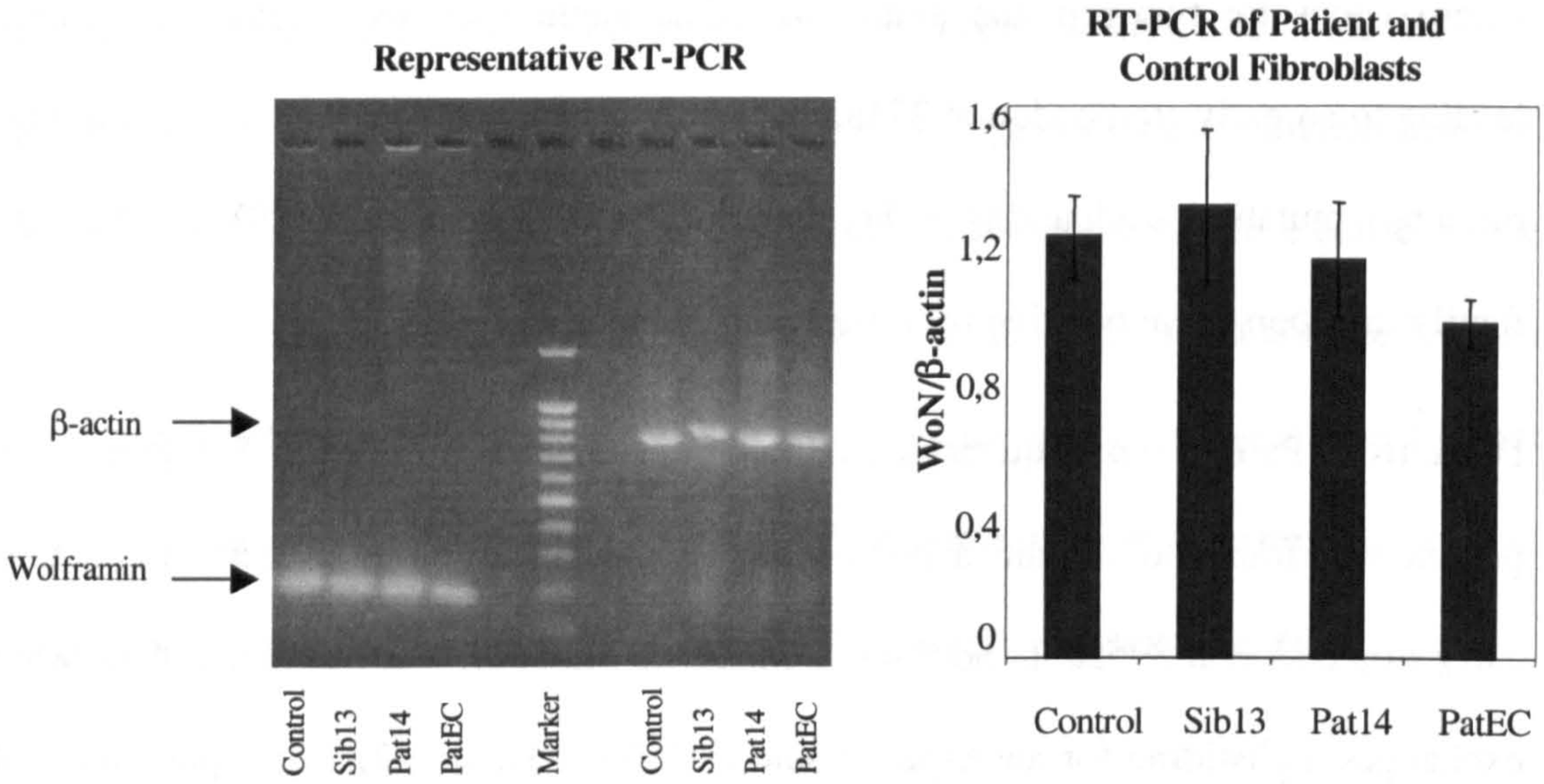

Figure 4.1 RT-PCR of fibroblast cells from DIDMOAD patients and controls. Wolframin expression was normalised by β-actin. Each RT-PCR was repeated three times. The gel picture shows a single representative RT-PCR result.

4.2 mRNA expression

It had already been shown that Wolframin mRNA is ubiquitously expressed in many tissues (Inoue, Tanizawa et al. 1998; Strom, Hortnagel et al. 1998). However its expression in fibroblast cells and other cell lines had not been observed. Therefore, Wolframin mRNA expression in fibroblast cells from these patients and from fibroblasts from control individuals was analysed with RT-PCR (figure 4.1). Primers used were: human Wolframin forward: 5'-AAA GAG GAA GAG GAA GTA GCC GAT GG-3', human Wolframin reverse: 5'-GAG GCT GAC GTT GAG GAT GAT GAA GT-3', β-actin forward: 5'-ATC TGG CAC CAC ACC TTC TAC AAT GAG CTG-3' and β-actin reverse: 5'-CGT CAT ACT CCT GCT TGC TGA TCC ACA TCT-3'. Wolframin mRNA expression was found in fibroblast cells, however, no notable differences were seen in expression between cells from controls and WS patients. Therefore, these mutations do not affect stable mRNA expression in addition

to their expected effect on the structure and function of the Wolframin protein. The fact that Wolframin is expressed in fibroblast cells, indicated that these cells could be suitable for functional analysis.

Chapter 5. Production of antibodies to recombinant protein and peptides

The Wolframin cDNA sequence encodes for a polypeptide of 890aa, with a predicted molecular mass of 100.29 kDa. Figure 5.1 shows the hydrophobicity plot of the deduced amino acid sequence. A transmembrane protein is predicted which transverses the membrane nine times. The protein contains, therefore, three structural domains, hydrophilic N- and C- terminal regions and a central hydrophobic core spanning the region from 330 – 650aa. Protein structure prediction programs (Stoffel, Duker et al. 1993; Rost, Casadio et al. 1995) preferentially placed the N-terminal hydrophilic part on the extracytoplasmic side and the C-terminal part on the intracytoplasmic side. This deduced amino acid structure contains no sequences targeting the protein to any function or cellular compartment, nor is it homologous to any known protein. In order to gain insight into this novel protein, antibodies were made to recognise its N- and C- terminal regions. Antibodies raised against both peptides and recombinant proteins were used in this work.

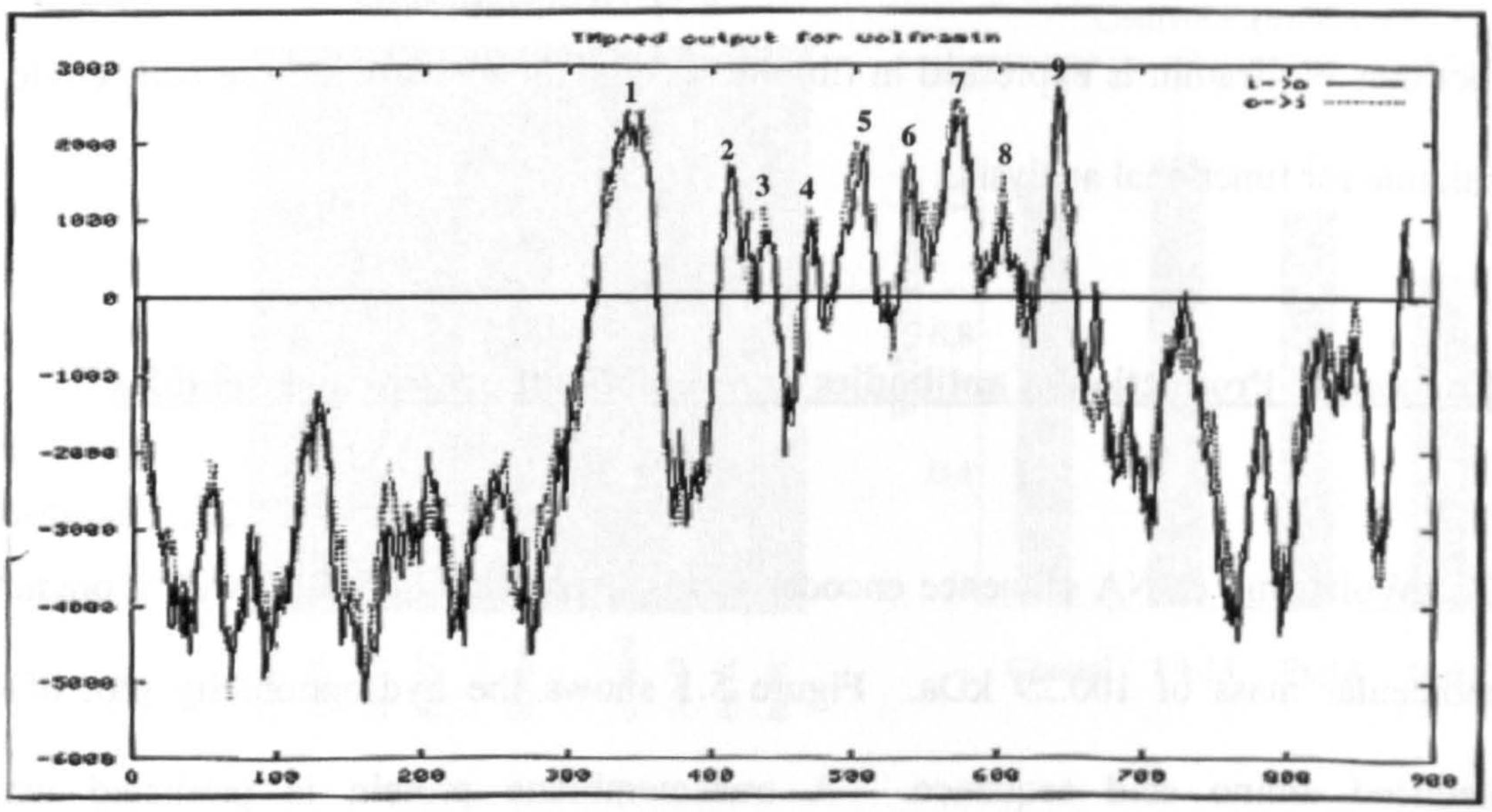

Figure 5.1 Prediction of possible transmembrane helices. 9 transmembrane helices were predicted from the Wolframin amino acid sequence.

.

5.1 Production of recombinant proteins as antigens for immunisation

The advantage to making antibodies against recombinant protein is that more epitopes are presented to the immune system and the antibody can recognise even the denatured state. However, in the case of such a large transmembrane spanning protein, it would be very difficult or even not possible to produce a recombinant protein to the entire sequence. Therefore, due to their hydrophilic nature, the N- and C- terminal regions were chosen as targets to be incorporated into recombinant protein to be used as antigens for antibody production. In these hydrophilic regions, the human and mouse sequences are relatively conserved (figure 5.2). The N-terminus region chosen for antigen production spans 1 – 295aa and is 83% identical to the mouse sequences at the amino acid level. The C-terminus region spans 625 – 890aa and its amino acid sequence is 91% similar to the mouse amino acid sequence.

```
human:   RSRLNATASLEQERSE----------------VRDAAAPAEPQAQHTRSRERADGTGPTK
mouse:   RARLNATASLEQDKIEPPRAPRPQADPSAGRSAGEAAAP-EPRAPQTGSREETDRAGPMK

human:   GDMEIPFEEVLERAKAGDPKAQTEVGKHYLQLAGDTDEELNSCTAVDWLVLAAKQGRREA
mouse:   ADVEIPFEEVLEKAKAGDPKAQTEVGKHYLRLANDADEELNSCSAVAWLILAAKQGRREA

human:   VKLLRRCLADRRGITSENEREVRQLSSETDLERAVRKAALVMYWKLNPKKKKQVAVAELL
mouse:   VKLLRRCLADRKGITSENEAEVKQLSSETDLERAVRKAALVMYWKLNPKKKKQVAVSELL

human:   ENVGQVNEHDGGAQPGPVPKSLQKQRRMLERLVSSESKNYIALDDFVEITKKYAKGVIPS
mouse:   ENVGQVNEQDGGAQPGPVPKSLQKQRRMLERLVSSESKNYIALDDFVELTKKYAKGIIPT

human:   SLFLQ--------LAGKSPEDLPLRLKVVKYPLHAIMEIKEYLIDMASRAGMHWLSTIIP
mouse:   NLFLQDEDEDEDELAGKSPEDLPLRQKVVKYPLHAIMEIKEYLIDVASKAGMHWLSTIVP

human:   THHINALIFFFIISNLTIDFFAFFIPLVIFYLSFISMVICTLKVFQDSKAWENFRTLTDL
mouse:   THHINALIFFFIISNLTIDFFAFFIPLVVFYLSFVSMVICTLKVFQDSKAWENFRTLTDL

human:   LLRFEPNLDVEQAEVNFGWNHLEPYAHFLLSVFFVIFSFPIASKDCIPCSELAVITGFFT
mouse:   LLRFEPNLDVEQAEVNFGWNHLEPYIHFLLSVVFVIFSFPLASKDCIPCSELAVISTFFT

human:   VTSYLSLSTHAEPYTRRALATEVTAGLLSLLPSMPLNWPYLKVLGQTFITVPVGHLVVLN
mouse:   VTSYMSLSSSAEPYTRRALVTEVAAGLLSLLPTVPVDWRFLKVLGQTFFTVPVGHFIILN

human:   VSVPC---------FFRMAQLRNFKGTYCYLVPYLVCFMWCELSVVILLESTGLGLLRAS
mouse:   VSLPCLLYVYLFYLFFRMAQLRNFKGTYCYLVPYLVCFMWCELSVVILLQSTGLGLVRAS

human:   IGYFLFLFALPI----------QFARWFTSLELTKIAVTVAVCSVPLLLRWWTKASFSV
mouse:   IGYFLFLFALPILVAGLALMGTVQFARWFLSLDLTKIMVTTVICGVPLLFRWWTKANFSV

human:   VGMVKSLTRSSMVKLILVWLTAIVLFCWFYVYRSEGMKVYNSTLTWQQYGALCGPRAWKE
mouse:   MGMVKSLTKSSMVKLILVWLTAILLFCWFYVYRSEGMKVYNSTLTWQQYGFLCGPRAWKE

human:   TNMARTQILCSHLEGHRVTWTGRFKYVRVTDIDNSAESAINMLPFFIGDWMRCLYGEAYP
mouse:   TNMARTQILCSHLEGHRVTWTGRFKYVRVTEIDNSAESAINMLPFFLGDWMRCLYGEAYP

human:   ACSPGNTSTAEEELCRLKLLAKHPCHIKKFDRYKFEITVGMPFSSGADGSRSREEDDVTK
mouse:   SCSSGNTSTAEEELCRLKQLAKHPCHIKKFDRYKFEITVGMPF--GTNGNRGHEEDDITK

human:   DIVLRASSEFKSVLLSLRQGSLIEFSTILEGRLGSKWPVFELKAISCLNCMAQLSPTRRH
mouse:   DIVLRASSEFKDVLLNLRQGSLIEFSTILEGRLGSKWPVFELKAISCLNCMTQLSPARRH

human:   VKIEHDWRSTVHGAVK----------LSAA
mouse:   VKIEQDWRSTVHGALKFAFDFFFFPFLSAA
```

Figure 5.2 Alignment of the human and mouse Wolframin amino acid sequences. Underlined sequences indicate transmembrane regions.

These two regions were PCR amplified and cloned into pQE40 (Qiagen) expression vectors using the sites BamHI and HindIII. Both enzymes do not cut Wolframin cDNA and were therefore introduced on the PCR primers. N- or C-terminal regions

were cloned in frame with the start codon located upstream from the His tag located on the pQE40 vector. pQE40 plasmids utilise the phage T5 promoter coupled with two lac operator sequences, which increase lac repressor binding to regulate the T5 promoter. The 6x His tag located on the 3' end of the multiple cloning site (MCS), allows for immobilisation of the expressed protein by binding to Ni-NTA agarose columns.

PQE40 vectors containing either C-terminal (WmrecC) or N-terminal (WmrecN) sequences were inoculated into E. coli and induced for expression of the respective protein with IPTG. In order to test for expression, aliquots of the pellet and supernatant (SN) were loaded onto a 12% SDS gel. As a control, a parallel experiment was done without induction with IPTG. Neither WmrecC nor WmrecN protein was detected when cells were lysed under native conditions. Instead, WmrecN and WmrecC both formed insoluble inclusion bodies and were impossible to solubilise without using 8M urea as a denaturing agent. In an attempt to solubilise the recombinant protein, clones were inoculated in E. coli and induced as before. The E. coli pellet was dissolved in 4 ml PBS and sonicated three times at 30 seconds each. The culture was divided into two halves and centrifuged. The combined supernatant was loaded (SN1) (figure 5.3). The pellets were dissolved in either 2 ml PBS plus 8M urea (P1 + urea) or 2 ml 2% SDS in PBS (P1 + SDS). The pellets were sonicated again twice for 20 seconds each time and re-centrifuged. The resulting pellets (P2) were dissolved in 1x Laemmli buffer and loaded along with the supernatants (SN2). This allowed some of the expressed protein to be transferred from the original pellet into subsequent supernatant fractions for WmrecN, but not for WmrecC (not shown). Therefore, only the N-terminal recombinant protein, WmrecN was isolated and used to inject rabbits. Sera from immunised rabbits were received and purified by binding to

protein G columns. Protein G binds to IgG regions to purify crude serum from possible unspecific proteins such as albumin, thereby improving antibody specificity.

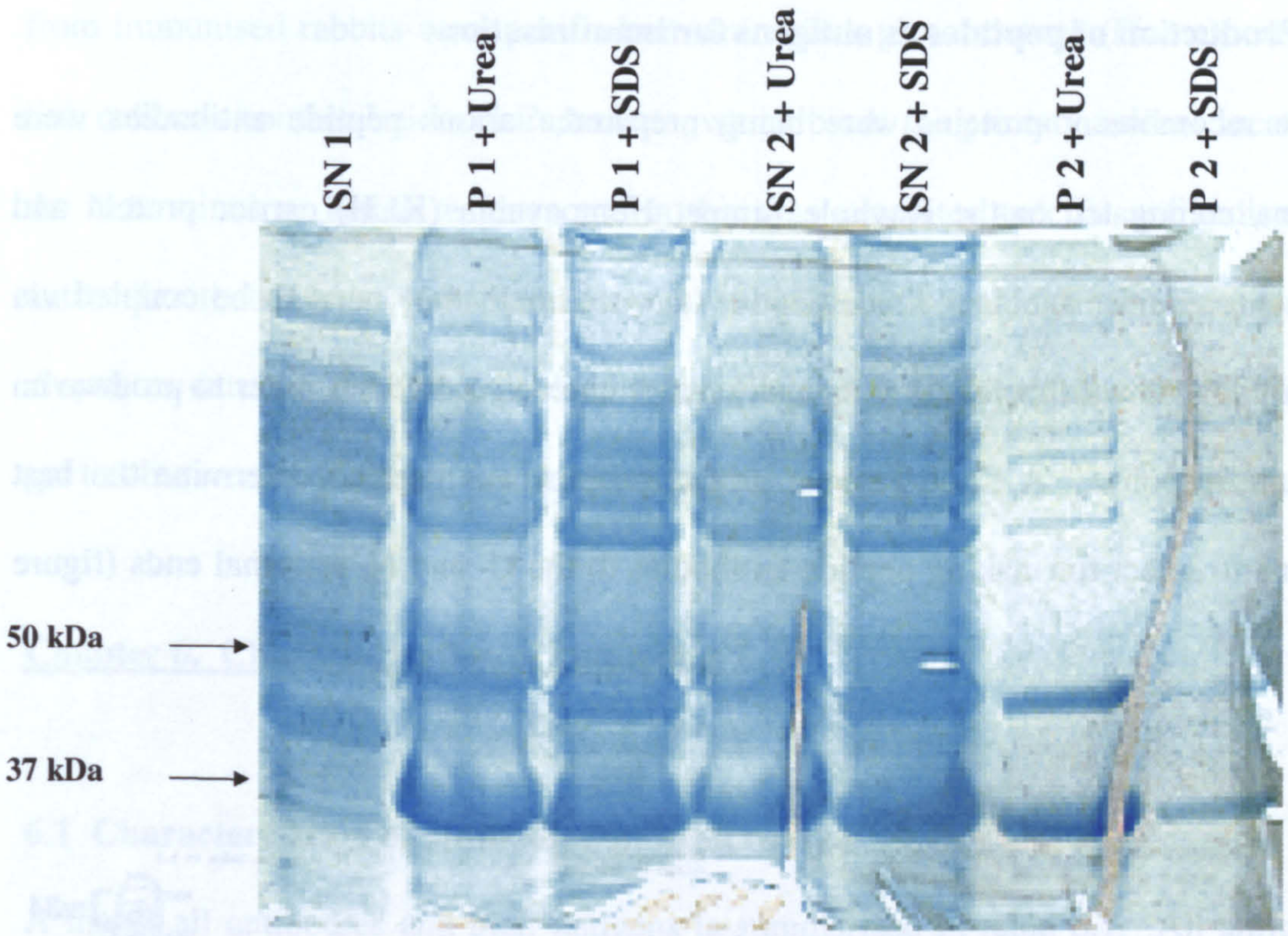

Figure 5.3 Bacterially expressed Wolframin N-Terminal protein. Mini-scale protein preparations from a WmrecN-pQE40 positive clone under denaturing conditions. Expected size of protein is 35 kDa. Supernatant and Pellet fractions are described in the text.

After this, the group of Dr. Sabine Hofmann decided to tackle this solubility problem by fusing Wolframin to the maltose binding protein, using the pMal-C2x vector (New England Biolabs). This system utilises the Ptac promoter and translation initiation signals of the maltose binding protein (MBP) to express large amounts of protein. MBP has been shown to enhance the solubility of protein expressed in E. coli (Kapust and Waugh 1999). Another advantage of the MBP is its ability to bind amylose and elute with low concentrations of maltose, excluding the need for harsh detergents. In

this way, it was possible to successfully express both N- and C-terminal proteins and use these for immunisation of rabbits.

5.2 Production of peptides as antigens for immunisation

While recombinant proteins were being prepared, various peptide antibodies were chosen, conjugated to the Keyhole Limpet Hemocyanin (KLH) carrier protein and used to immunise rabbits. Since peptides are so small, they need to be coupled via glutaraldehyde with the immunologically rather unreactive KLH in order to produce an immune response. A Chou-Fasman prediction plot was used to determine the best regions to select for making peptide antibodies to the C- and N- terminal ends (figure 5.4).

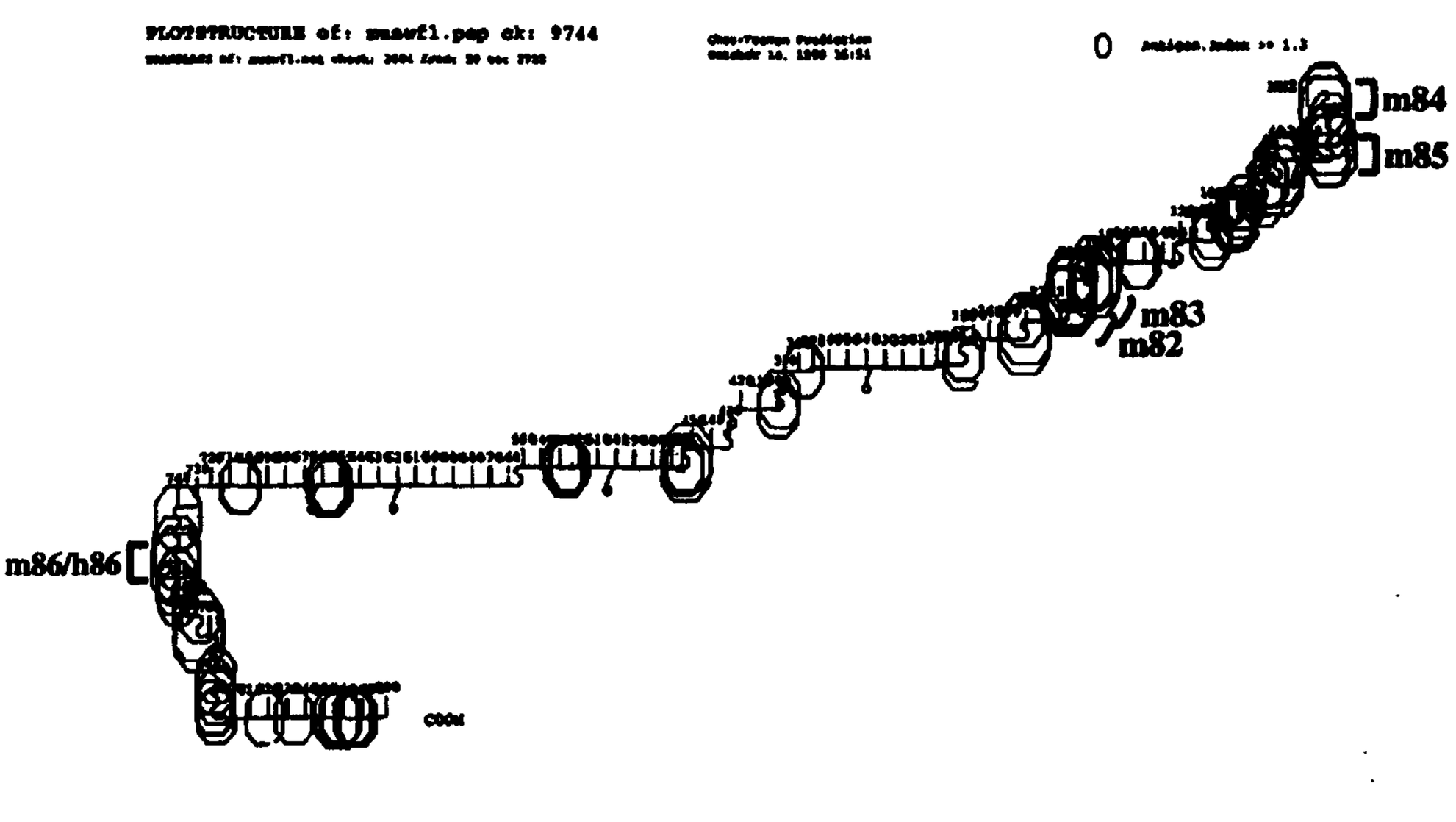

Figure 5.4 The Chou-Fasman topological prediction plot for Wolframin. Circles indicate hydrophilic regions.

Four N-terminal peptides were chosen, two of which were targeted to both mouse and human sequences and two were targeted only to mouse sequences. Two C-terminal peptides were made, one targeted to the human and one to the mouse sequence. Sera from immunised rabbits were purified on amino-link plus columns (Pierce). Amino-link columns contain Imidazol Carbamate, which binds the primary amines located on the N-terminus or lysine residues and in this way separates specific antibodies from antibodies that bind to unknown antigens. OD 280 nm readings were taken of the eluates to determine the best pools and equal amounts were loaded onto a 12% SDS gel to observe the quality of the resulting eluates.

Chapter 6. Characterisation of antibodies

6.1 Characterisation of antibodies on western blot

A list of all antibodies and their antigens is summarised in table 6.1. All antibodies tested positive for reactivity against their respective antigen by using ELISA (data not shown). It had recently been shown by Takeda et al. that the Wolframin protein is very weakly expressed in Cos-7 cells and a large difference can be seen between transfected and non-transfected cells. Therefore, as a test to determine which antibodies were specific and which were not, western blot analyses were performed comparing untransfected Cos-7 cells and those transfected with the Wolframin expression construct. This analysis is shown in figure 6.1. Only two antibodies showed specific immunoreactivity on the western blot. These were WoN; the antibody against the N-terminal recombinant protein fused with MBP and h86; an antibody to the human C-terminal peptide. However, h86 only reacted weakly on western blots and did not improve when purification was repeated once more with AminoLink and

then with SulfoLink affinity chromatography. SulfoLink columns contain Iodoacetyl, which binds to the sulfhydryl groups located on cystein residues. In this case, Iodoacetyl was able to bind to the internal cystein located on the h86 peptide sequence. Interestingly, the h86 antibody was able to immunoprecipitate the Wolframin protein specifically from native pancreatic tissue extracts. For example, when protein homogenate was precipitated with h86, a strong signal at 100 kDa for Wolframin was seen using WoN on western blot analysis. However, when h86 was used to detect an h86 precipitated Wolframin protein, no signal was seen. This indicates that h86 recognises the Wolframin protein, but shows only weak reactivity on western blot.

Antibody	Antigen	Region	Western Reactivity	IF Reactivity
m84	N-terminal peptide	aa 30 - 49	-	weak
m85	N-terminal peptide	aa 61 - 79	-	-
m83	N-terminal peptide	aa 187 - 206	-	-
m82	N-terminal peptide	aa 203 - 222	-	weak
m86	C-terminal peptide	aa 745 – 764	-	-
h86	C-terminal peptide	aa 745 – 764	weak	-
WmrecN.	N-terminal recombinant	aa 1 - 295	-	-
WmrecC.	C-terminal recombinant	aa 625 - 890	n.a.	n.a.
WoN	N-terminal recombinant	aa 39 - 288	strong	strong

Table 6.1 List of antibodies used for immunisation. IF = Immunofluorescence, n.a. = not analysed.

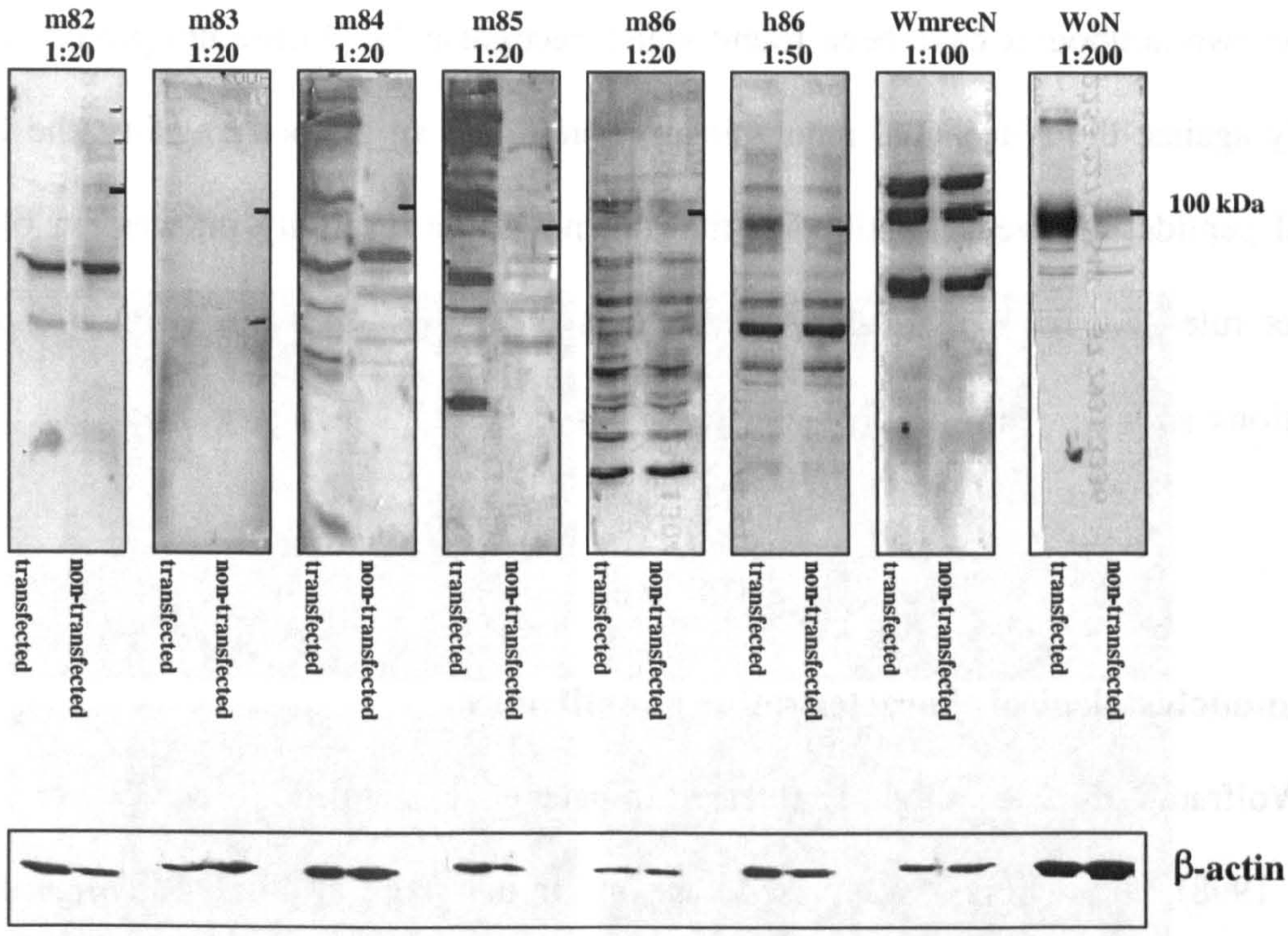

Figure 6.1. Western blot analysis of Wolframin antibodies on total protein extracts from either transfected or non-transfected cos-7 cells. 50μg total cell homogenate was loaded. WoN and h86 recognize the Wolframin protein as a band of 100 kDa, which is more intense in protein from cos-7 cells transfected with Wolframin cDNA.

The antibody to recombinant N-terminal protein fused with 6xHis tag, WmrecN, produced a strong band at the expected size, however, this band was present in equal concentration in untransfected cells and those transfected with Wolframin, indicating unspecific binding. This antibody produced a 100 kDa band in all fractions, including both soluble and insoluble cell extracts and non-membrane fractions (data not shown). m82 and m83 showed no transfection specific reactivity in the range of the expected size of 100 kDa and m84, m85 and m86 showed only weak, if any transfection specific activity. This can be seen in figure 6.1. Based on this information, the antibody WoN was used for all future western analyses.

Thus far, two antibodies have been found which recognise the Wolframin protein, an antibody against the N-terminal recombinant protein and an antibody against the C-terminal peptide. However, antibodies that did not show reactivity on western blot were not ruled out for their possible recognition of the Wolframin protein in other applications and were further characterised by immunohistochemistry on pancreatic slices.

6.2 Immunohistological characterisation of antibodies

Since Wolframin mRNA is highly expressed in pancreatic islet cells (Inoue, Tanizawa et al. 1998), this tissue was used as an initial control for studying the immunohistological reactivity of these antibodies. In addition, it is not understood what causes the loss of pancreatic β-cells in Wolfram patients. Therefore, it was important to determine whether the β-cell loss is a direct defect originating in the cells themselves or caused by a secondary effect from α-cells, pancreatic polypeptide (PP) or delta cell impairment. Pancreatic slices from control mice were treated with antibody and detected using a secondary goat anti-rabbit conjugated to FITC-fluorescent dye. Immunofluorescence studies of all the antibodies made revealed four antibodies which showed a staining pattern different to the preserum: three antibodies against the N-terminal region; WoN, m82 and m84 and one against the C-terminal region, h86 (figure 6.2).

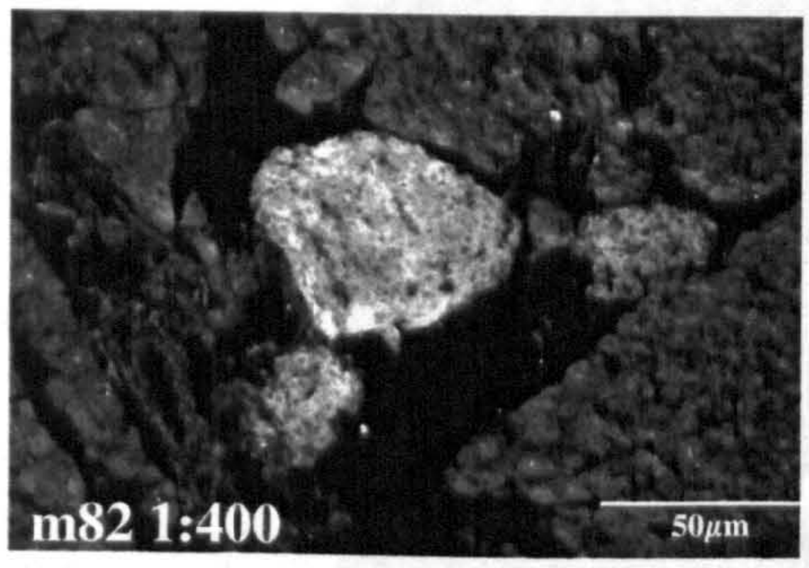
m82 1:400
50µm

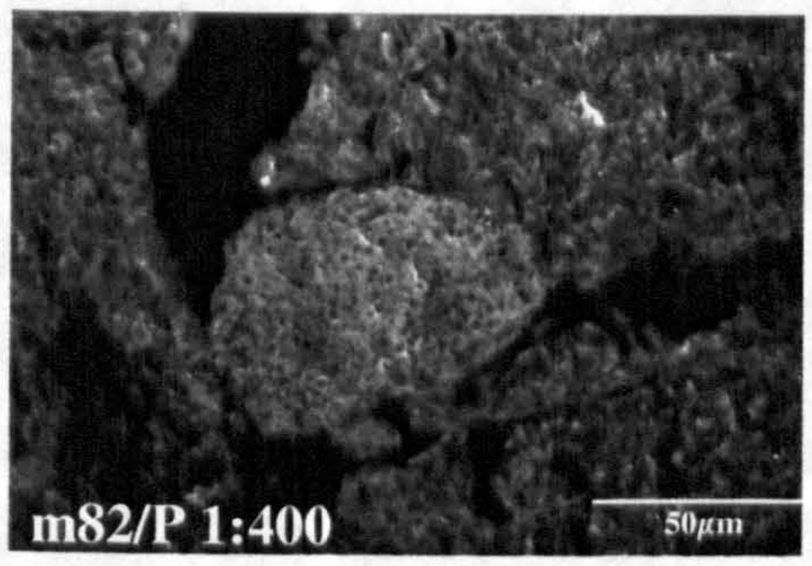
m82/P 1:400
50µm

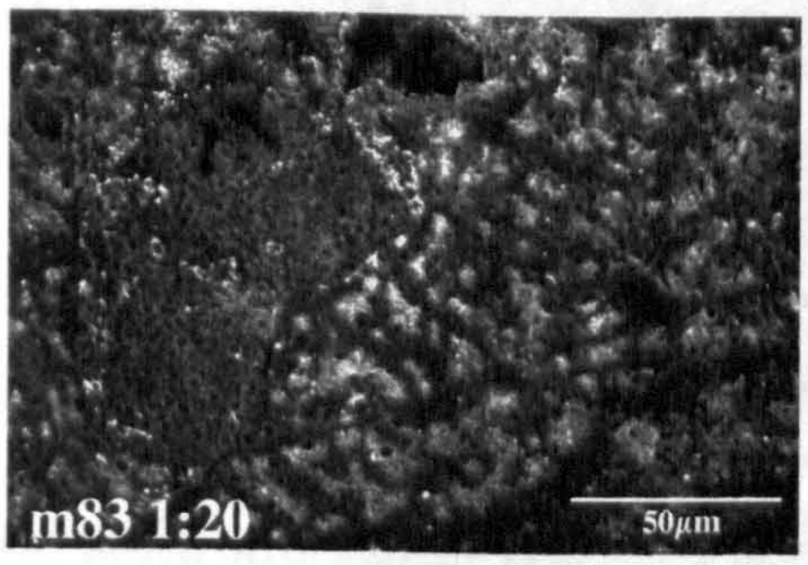
m83 1:20
50µm

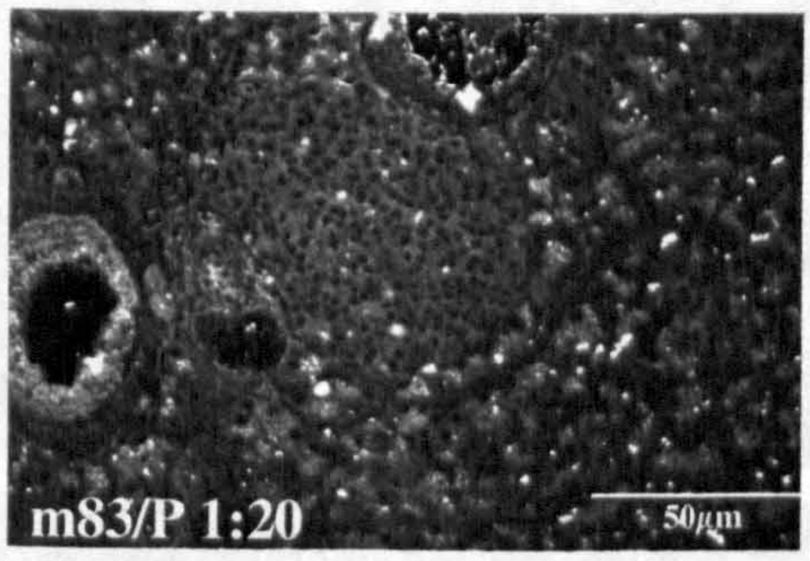
m83/P 1:20
50µm

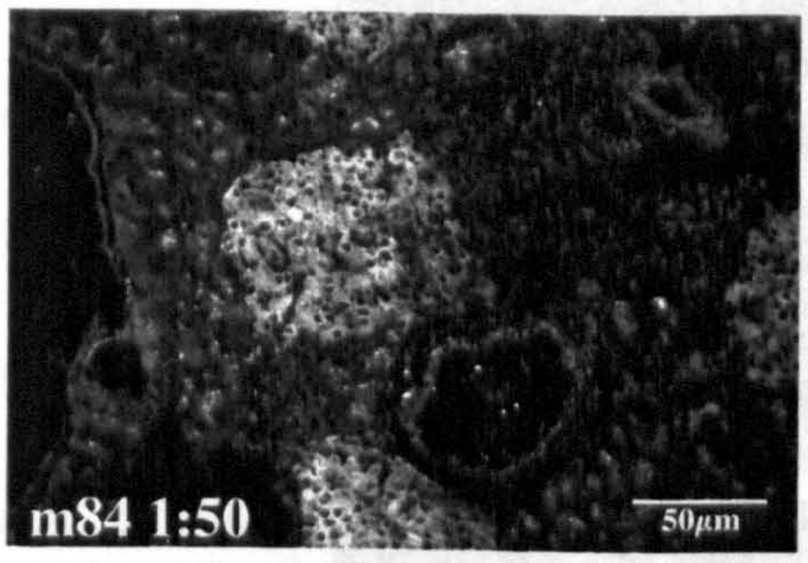
m84 1:50
50µm

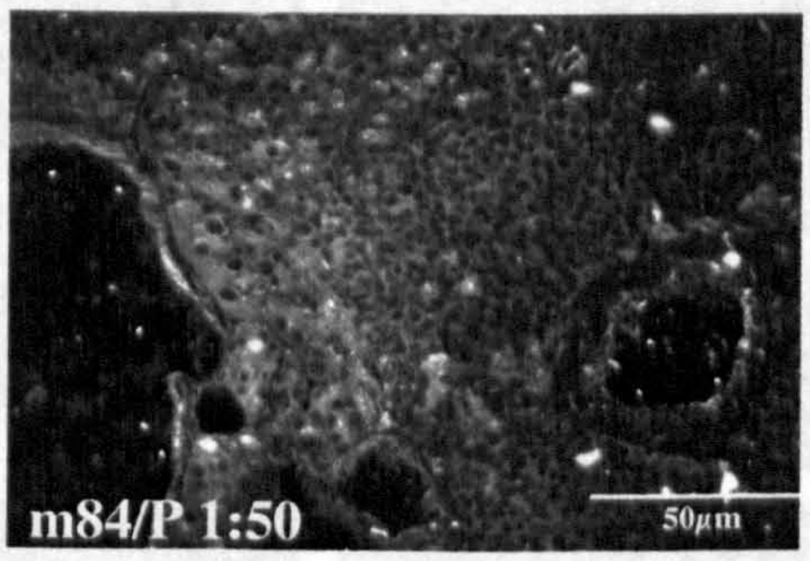
m84/P 1:50
50µm

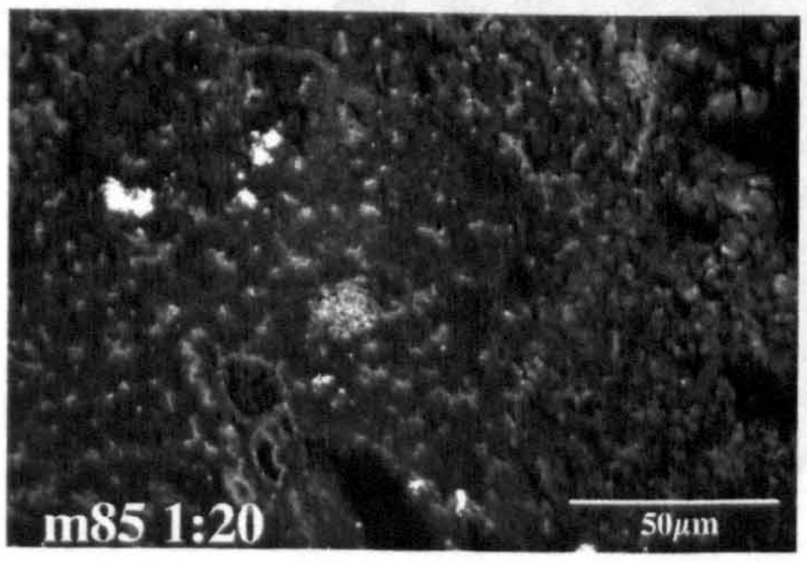
m85 1:20
50µm

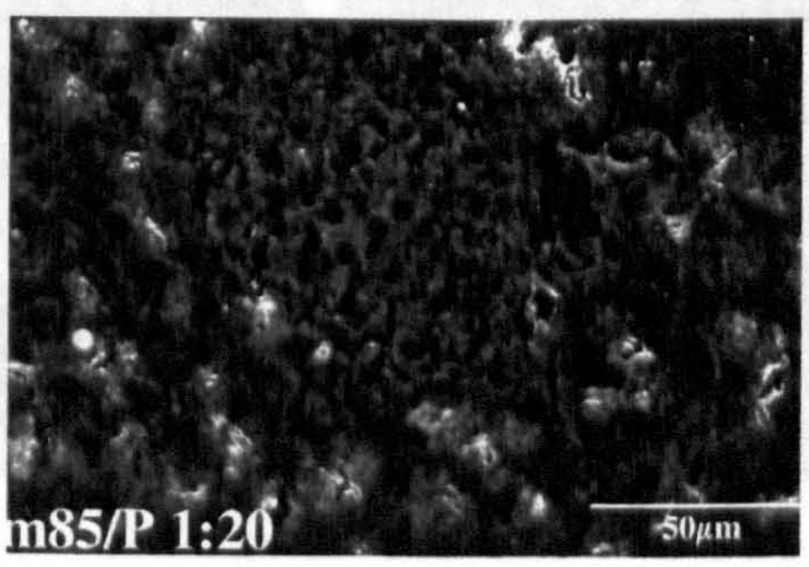
m85/P 1:20
50µm

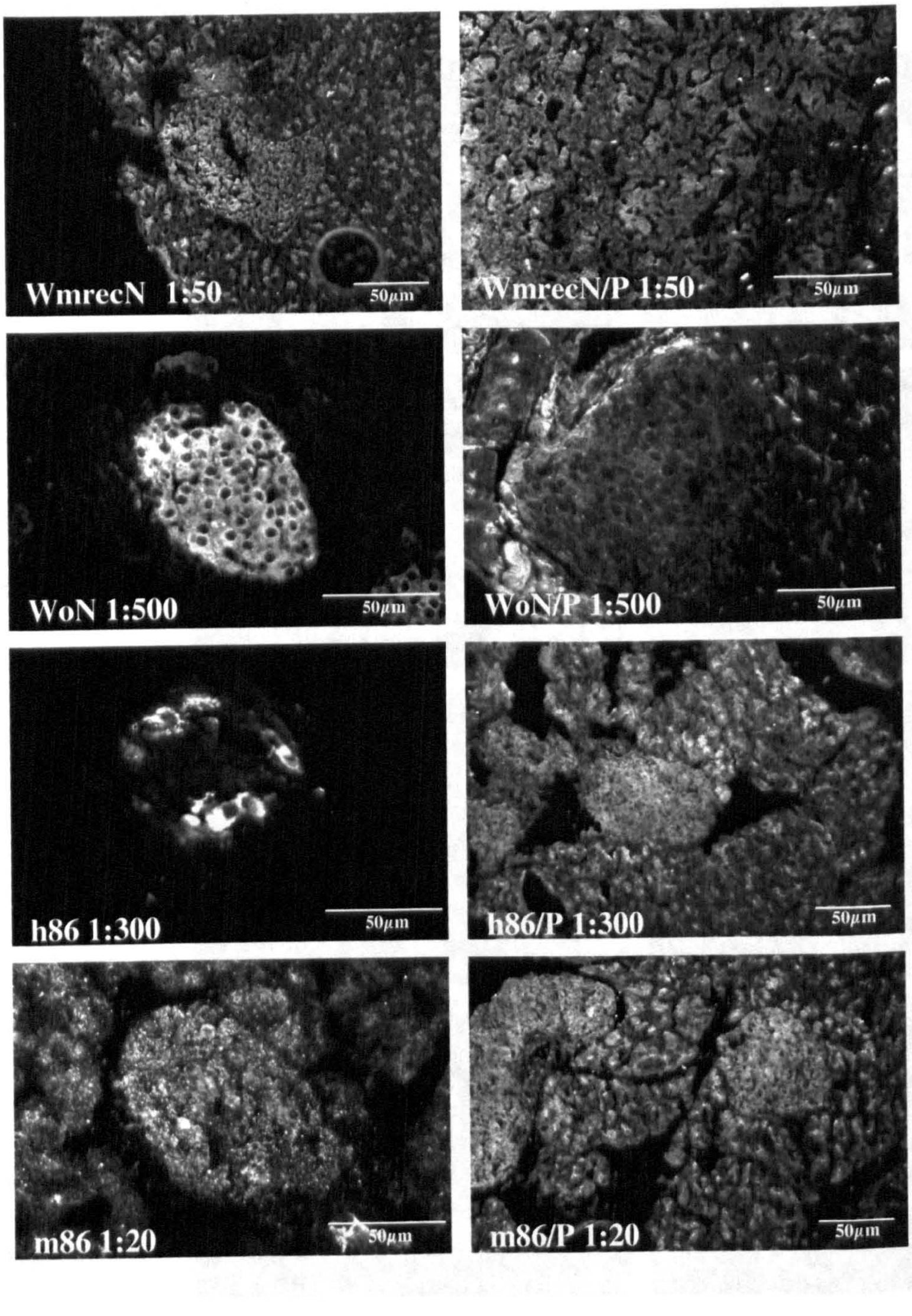

Figure 6.2 Immunofluorescence studies of all antisera produced on pancreas slices. /P refers to preserum. WoN, m82, m84 and h86 are the only antisera, which showed a difference to preserum.

WoN, m82 and m84 all showed the same pattern, although the signal from WoN was the most intense. h86 showed a strong signal that was different from the other three. In order to check the specificity of this staining, pancreas slices were stained with anti-insulin antibody as a control for β-cells and with anti-glucagon antibody for α-cells. These antibodies were detected using anti-guinea pig and anti-mouse TRITC-conjugated secondary antibodies for insulin and glucagon respectively. Superimposing images from the exact location showed that the signal from antibodies WoN, m82 and m84 over-lapped with insulin and not with glucagon. h86 showed an α-cell similar structure, but did not co-localise to glucagon (figure 6.3). Localisation to the polypeptide product or delta cells was not tested using the h86 antibody. Thus, WoN, m82 and m84 localised to the β–cells of the pancreas. However, the signal for WoN was much stronger than for m82 or m84 and the expression for m82 was stronger than for m84. The expression of Wolframin in β-cells indicates that the diabetes mellitus in Wolfram patients is likely due to a direct defect in β-cell functioning. Here again, WoN was the antibody with the strongest immune reactivity and was subsequently used for sub-cellular localisation studies and all other antibody requiring analyses.

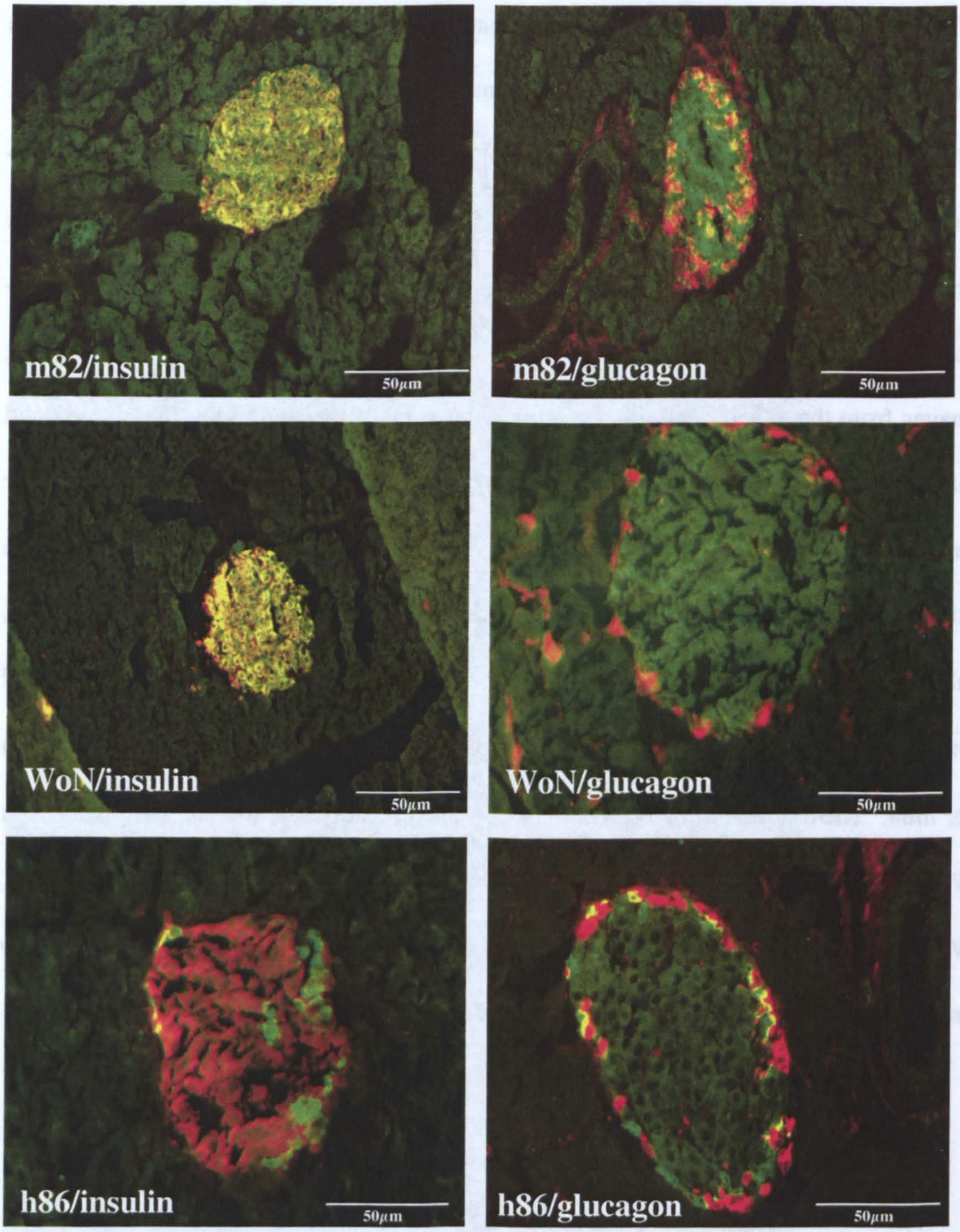

Figure 6.3 Immunofluorescence studies of Wolframin in pancreatic β-cells. Control mouse pancreata were detected with both Wolframin specific antibodies (FITC-conjugated secondary antibody) and either anti-glucagon or anti-insulin (TRITC-conjugated secondary).

6.3 Localisation to the limbic system of the brain

The neurological complications found in DIDMOAD patients are due to generalized brain atrophy (Barrett, Bundey et al. 1995). For example, the optic atrophy is caused by degeneration of the nerves leading to the eye. Therefore, it is probable that the protein is expressed in areas responsible for the various neurological symptoms. To observe localisation in the brain, 5μm thick sagittal slices from a mouse brain were incubated with the WoN antibody at a dilution of 1:500 and detected using a secondary goat anti-rabbit conjugated to FITC (figure 6.4).

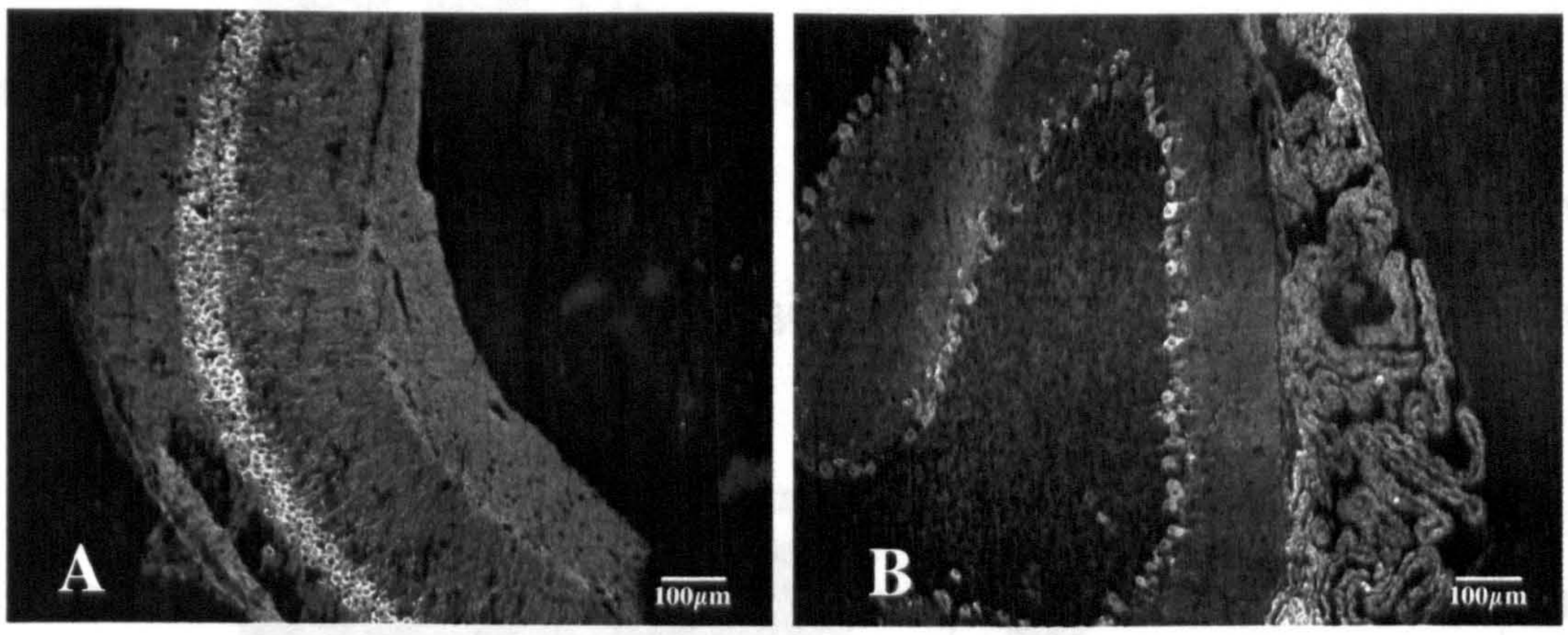

Figure 6.4 Immunofluorescence studies of the expression of Wolframin in sagittal mouse brain slices. Strong signal can be seen in the CA1 region pyramidal cells of Ammon's horn in the hippocampus (A) and in the purkinje cells of the cerebellar cortex (B).

Localisation in the brain was found in the CA1 region of the pyramidal cells of the Ammon's horn in the hippocampus. Strong expression was seen in the ependymal layer and in individual brain nerve nuclei and neuronal groups from the forebrain. Purkinje cells of the cerebellar cortex were the only cells stained in this area. The hippocampus and cerebellar cortex both belong to the limbic system and are responsible for emotion, behaviour, anxiety and/or panic including depression. These findings suggest a function for the Wolframin protein in the control of emotion and

behaviour and are in accordance with the fact that WS patients and even heterozygous individuals are susceptible to psychiatric illness (Swift, Polymeropoulos et al. 1998). Therefore, destruction of the Wolframin protein could lead to abnormal psychiatric functioning in these patients by directly disturbing interactions in the limbic system of the brain.

Chapter 7. Test of WoN on various tissues, cell lines and fibroblast cells from controls and our patients

After discovering that Wolframin protein expression was found in the β-cells of the pancreas, expression of isolated islet cells and exocrine tissue from control mouse pancreas was investigated on western blot (figure 7.1).

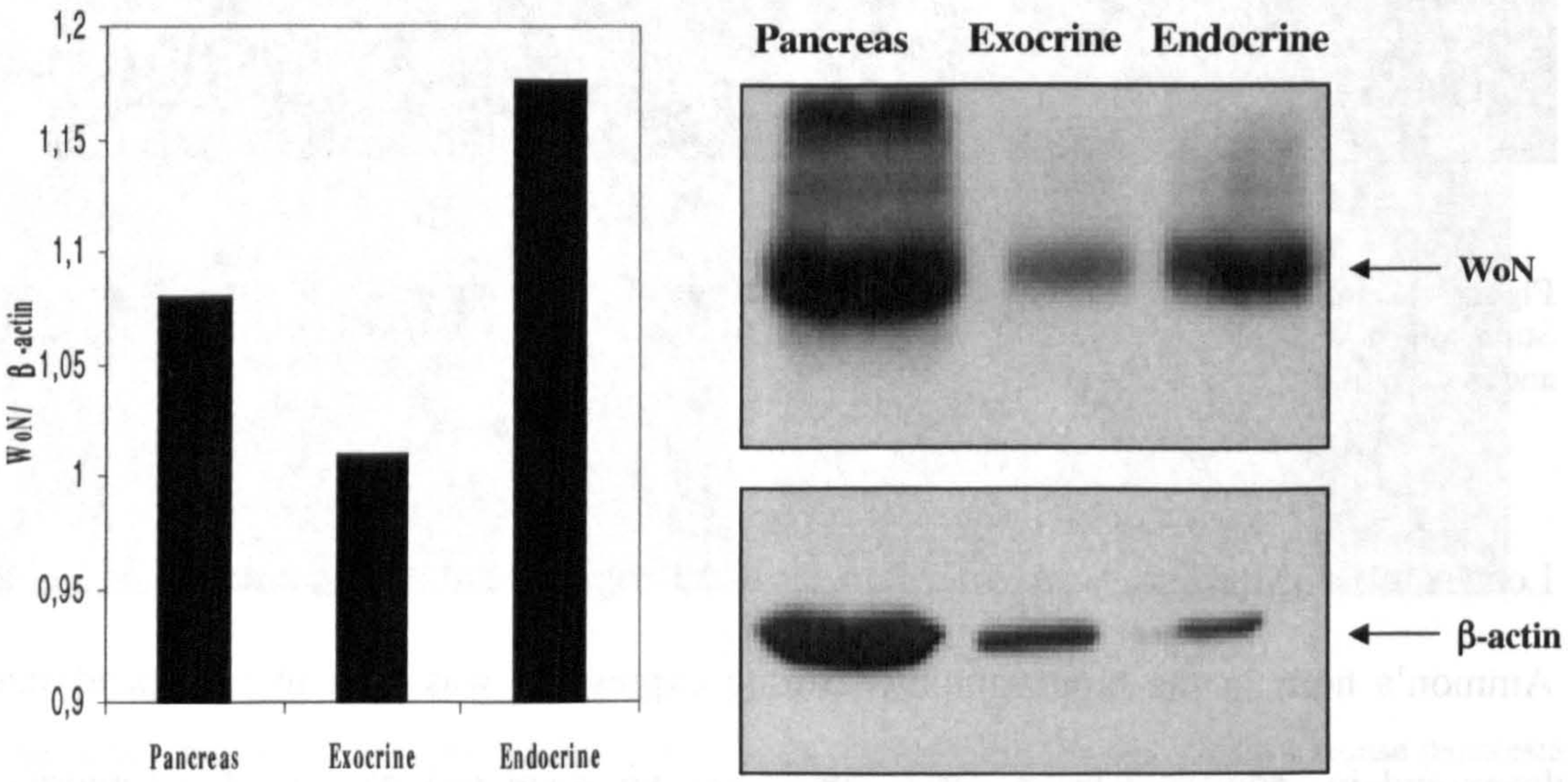

Figure 7.1 Expression of Wolframin in Pancreas homogenate and endocrine and exocrine fractions. High expression can be seen in the endocrine fraction as compared to pancreas homogenate and the exocrine fraction. Normalisation of band intensities was done using the AIDA program.

Dr. Schremmer-Danninger (Institute for Diabetes Research) provided the endocrine and exocrine fractions for this analysis. A much higher expression level in endocrine pancreas than in exocrine pancreas was seen. However, it was surprising that there was expression at all in exocrine fractions. It could be possible that the exocrine fractions are slightly contaminated with endocrine tissue.

The cell lines tested were two β-cells lines: βTC-tet and R7T1 and an α-cell line: In-R1-G9 (figure 7.2).

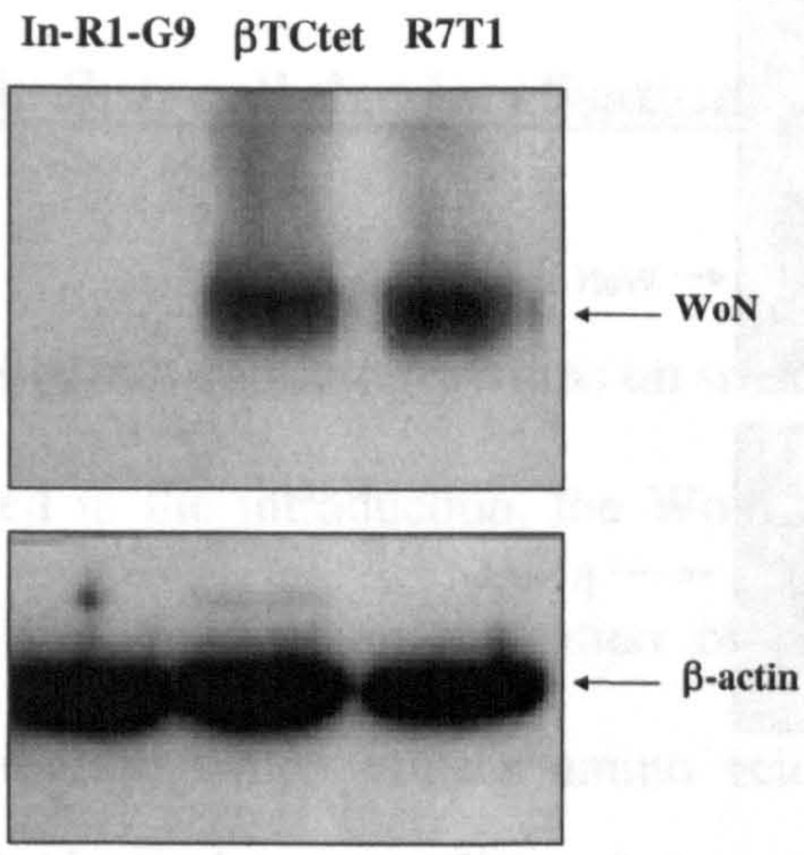

Figure 7.2 Expression of Wolframin in cell lines. 50 μg of total protein homogenates from either In-R1-G9, βTC-tet or R7T1 cell lines were loaded onto a 10% SDS-PAGE gel and detected with WoN. A very weak band could be seen with longer exposures in the lane 1.

βTC-tet cells come from a non-clonal cell line derived from a male mouse insulinoma of transgenic background expressing the SV40T antigen oncoprotein in pancreatic β-cells under control of the bacterial tetracycline repressor/operator system (Efrat, Fusco-DeMane et al. 1995). These cells use the tet-off approach, in which cells proliferate in the absence of tet ligands and undergo growth arrest in their presence. R7T1, on the other hand, utilises the tet-on regulatory system, in which cells divide in the presence of ligands and undergo growth arrest in their absence. This cell line is derived from

insulinomas from transgenic mice treated with the tetracycline derivative, doxycycline (dox) (Milo-Landesman, Surana et al. 2001). The R7T1 cell line is advantageous for in vivo experiments and transplantation because no ligand is needed for long-term maintenance of growth arrest in vivo. The α-cell cell line, In-R1-G9, comes from the hamster insulinoma cell line, In-111-R1, and produces glucagon (Takaki, Ono et al. 1986). This analysis revealed high expression in islet cells and both β-cell lines and a low expression in the α-cell line.

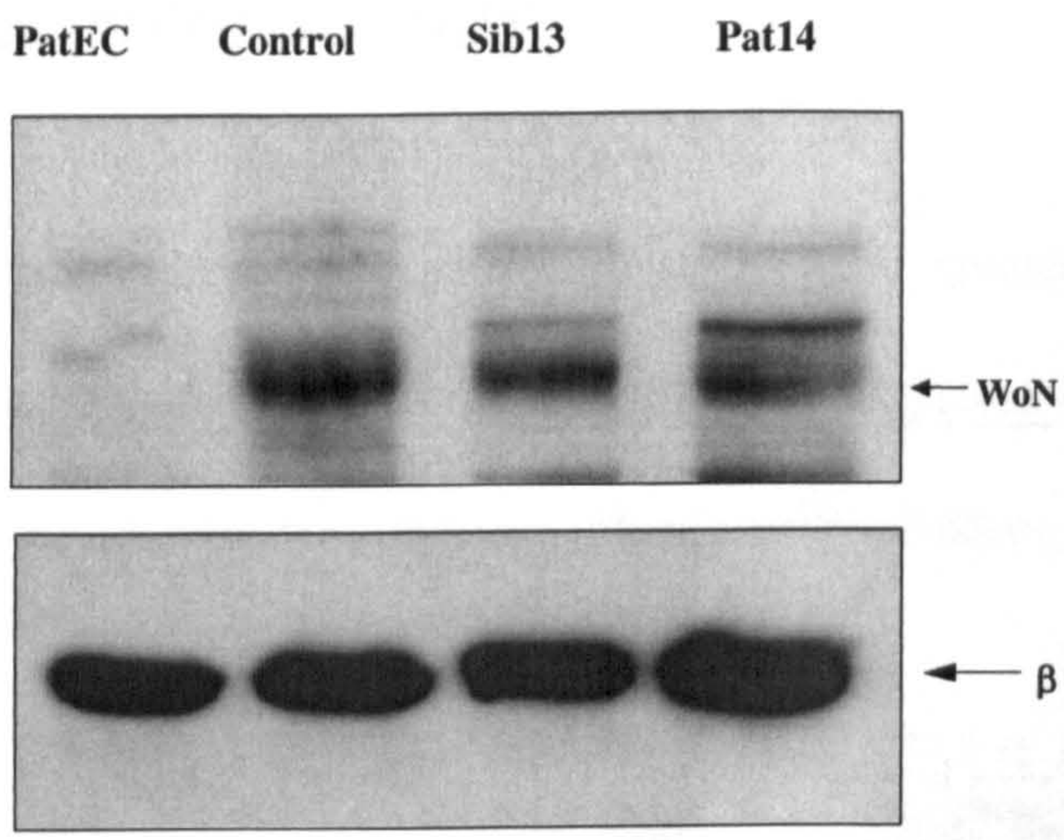

Figure 7.3 Expression of Wolframin in fibroblast cells from WS patients and control individuals. 50μg total protein homogenate was loaded from PatEC, Control, Sib13 and Pat14.

Moderate expression was seen in fibroblast cells from healthy individuals and Sib13 (figure 7.3). Pat14 showed a slightly lower level of expression as Sib13, indicating that protein is produced in this patient. Since this patient contains a nonsense mutation leading to an early truncation on one allele and a missense mutation on the other allele, production of the full-length protein is possible. These mutations on both alleles could cause the phenotype seen in this patient by not allowing the protein to appropriately interact or complete its normal functions. This analysis does not give any insight into how much function is retained in the produced protein. It is possible, for example, that

this protein cannot be properly folded or is not able to react with other proteins as it otherwise would. PatEC showed no band at 100 kDa, as was expected from the mutational analysis. This patient contains an insert resulting in a severely truncated protein on both alleles and should not be able to produce the full-length protein. In addition, the N-terminal specific antibody, WoN, did not detect a lower molecular weight band that could result from the truncated protein. Therefore, the truncated version of the Wolframin protein in PatEC is most likely not stable enough for detection.

Chapter 8. Sub-cellular localisation

8.1 Analysis of sub-cellular fractions on western blot

As mentioned in the introduction, the Wolframin gene contains no signal sequence recognition sites to give an indication of sub-cellular localisation. PSORT is a computer program which utilises amino acid sequences to determine where such proteins will most likely localise (Nakai and Horton 1999). The amino acid sequence encoded by Wolframin predicts an integral transmembrane protein with 65% probability for localisation to the plasma membrane, 26% to the endoplasmic reticulum and 4% to the mitochondria. The symptoms seen in the Wolfram syndrome are similar to many known mitochondrial disorders, as discussed in the introduction. It was therefore hypothesised that despite the structure predictions, this protein could localise to the mitochondria. Determining the sub-cellular localisation of a novel protein is essential to ascertaining its function and provides a starting point for further analysis. In order to check this, both western blot and immunofluorescence techniques were used. Mouse brain was used to extract cell fractions for western blot analysis. Nuclear

(N), mitochondrial (Mit), microsomal (Mic) and cytosolic (Cyt) fractions were collected (figure 8.1). Anti-protein disulfide isomerase (α-PDI) was used as an ER marker and anti-translocon inner membrane protein complex 23 (α-Tim23) as a mitochondrial marker to check these fractions for purity. PDI sits on the lumen of the ER and is involved in protein folding. Calnexin, an ER membrane localised protein was also used to check individual fractions, however, this protein has approximately the same molecular weight as the Wolframin protein and could be not used for double staining. Calnexin showed ER staining in the same fractions as PDI (data not shown). Tim23 is a mitochondrial protein complex, which mediates the translocation of proteins into the mitochondrial matrix and is located on the inner membrane of the mitochondria. Surprisingly, Wolframin co-localised exclusively to the ER-containing microsomal fraction and not to the mitochondria as was previously suspected based on the disease phenotype.

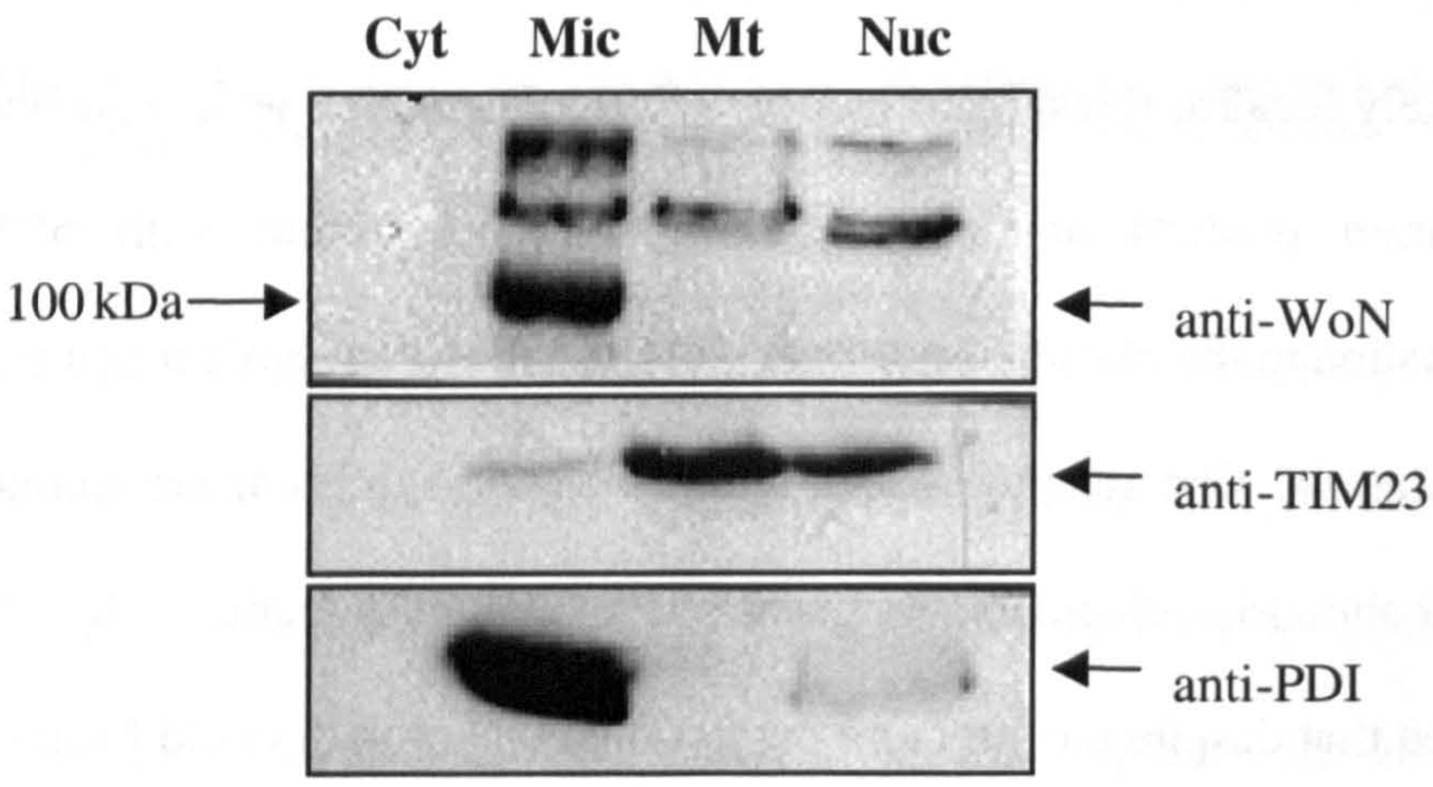

Figure 8.1 Localisation of the Wolframin protein in cell fraction extracts. Whole mouse brains were homogenised and fractionated into nuclear (Nuc), mitochondrial (Mit), microsomal (Mic) and cytostolic (Cyt) fractions. 50μg of each protein was loaded and detected using either anti-WoN (1:200), anti-TIM23 (1:500) or anti-PDI (1:1000). The WoN antibody recognised a 100 kDa band for the Wolframin protein in the ER enriched fraction.

8.2 Sub- cellular localisation on cell lines

Fibroblasts, which were shown in figure 7.3 to express the Wolframin protein, were tested for immunofluorescence studies. Cells were grown overnight on chamber slides and incubated on the next day with various antibodies and again detected with FITC or TRITC conjugated secondary antibodies depending on the host animal of the primary antibody. In contrast to immunohistochemical studies on tissue slices, the expression in fibroblast cells from control individuals was too weak to see a significant signal (figure 8.2). There was hardly a difference between preserum and WoN. Myoblast cells (obtained from Dr. Sabine Hofmann), which showed a slightly higher protein expression on western blots as fibroblasts also showed no distinct difference between preserum and WoN. Therefore, immunofluorescence was tested with βTC-tet cells, since they show a very high expression on western blot. These cells showed a definite difference between preserum and WoN and the intracellular distribution appeared to be very similar to that of α-PDI. However, due to their size and the fact that they grow in clumps, even in a differentiated state, distinct intracellular structure could not be properly observed (figure 8.2). Finally, Cos-7 cells were transfected with Wolframin using pIRES vector under regulation of the CMV promoter with Lipofectamine (Gibco). This showed a much stronger signal, which differed greatly in its structure from preserum (figure 8.2). In order to determine its localisation, antibodies to the ER (anti-PDI), mitochondria (Mitotracker red) and golgi (anti-58k protein) were observed on transfected Cos-7 (figure 8.3). The WoN staining pattern was very similar to cells stained with ER antibodies and not similar to golgi or mitochondrial structures. WoN was then co-localised with anti-PDI, Mitotracker Red and anti-58k (figure 8.4). Superimposing the green images of WoN with the red images of organelle-specific

antibodies showed virtually identical overlap with PDI and only partial overlap with anti-58k, as indicated by the yellow colour.

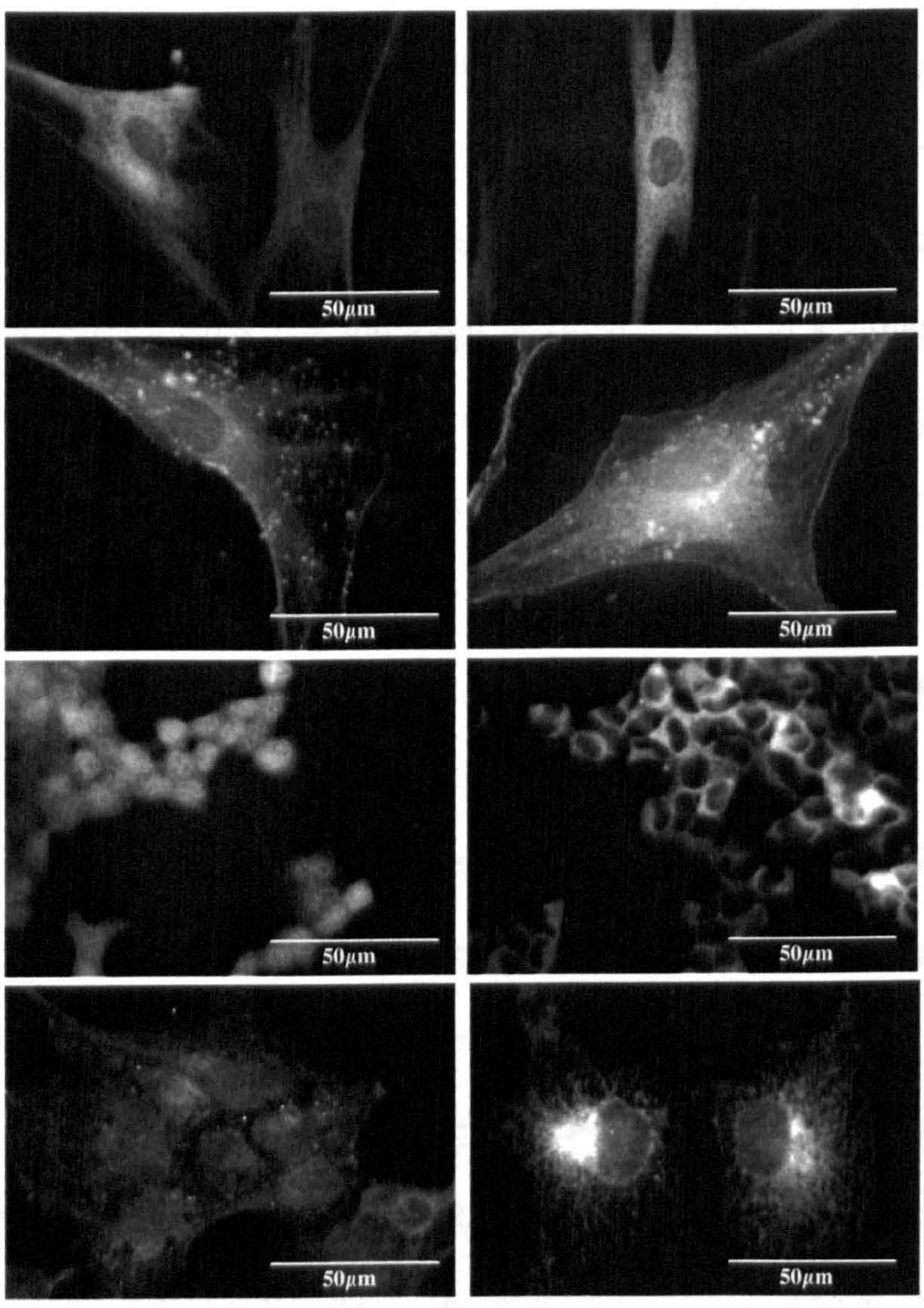

Figure 8.2 Expression of Wolframin in various cell lines. Cells were incubated with either rabbit preserum (1:50) or anti-WoN (1:50) serum decorated with FITC conjugated anti-rabbit second antibody.

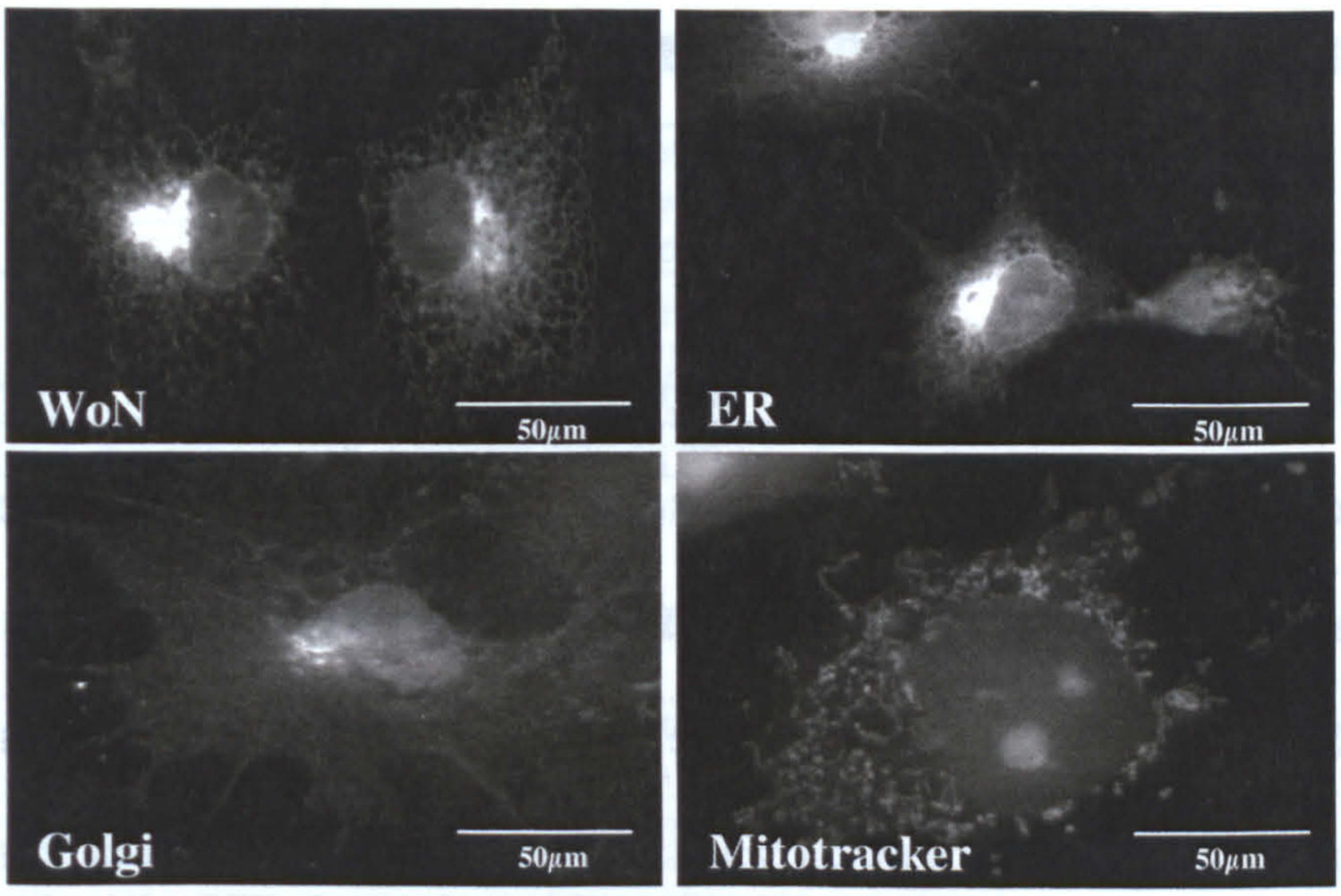

Figure 8.3 Immunofluorescence of various antibodies on Cos-7 cells transfected with the Wolframin cDNA.

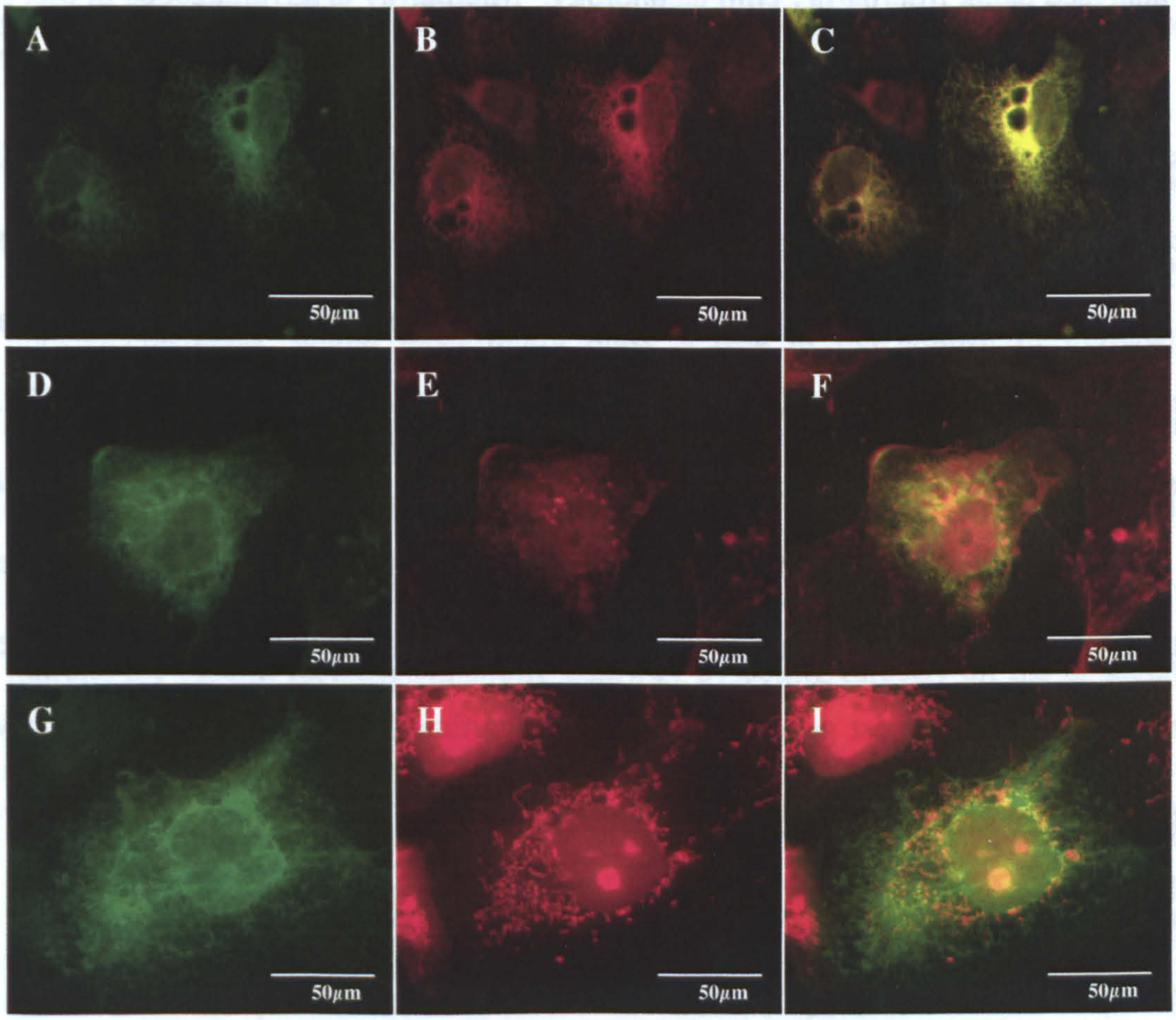

Figure 8.4 Co-localization of Wolframin in transfected Cos-7 cells. Cos-7 cells were transfected withWolframin cDNA vector and incubated with WoN antibody (1:50) (A, D, G). The same cells were incubated with either (B) anti-PDI for the ER, (E) anti-Golgi 58k for the Golgi or (H) mitotracker for the mitochondria. Overlaying these signals (C, F and I) shows overlap between the green WoN and the red anti-PDI (ER), a slight overlap can be seen with the red anti-Golgi 58k and no overlap is seen with the red mitotracker.

Chapter 9. Functional analysis of Wolfram syndrome patient cells

9.1 Microarray

After determining that Wolframin is expressed in fibroblast cells, it was decided to use these cells or cell extracts for various functional tests. An attempt was made to determine what other genes could possibly be affected by a malfunction in the Wolframin gene. Such information was desirable as a starting point for further functional analyses since at this point no data was known about the function of this protein. The effects of the Wolframin gene defect on the expression of other genes was analysed using Microarray chip technology. Microarray is advantageous in that it can quantitatively analyse expression levels of many thousands of genes in parallel. This method can identify genes involved in many diseases and developmental processes. For this purpose, poly A^+ RNA was isolated and 600 ng at 50 ng/μl was sent to Incyte Genomics for analysis. Poly A^+ RNA from Sib13 was labelled in a reverse transcription reaction with Cye3-dUTP and Pat14 labelled with Cye5-dUTP. These samples were used to probe the human UniGEMV2.0 microarray chip, which at this point contained approximately 10,000 genes per analysis. Comparing first-grade relatives lowers the possibility of differences due to altered genetic backgrounds. The expression pattern of most genes did not differ significantly from one another. Only very few genes appeared to be differentially expressed by a factor of 1.8 or more. Table 9.1 shows a list of the genes with the largest differences between siblings.

Genes with lower expression in Pat14 cells

-3.8	ectonucleotide pyrophosphatase/phosphodiesterase (PC-1 plasma cell membrane glycoprotein)
-2.5	glioma pathogenesis-related protein (RtP)
-2.0	desmoplakin (DPI,DPII)
-2.0	microtubule-associated protein 1B
-1.9	Homo sapiens cDNA FLJ11245 fis, clone
-1.9	HIV-1 reverse binding protein 2

Genes with higher expression in Pat14 cells

2.1	EGF-containing fibulin-like extracellular matrix protein 1 (Fibulin 3)
2.0	ferritin, heavy polypeptide 1
2.0	zinc finger protein 238
1.9	collagen, type VIII, alpha 1
1.8	cysteine-rich protein 1 (intestinal)
1.8	microseminoprotein, beta

Table 9.1 List of genes found to up and down regulated after microarray analysis comparing poly A+ RNA from fibroblast cells from Pat14 and Sib13.

Interesting to note is the 3.8 times down regulated expression of the human plasma membrane glycoprotein, PC-1. PC-1 is an ecto-nucleotide pyrophosphatase/ phosphodiesterase, which most likely plays a role in the control of extracellular pyrophosphate, insulin signalling and in the calcification of bone and cartilage (Okawa, Nakamura et al. 1998; Johnson, Vaingankar et al. 1999). Knocking out the PC-1 gene in mice causes calcification in and around joints and ligaments. This gene inhibits the insulin receptor signalling pathway by acting directly on the α-subunit of the insulin receptor (IR) (Maddux and Goldfine 2000). In cells, including skin fibroblasts from insulin resistant Type 2 diabetics, as well as in those from non-obese, insulin resistant, non-diabetic subjects, the phosphatase expression is significantly higher (Maddux, Sbraccia et al. 1995). This is exactly opposite in fibroblast cells from WS patients. In these fibroblast cells, PC-1 mRNA expression is lower than in control persons. This is not too surprising, since the diabetes in DIDMOAD patients is not based on insulin resistance as in Type 2 diabetes, but is due to a selective loss of β-

cells. It appears however interesting, that a gene which is over-expressed in Type 2 diabetics is down regulated in DIDMOAD patient cells.

Of the genes up regulated in DIDMOAD fibroblasts, EFEMP1 (epidermal growth factor-containing fibrillin-like extracellular matrix protein 1 or fibulin 3) was the most interesting. EFEMP1 is a widely expressed extracellular matrix protein of unknown function. It has been shown to be over-expressed in senescence cells from Werner patients and can be induced by serum-deprivation of young cells (Lecka-Czernik, Lumpkin et al. 1995). The fact that EFEMP1 is over-expressed in cells from both Wolframin and Werner patients led to a later experiment testing our cells for their sensitivity to γ– radiation and apoptotic induction. In addition, a single mutation, R345W, in the EFEMP1 gene causes the disease, Malattia Levantinase (ML) or Doyne honeycomb retinal dystrophy (Katsanis, Venable et al. 2000). This is an autosomal dominant disease characterised by the build-up of drusen (sub-retinal pigment epithelium deposits), geographical atrophy, decreased visual acuity and blindness. These drusen accumulations are due to misfolding of the mutated EFEMP1 protein (Marmorstein, Munier et al. 2002). Considering the fact that optical atrophy is a requirement for WS, it might be possible that a defect in Wolframin could indirectly cause changes in EFEMP1 that in turn cause optical atrophy and blindness.

EFEMP1 protein expression clearly shows a stronger signal in Pat14 fibroblast cell homogenate than in Sib13, as can be seen in figure 9.1. This protein expression difference is in accordance with microarray results.

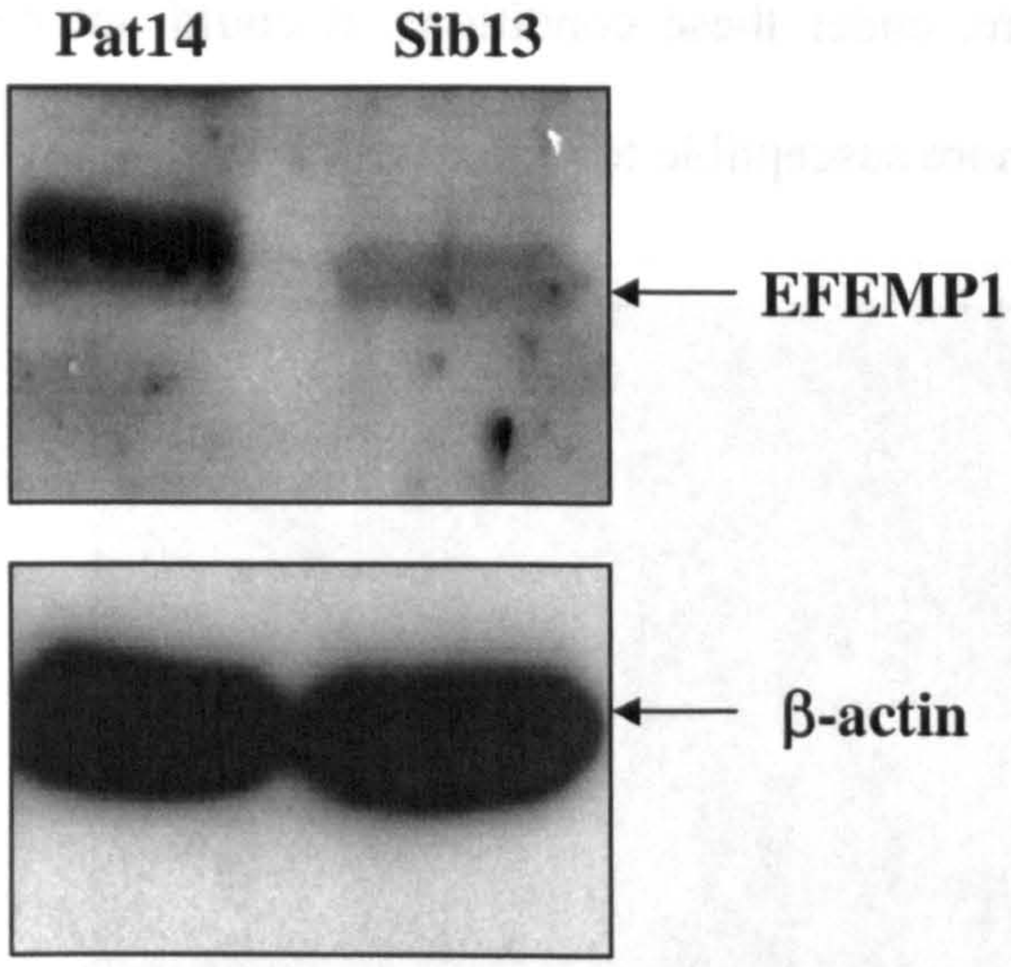

Figure 9.1 Western analysis of the EFEMP1 antibody on fibroblast cell extracts from Pat14 and Sib13. EFEMP1 showed a stronger expression in Pat14 cells then in Sib13 cells.

9.2 Susceptibility to X-ray radiation

According to Microarray analysis, EFEMP1 is over-expressed in fibroblasts lacking functional Wolframin. An over-expression of EFEMP1 has also been reported for senescent cells and cells from Werner Syndrome patients (Lecka-Czernik, Lumpkin et al. 1995). Therefore, two senescence markers, growth rate and sensitivity to radiation, were compared between cells from Pat14 and Sib13 (figure 9.2). 10.000 cells were plated per well of 24-well dishes. Two hours following plating, the cells were irradiated with either 1 Gray or 5 Gray using a Co-Gamma source (9,76 Gray/min) or mock treated. At the times indicated, all cells of a single 24 well were thoroughly trypsinised and the total cell number (not discriminating potentially dead or apoptotic cells) were determined by Coulter counting (Coulter Electronics/Beckmann). During the time-course examined, non-irradiated control cells were not reaching cell numbers that lead to density inhibition, as was evident from the respective growth curves. As seen in figure 9.2, both treated and untreated cells showed no significant differences

with regard to their genotypes. Therefore, under these conditions, it could not be proven that Wolframin deficient cells are more susceptible to radiation.

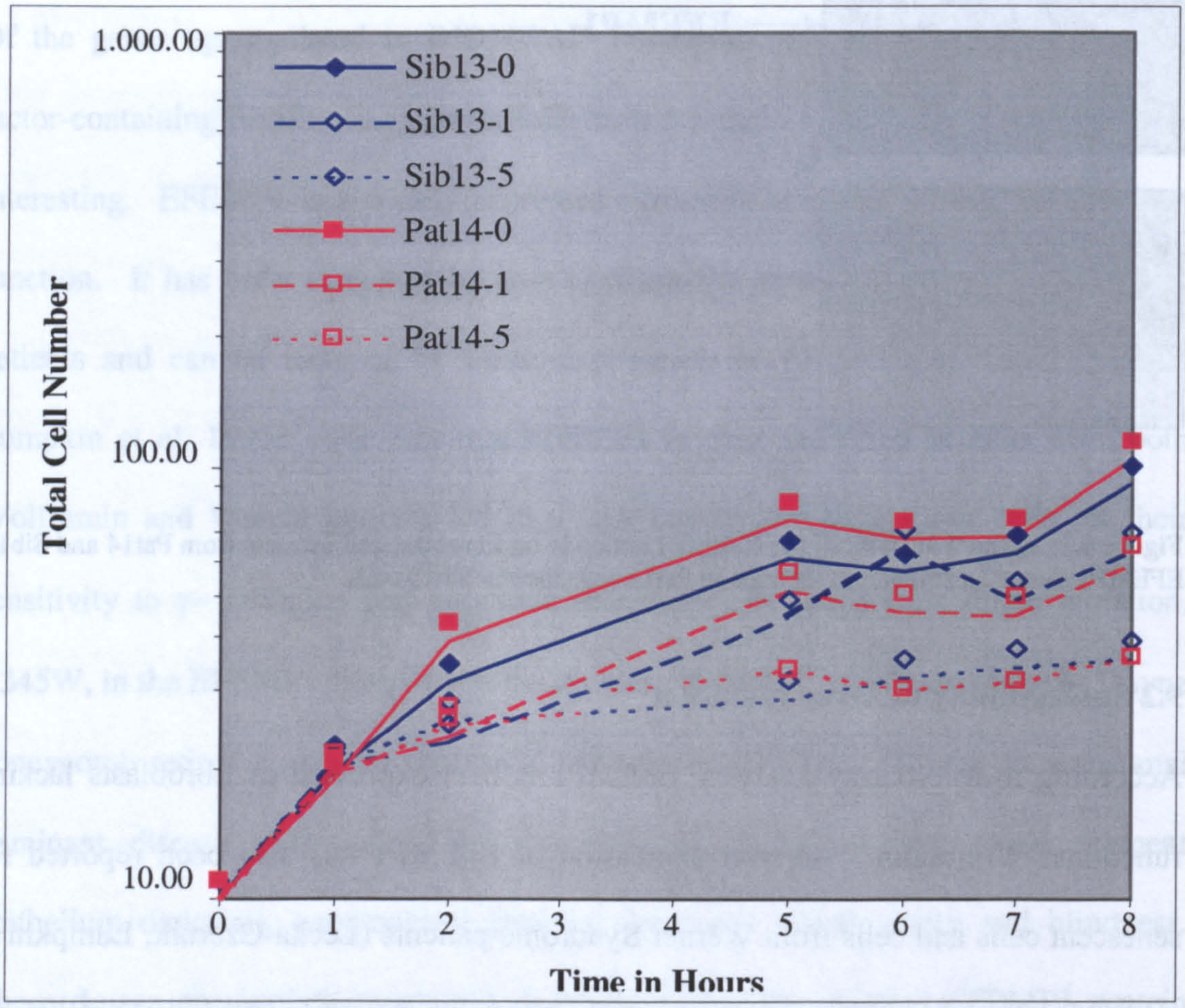

Figure 9.2 Radiation sensitivity test to determine if fibroblast cells from Wolfram syndrome patients are more susceptible to senescence. -0 = 0 Gray, -1 = 1 Gray and -5 = 5 Gray used for radiation.

9.3 Apoptosis

The atrophy of selective neurons in the brain and the loss of β-cells in the pancreas in WS patients gave an indication that these cells or tissues are more sensitive to apoptosis. For this reason, it was hypothesised that fibroblast cells from our patients could be more susceptible to induced cell death. Therefore, a staurosporine induced apoptosis assay was used to examine the difference between healthy and diseased cells (figure 9.3).

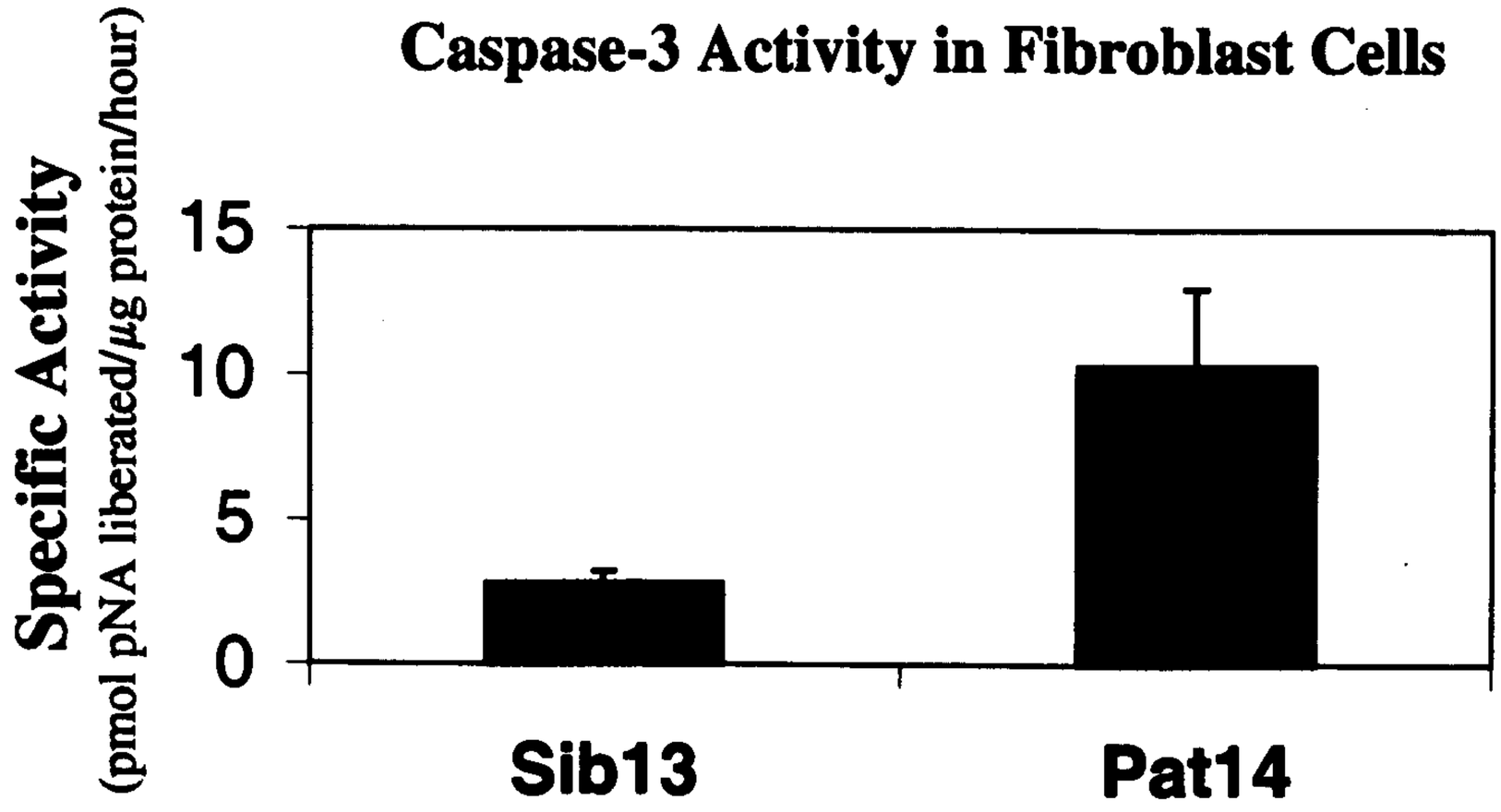

Figure 9.3 Specific activity of caspase-3 in Sib13 and Pat 14 fibroblast cells. Fibroblast cells were induced for apoptosis with staurosporine alone or staurosporine and apoptosis inhibitor for 6 hours and specific activity calculated. Pat14 is 3.8 times more susceptible to staurosporine-induced apoptosis than Sib13.

Staurosporin inhibits protein kinase C (PKC) by interaction with the catalytic domain close to the ATP-binding site (Nakano, Kobayashi et al. 1987). Pat14 and Sib13 cells were seeded onto 6-Well plates, grown overnight and staurosporine was subsequently added at a concentration of 0.5μM for 6 hours. The cells were then trypsinised and lysed in cell lysis buffer from the CaspACE assay system, colorimetric kit (Promega). The activity of caspase-3 was measured after induction for apoptosis with staurosporine, a common induction route for programmed cell death. Caspase-3 is a member of the cysteine aspartic acid specific protease family involved early on in the apoptotic process as a main effector caspase. It cleaves on the aspartate residue of the sequence Asp-Glu-Val-Asp (DEVD) (Gurtu, Kain et al. 1997). In this assay, the substrate, Ac-DEVD-pNa is added to equal concentrations of protein lysate on a 96-Well plate. p-Nitroaniline (pNa) is a chromophore, which produces a yellow colour

after caspase-3 has cleaved Ac-DEVD-pNa and released free pNa. This colour can be read at 405 nm and samples compared with one another. Calculation of the specific activity of caspase-3, taking into consideration natural cell death by inhibition with the caspase inhibitor, Z-VAD-FMK, was recorded as pmol pNa liberated per hour per μg protein. This revealed 3.8 times more caspase-3 activity for Pat14 as for Sib13. Therefore, Wolframin patient fibroblast cells are more susceptible to stauroporine-induced apoptosis.

9.4 Glycosylation

The Wolframin gene product is an N-glycosylated ER membrane protein. It could be possible that the symptoms in DIDMOAD are due to a defect of glycosylation. For example, features of congenital disorders of glycosylation (CDG) include atrophy and polyneuropathy (Freeze 2001). Therefore, general glycosylation patterns in Wolframin deficient fibroblast cells were tested. For this experiment, serum from PatEC and one parent were obtained. Transferrin glycosylation is a commonly used marker for such disruption. The transferrin receptor is highly expressed in all non-eurythroid cells. In fact, on the surface of proliferating cells, 10,000 to 100,000 molecules per cell are expressed (Chitambar, Massey et al. 1983; Gatter, Brown et al. 1983), thereby making this a good indicator of general glycosylation. Improper glycosylation of the transferrin receptor confers inability to bind transferrin, which results in an inability to deliver iron to tissues. Normal human transferrin can be found in several isoforms depending on differences in glycosylation (de Jong and van Eijk 1988). These transferrin isoforms can be characterized by the number of sialic acid residues present (de Jong, van Dijk et al. 1990). Dr. Klaus Gempel (Institute for Clinical Chemistry,

Munich, Germany) performed capillary electrophoresis analysis to determine the levels of transferrin isoforms.

However, as can be seen in figure 9.4, the various transferrin glycosylation levels are the same in patient and control sera. Therefore, the defects seen in DIDMOAD are most likely not due to improper glycosylation.

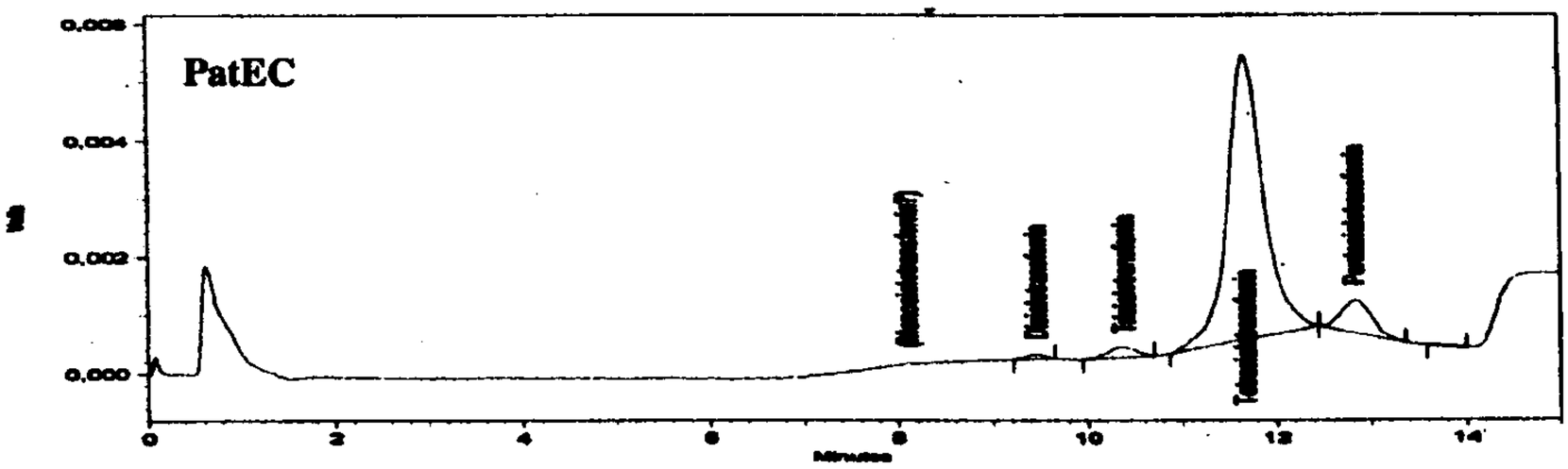

Detector A (460nm) Name	Retention Time	Height Percent	Area Percent
Monosialotransferrin?	9.467	1.35	0.74
Disialotransferrin	10.392	2.96	2.49
Trisialotransferrin	11.675	85.59	87.80
Tetrasialotransferrin	12.825	9.75	8.75
Pentasialotransferrin	13.650	0.35	0.22

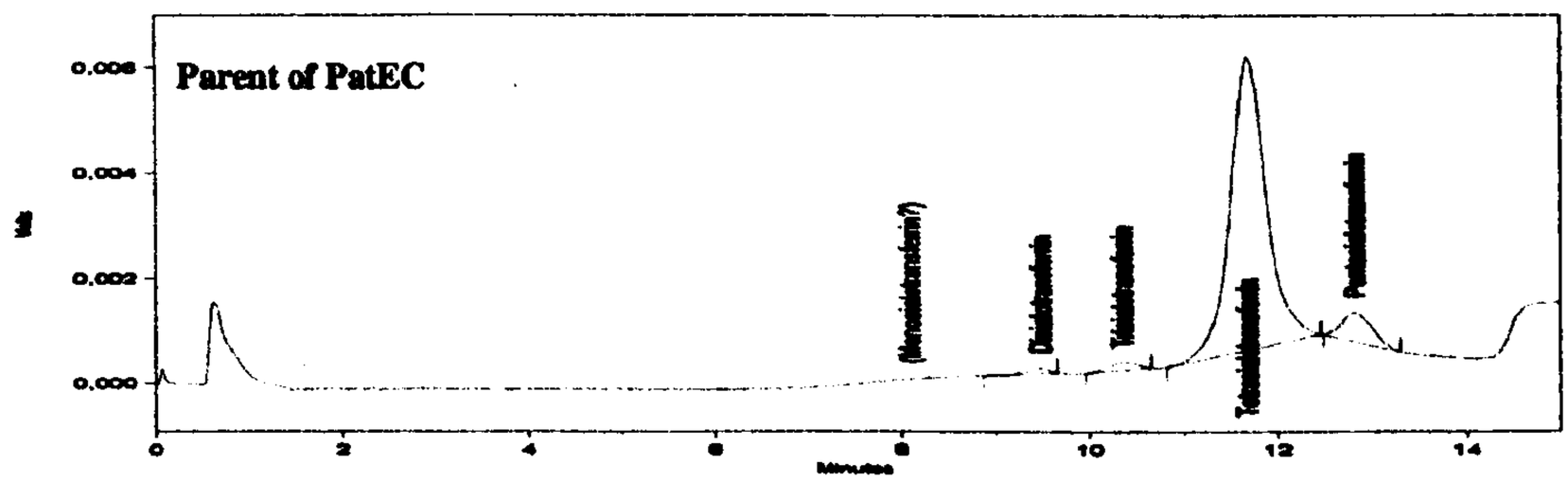

Detector A (460nm) Name	Retention Time	Height Percent	Area Percent
Monosialotransferrin?	9.492	1.54	0.98
Disialotransferrin	10.350	2.50	2.01
Trisialotransferrin	11.683	87.25	89.42
Tetrasialotransferrin	12.825	8.71	7.59
Pentasialotransferrin			

Figure 9.4 Capillary electrophoresis experiment to determine transferrin glycosylation in PatEC and a parent of PatEC. No difference was seen in levels of transferrin isoforms between these two samples.

Chapter 10. Wolframin knock-out mouse

DIDMOAD is a very rare disease and material to study is difficult to obtain. In addition, not all WS patients contain mutations resulting in a complete loss of functional protein. For these reasons, a knock-out mouse construct was planned. Sequence analysis has shown no yeast homologue and no known natural mutant mice have been found to exist. Strom et al. (1999) showed that the mouse homologue of Wolframin is 83% identical to the human variant. Therefore, in order to investigate the ramification of a complete loss-of-function of the Wolframin gene in various tissues, a knock-out mouse model was planned that would render the last exon, exon 8, non-functional. In addition, there is no phenotypic difference between patients containing homozygous mutations leading to a truncated protein and less severe mutations. This exon was chosen because it encodes 72% of the entire gene, covers all transmembrane regions and a majority of mutations are found in this region. Initially, no information was known about the genomic sequence of Wolframin, therefore, a mouse 129/OLA cosmid library from the Resource Center of the German Human Genome Project (RZPD, Berlin, Germany) was searched to determine which pools contained Wolframin genomic sequences. Primary and secondary PCR pools were screened for positive clones. Only one positive clone was found in this search and the clone was requested. Unfortunately, this clone was a false positive as it contained sequences from the Wolf-Hirschorn Syndrome, interestingly also located on Chromosome 4p16 and the Wolframin gene was not present. In a second attempt, genomic DNA was sequenced using the GenomeWalker kit from Clontech. Using this method, a 3 kb fragment was produced as the 5' arm for homologue recombination in this knock-out mouse construct. A 1.1 kb long 3' fragment from the end of exon 8 was

amplified and both fragments were cloned into the pBluescript II cloning vector. In order to interrupt exon 8 and render the resulting protein inactive, the neomycin gene was inserted between the 5' and 3' arms on the pBluescript II clone. The neomycin gene was also used as a positive selection marker to allow selection of homologue recombination events with Genticin (G418). This construct was linearised and electroporated into the embryonic stem cell line, R1-ES. I performed all R1-ES cell techniques at the Max Planck Institute for molecular neurobiology in Heidelberg, Germany in the laboratory of Dr. Rolf Sprengel. 600 colonies were picked, plated onto 96-well plates and PCR screened in pools of 6 with a nested PCR using two reverse primers that anneal to the target chromosomal sequences just outside of the homology used in the vector and two forward primers from the 3' end of the neomycin insert. Unfortunately, no positive knock-out clones were found with PCR screening. Since the 5' region used in our construct was relatively short and this could have lead to a lower probability of homologue recombination, this region was chosen as a target for improving the construct. Luckily, the full genomic sequence became available to the public in this time. This information was used to produce a Wolframin knock-out mouse construct consisting of a 5.3 kb long 5' fragment and a 3' fragment 1.1 kb long (figure 10.1).

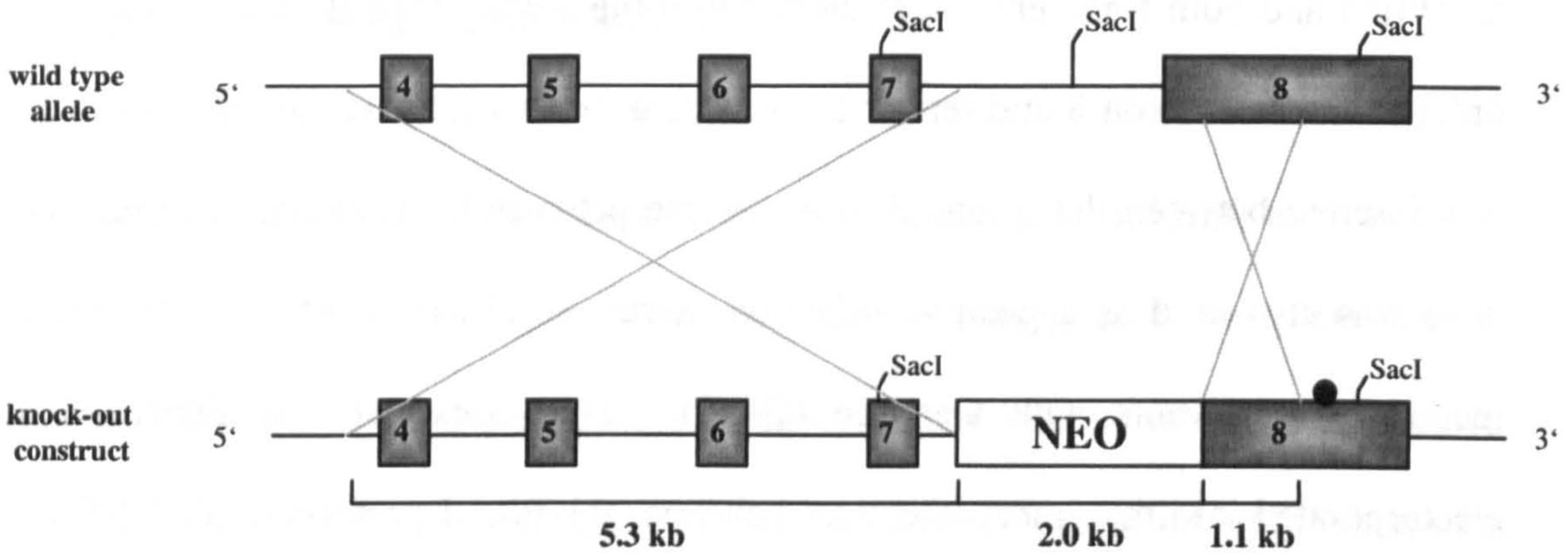

Figure 10.1 Wolframin knock-out mouse construct. The 5' homologous region is 5.3 kb long and contains sequences spanning from intron 3 to intron 7, the neomycin positive selection vector was inserted into the region spanning from intron 7 to the beginning of exon 8, thereby excluding 1.9 kb of seqnences and rendering exon 8 inactive. The regions of homologue recombination are indicated by X's. The closed circle indicates position of the southern probe.

A neomycin selection vector was placed in the exon 8 coding region to disrupt this exon and result in a non-functional protein. In addition, 1.9 kb of Wolframin sequence were excluded by amplifying the 3' and 5' segments around this area. This construct was also linearised and electroporated into R1-ES cells. From this analysis, two positive pools were found and propagated from 96-wells into 24-wells and the individual pools screened again by PCR. At this stage, two individual clones were found and propagated to several 10 cm dishes. Genomic DNA was isolated and the clones checked by southern blot analysis. The DNA was cut with Sac1 and a 3' probe was used to determine the size difference in knock-out DNA and genomic DNA. The sequences for a Sac1 site were present in the section that was excluded in the knock-out construct. Therefore, digestion with Sac1 should have resulted in 2082 bp fragment for wild-type and 4103 kb for the transgenic allele. As can be seen in figure 10.2, only the band for wild-type was present. Thus, neither of these clones proved to be correct. At the moment, a new knock-out mouse construct is being produced, which includes 7 kb of sequences for the 5' homologue recombination and 1.4 for the

3' region. The 3' region is also being changed and new primers selected for PCR screening to allow positive clones to be found.

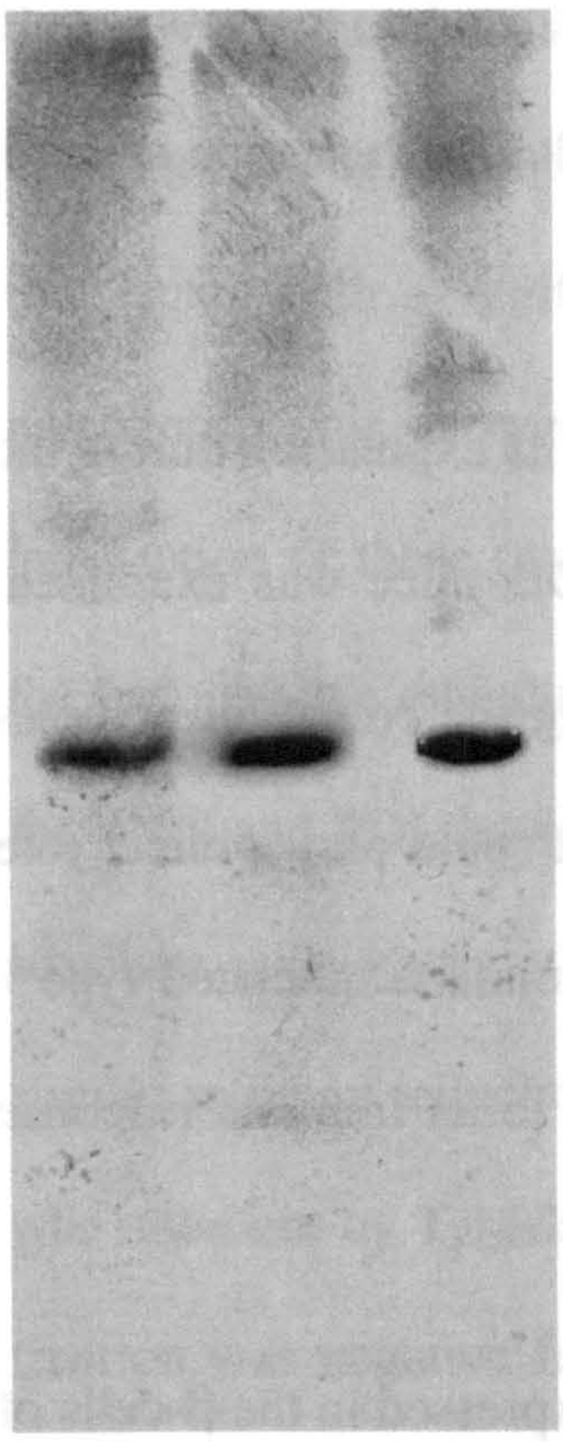

Figure 10.2 Southern blot of PCR positive Wolframin mouse knock-out clones. DNA was cut with SacI and probed with a 3' end PCR product. The wt allele should result in a 2082 bp band and the knock-out allele in a 4103 bp band. Both clones produced only the band representative of the wt allele.

Chapter 11. Discussion

Wolframin was discovered in 1998 by two unrelated groups to be the gene responsible for the Wolfram Syndrome. Both groups found loss-of-function mutations on two alleles in a majority of patients tested. Wolframin was a novel gene and its encoded product was completely uncharacterised at the start of this thesis. Using the amino acid sequences, a transmembrane protein was predicted that showed no resemblance to any other known protein. The Wolframin sequence contained no information as to its possible localisation or function.

In order to gain insight into the possible function of this gene, its expression during the development of cyclophosphamide enhanced diabetes in NOD mice was examined. The expression changes in brain and pancreas detected during the course of diabetes induction gave the first indications that the Wolframin protein could play a direct role in the tissues affected in WS patients. In contrast, the auto-immune mediated type 1 diabetes mellitus is a result of at least 18 genes contributing to an immune response (Davies and Day 1994).

The next step was then to determine if the protein itself was expressed in the β-cells of the pancreas. In order to investigate this, antibodies were raised against various C- and N- terminal peptides and recombinant proteins. One antibody, WoN, showed proper expression on western blot and immunohistological analysis. Indeed, it was shown that the Wolframin protein is expressed in insulin-producing β-cells. Since WS patients show a selective loss of β-cells and the Wolframin protein is expressed in these cells, it is possible that the Wolframin gene product plays a role in the survival of β-cells.

Exactly what functions or interactions are important for the Wolframin protein could be better understood by determining its sub-cellular localisation. A 100 kDa band, which was the expected size based on amino acid sequences for the Wolframin protein was seen in western analysis of purified microsomal fractions. No band was seen in the nuclear, mitochondrial or cytosolic fraction.

Unfortunately, the cell types tested for immunofluorescence studies were not adequate to determine the endogenous expression. Either expression was too low or cells were not large enough to observe structural patterns. Therefore, Cos-7 cells were first transfected with a Wolframin expression construct and used for immunofluorescent detection. This showed a pattern similar to the ER specific antibody, PDI. Co-localisation of these two antibodies proved that the Wolframin protein does reside in the endoplasmic reticulum. βTC-tet cells also showed an over-lapping staining pattern for WoN and PDI, however, these cells were too small to observe proper intracellular structure. This was a surprising result, as the symptoms seen in DIDMOAD are similar to many mitochondrial related diseases. Localisation to the plasma membrane was ruled out by Takeda et al. (2001) by showing that the plasma membrane enriched fraction was negative for Wolframin. Microsomal fractions have been tested for N-glycosylation and Endo H sensitivity (Takeda, Inoue et al. 2001) and by others at the Institute for Diabetes Research (unpublished data). In both cases, a shift in band size was seen. This is additional evidence that the Wolframin protein does localise properly to the ER. Thus, the Wolframin protein is an Endo H sensitive type 2 (cytoplasmic amino terminus) integral membrane glycoprotein of unknown function.

It has been previously reported that β-cells have a highly developed ER needed for insulin secretion (Oyadomari, Araki et al. 2002). Disturbing proper functioning of the ER results in cellular damage and eventually apoptosis. The ER is an organelle

responsible for the processing, trafficking, proper folding of newly synthesised proteins and regulation of calcium stores. When any of these functions are disturbed, the ER finds itself in a stage of "ER stress". As a self-protective mechanisms against ER stress, cells undergo what is called the ER stress response (Kaufman 1999). Prolonged periods of ER stress lead to apoptotic cell death by several different pathways (Oyadomari, Araki et al. 2002). In fact, it has been reported that β-cells, the first cells affected in the WS, are among the most susceptible cells to ER stress mediated apoptosis (Oyadomari, Koizumi et al. 2002).

The Wolcott-Rallison syndrome, as described in the introduction, is due to mutations found in the ER-localised EIF2AK3 gene. EIF2AK encodes for pancreatic ER kinase (PERK) (Delepine, Nicolino et al. 2000). PERK attenuates translation initiation in response to ER stress, thereby protecting β-cells from ER stress (Harding and Ron 2002). PERK deficient mice develop hyperglycaemia at four weeks of age and show increased apoptosis in β-cells (Harding, Zeng et al. 2001). The Wolcott-Rallison syndrome is an example of a diabetic phenotype resulting from mutations in an ER-localised β-cell residing protein. In this case, the ability to respond to ER stress is important for the survival of β-cells.

This thesis provides evidence that the Wolframin protein is also localised to the ER and β-cells of the pancreas. The Wolframin gene product has some sequence similarity to SEL-1 and Hrd3p, from *Caenorhabditis elegans* and yeast respectively. These proteins play an important role in degrading malfolded ER proteins. If Wolframin also had a role in degrading malfolded ER proteins, then Wolframin defective cells should show a difference to non-defective cells undergoing ER stress. Indeed, fibroblast cells from a Wolfram patient showed a 3.8 fold higher increase in caspase-3 activity than a non-affected sibling after induction for apoptosis with

staurosporine. The next step in determining Wolframin's possible function in ER stress response will be to induce these fibroblast cells with more ER stress-specific inducers. In addition, caspase-12, a recently identified caspase, responds specifically to ER stress to activate downstream caspases to induce apoptosis (Rao, Hermel et al. 2001). It would be interesting to observe the levels of caspase-12 in addition to caspase-3. If Wolframin is indeed involved in the ER stress response, than it could be possible that its own protein expression increases in states of ER stress. Such an experiment could also be done on pancreatic β-cells, which would be advantageous, since the diabetic phenotype suggests more activity in β-cells.

It is also possible that the Wolframin protein functions as a channel or as a mediator by interacting with other proteins. At least the last 8 residues are important for the function of the entire protein (Barrett, Bundey et al. 1995). The importance of these residues could feasibly lie in their protein-protein interaction with yet unknown partners. The PERK protein, for example, has its stress-sensing domain in the ER lumen, where it interacts with the binding protein, BiP (Bertolotti, Zhang et al. 2000; Liu, Schroder et al. 2000). When proteins accumulate in the ER luman, BiP detaches and allows PERK to become active. Maybe the last 8 residues of Wolframin, which also lie in the lumen, are important for activation in ER stress. When the ER stress response does not function properly, an increase in apoptosis could occur. Interactions of this protein with others is currently being investigated here at the Institute for Diabetes Research and should prove to be valuable information for determining a more precise function of this protein.

In another attempt to gain functional data about the Wolframin gene, a microarray analysis was performed with mRNA isolated from fibroblast cells from a WS patient, Pat14, and a sibling, Sib13. This analysis resulted in two interesting genes; PC-1 and

EFEMP1. The PC-1 gene was down regulated in DIDMOAD patient fibroblast cells and is an ecto-nucleotide pyrophosphatase/phosphodiesterase of unknown function. It is interesting to note that members of the phophodiesterase/nucleotide pyrophsphatase (PDNP) family play a role in neuromodulation in CNS and PNS, renal function and nociception (pain awareness) (Burnstock 1995; Buell, Collo et al. 1996; Thorn and Jarvis 1996). Considering the neurological and endocrine symptoms associated with WS, the significance of the down-regulation of PC-1 may be in its interaction with these neurological functions. It would be interesting to know to what degree, PC-1 plays a role in these functions. For example, comparing PC-1 staining patterns in the brain to those of Wolframin would give an indication of their possible interaction. This will have to be investigated in future experiments.

EFEMP1 is a widely expressed extracellular matrix protein of unknown function and was up regulated in DIDMOAD patient fibroblast cells. This gene has been shown to be over-expressed in Werner patients and can be induced by serum deprivation (Katsanis, Venable et al. 2000). Werner patient cells and serum deprived cells are both senescent. An attempt to determine if Wolframin plays a role in senescence by ascertaining its susceptibility to radiation proved negative. A single mutation in EFEMP1 causes build-up of misfolded EFEMP1 protein resulting in the Malattia Levantinase (ML) disease. Normally, the EFEMP1 protein is found in the nerve fiber layer (NFL) and the photoreceptor inner and outer segments in the eye (Marmorstein, Munier et al. 2002). In ML patient eyes, the retinal pigment epithelium is strongly stained with EFEMP1 antibody. Abnormal protein accumulation can be due to defects in either: protein folding, transport or degradation, all of which involve ER membrane proteins. Defective protein processing is a cause of several neurodegnerative diseases. For example, abnormal processing of the ER membrane amyloid precursor protein is

responsible for Alzheimer's disease and results in vulnerability to apoptosis (Haass, Grunberg et al. 1998). In order to understand the relationship of the Wolframin protein in the eye, histological staining patterns in the retina for Wolframin protein need to be investigated. Observation of the expression of EFEMP1 in retina from Wolframin negative mice would also provide valuable information.

The expressed genes found in this microarray analysis did not differ greatly from one another. A more prominent difference may have been better observed between normal βTC-tet cells and βTC-tet containing a disrupted Wolframin protein because the patient phenotype suggests that Wolframin plays a large role in endocrine tissue. Disrupting the Wolframin gene can be achieved for example using antisense technique. The best comparison would have been the difference between heterozygous and homozygous Wolframin knock-out mice. However, the production of these mice could not be completed during the course of this work.

After determining that the Wolframin protein is expressed in the β-cells of the pancreas, the expression pattern in the mouse brain was investigated. These findings corresponded with findings from Takeda et al. 2001, who also discovered expression in areas of the limbic system of the rat brain. This expression pattern is interesting since a majority of WS patients develop psychiatric and emotional abnormalities, including depression. Strom et al. (1998) have also reported that even individuals harbouring mutations on only a single allele are at a 26-fold higher risk of developing affective disorder. Expression of the Wolframin protein in these areas suggests a possible role for Wolframin in control of emotion and motivation. Lower expression was found in the cerebellum compared to other areas, although MRI from patients has revealed major atrophy of this area. However, it is not essential for protein expression to correlate exactly with affected areas. It could very well be that effects of the

malfunctioning protein lead to ER stress, which causes apoptosis in other areas of the brain. Wolframin might also be important for the activation of other proteins that have functions in other areas. These aspects need to be further investigated.

Many of the results obtained from these experiments lead to further ideas, which could be tested in knock-out mice. Two attempts have already been made to produce a knock-out mouse without success. In the last mouse construct, 5.3 kb of sequences were made available for homologue recombination, however no positive clones were obtained. It appears that the Wolframin locus only very inefficiently undergoes homologue recombination. It may be that 5.3 kb of homology are not enough. It has been reported that the relationship between targeting frequency and the length of homology in a replacement vector are found to increase linearly (Hasty, Rivera-Perez et al. 1991). Therefore, in another attempt to produce a knock-out mouse, a new construct is being designed containing over 7 kb of homology at the 5' end and 1.4 kb at the 3' end. The region at the 3' end is also being changed so that the PCR analysis hopefully will not result in false positives as encountered before. Should this new construct result in a Wolframin knock-out mouse, it will be a valuable tool for understanding the Wolframin gene and gene product.

This thesis presents data, which give the first indication towards characterisation of the Wolframin gene. It encodes for a transmembrane protein that resides in the ER membrane and localises to all tissue homogenates tested thus far and more specifically to the β-cells of the pancreas and structures of the limbic system of the brain. Fibroblast cells from DIDMOAD patients are more susceptible to caspase-3 activation after induction for apoptosis. Therefore, increased susceptibility to apoptosis in neurons and cells of the endocrine system may be involved in the pathogenesis of the Wolfram syndrome. However, the exact function of this gene still needs to be

investigated. Understanding the molecular mechanisms underlying the Wolframin gene is important for understanding the relationship of neurodegeneration and diabetes mellitus in Wolfram syndrome patients.

References

Ausubel, Frederick M., et al. (1993). "Preparation and analysis of DNA " Current Protocols Supplememnt 2.1 Wiley, John and sons, Inc. **1**: 2.9.4.

Baekkeskov, S., H. J. Aanstoot, S. Christgau, A. Reetz, M. Solimena, M. Cascalho, F. Folli, H. Richter-Olesen, P. De Camilli and P. D. Camilli (1990). "Identification of the 64K autoantigen in insulin-dependent diabetes as the GABA-synthesizing enzyme glutamic acid decarboxylase." Nature **347**: 151-6.

Barrett, T. G. and S. E. Bundey (1997). "Wolfram (DIDMOAD) syndrome." J Med Genet **34**: 838-41.

Barrett, T. G., S. E. Bundey, A. R. Fielder and P. A. Good (1997). "Optic atrophy in Wolfram (DIDMOAD) syndrome." Eye **11 (Pt 6)**: 882-8.

Barrett, T. G., S. E. Bundey and A. F. Macleod (1995). "Neurodegeneration and diabetes: UK nationwide study of Wolfram (DIDMOAD) syndrome." Lancet **346**: 1458-63.

Bauer, M. F., U. Rothbauer, N. Muhlenbein, R. J. Smith, K. Gerbitz, W. Neupert, M. Brunner and S. Hofmann (1999). "The mitochondrial TIM22 preprotein translocase is highly conserved throughout the eukaryotic kingdom." FEBS Lett **464**: 41-7.

Bertolotti, A., Y. Zhang, L. M. Hendershot, H. P. Harding and D. Ron (2000). "Dynamic interaction of BiP and ER stress transducers in the unfolded-protein response." Nat Cell Biol **2**: 326-32.

Bertrams, J., U. Wendel and S. Koletzko (1983). "HLA and Wolfram (DIDMOAD) syndrome." Lancet **2**: 573.

Bespalova, I. N., G. Van Camp, S. J. Bom, D. J. Brown, K. Cryns, A. T. DeWan, A. E. Erson, K. Flothmann, H. P. Kunst, P. Kurnool, T. A. Sivakumaran, C. W. Cremers, S. M. Leal, M. Burmeister and M. M. Lesperance (2001). "Mutations in the Wolfram syndrome 1 gene (WFS1) are a common cause of low frequency sensorineural hearing loss." Hum Mol Genet **10**: 2501-8.

Bogardus, C., S. Lillioja, B. L. Nyomba, F. Zurlo, B. Swinburn, A. Esposito-Del Puente, W. C. Knowler, E. Ravussin, D. M. Mott and P. H. Bennett (1989). "Distribution of in vivo insulin action in Pima Indians as mixture of three normal distributions." Diabetes **38**: 1423-32.

Bradford, M. M. (1976). "A rapid and sensitive method for the quantitation of microgram quantities of protein utilizing the principle of protein-dye binding." Anal Biochem **72**: 248-54.

Buell, G., G. Collo and F. Rassendren (1996). "P2X receptors: an emerging channel family." Eur J Neurosci **8**: 2221-8.

Burnstock, G. (1995). "Noradrenaline and ATP: cotransmitters and neuromodulators." J Physiol Pharmacol **46**: 365-84.

Chinnery, P. F., N. Howell, R. M. Andrews and D. M. Turnbull (1999). "Clinical mitochondrial genetics." J Med Genet **36**: 425-36.

Chitambar, C. R., E. J. Massey and P. A. Seligman (1983). "Regulation of transferrin receptor expression on human leukemic cells during proliferation and induction of differentiation. Effects of gallium and dimethylsulfoxide." J Clin Invest **72**: 1314-25.

Chu, P., W. G. Staff, J. A. Morris and J. M. Polak (1986). "DIDMOAD syndrome with megacystis and megaureter." Postgrad Med J **62**: 859-63.

Collier, D. A., T. G. Barrett, D. Curtis, A. Macleod, M. J. Arranz, J. A. Maassen and S. Bundey (1996). "Linkage of Wolfram syndrome to chromosome 4p16.1 and evidence for heterogeneity." Am J Hum Genet **59**: 855-63.

Davies, M. and J. Day (1994). "Screening for diabetes." Bmj **308**: 1160-1.

de Jong, G., J. P. van Dijk and H. G. van Eijk (1990). "The biology of transferrin." Clin Chim Acta **190**: 1-46.

de Jong, G. and H. G. van Eijk (1988). "Microheterogeneity of human serum transferrin: a biological phenomenon studied by isoelectric focusing in immobilized pH gradients." Electrophoresis **9**: 589-98.

Delepine, M., M. Nicolino, T. Barrett, M. Golamaully, G. M. Lathrop and C. Julier (2000). "EIF2AK3, encoding translation initiation factor 2-alpha kinase 3, is mutated in patients with Wolcott-Rallison syndrome." Nat Genet **25**: 406-9.

Diaz, G. A., M. Banikazemi, K. Oishi, R. J. Desnick and B. D. Gelb (1999). "Mutations in a new gene encoding a thiamine transporter cause thiamine-responsive megaloblastic anaemia syndrome." Nat Genet **22**: 309-12.

Efrat, S., D. Fusco-DeMane, H. Lemberg, O. al Emran and X. Wang (1995). "Conditional transformation of a pancreatic beta-cell line derived from transgenic mice expressing a tetracycline-regulated oncogene." Proc Natl Acad Sci U S A **92**: 3576-80.

El-Shanti, H., A. C. Lidral, N. Jarrah, L. Druhan and K. Ajlouni (2000). "Homozygosity mapping identifies an additional locus for Wolfram syndrome on chromosome 4q." Am J Hum Genet **66**: 1229-36.

Evans, K. L., D. Lawson, T. Meitinger, D. H. Blackwood and D. J. Porteous (2000). "Mutational analysis of the Wolfram syndrome gene in two families with chromosome 4p-linked bipolar affective disorder." Am J Med Genet **96**: 158-60.

Filiano, J. J., M. J. Goldenthal, A. C. Mamourian, C. C. Hall and J. Marin-Garcia (2002). "Mitochondrial DNA depletion in Leigh syndrome." Pediatr Neurol **26**: 239-42.

Fleming, J. C., E. Tartaglini, M. P. Steinkamp, D. F. Schorderet, N. Cohen and E. J. Neufeld (1999). "The gene mutated in thiamine-responsive anaemia with diabetes and deafness (TRMA) encodes a functional thiamine transporter." Nat Genet **22**: 305-8.

Fraser, F. C. and T. Gunn (1977). "Diabetes mellitus, diabetes insipidus, and optic atrophy. An autosomal recessive syndrome?" J Med Genet **14**: 190-3.

Freeze, H. H. (2001). "Congenital disorders of glycosylation and the pediatric liver." Semin Liver Dis **21**: 501-15.

Furlong, R. A., L. W. Ho, J. S. Rubinsztein, A. Michael, C. Walsh, E. S. Paykel and D. C. Rubinsztein (1999). "A rare coding variant within the wolframin gene in bipolar and unipolar affective disorder cases." Neurosci Lett **277**: 123-6.

Gabreels, B. A., D. F. Swaab, D. P. de Kleijn, A. Dean, N. G. Seidah, J. W. Van de Loo, W. J. Van de Ven, G. J. Martens and F. W. Van Leeuwen (1998). "The vasopressin precursor is not processed in the hypothalamus of Wolfram syndrome patients with diabetes insipidus: evidence for the involvement of PC2 and 7B2." J Clin Endocrinol Metab **83**: 4026-33.

Galluzzi, P., G. Filosomi, I. M. Vallone, A. M. Bardelli and C. Venturi (1999). "MRI of Wolfram syndrome (DIDMOAD)." Neuroradiology **41**: 729-31.

Gatter, K. C., G. Brown, I. S. Trowbridge, R. E. Woolston and D. Y. Mason (1983). "Transferrin receptors in human tissues: their distribution and possible clinical relevance." J Clin Pathol **36**: 539-45.

Genis, D., A. Davalos, A. Molins and I. Ferrer (1997). "Wolfram syndrome: a neuropathological study." Acta Neuropathol (Berl) **93**: 426-9.

Gerbitz, K. D., K. Gempel and D. Brdiczka (1996). "Mitochondria and diabetes. Genetic, biochemical, and clinical implications of the cellular energy circuit." Diabetes **45**: 113-26.

Gurtu, V., S. R. Kain and G. Zhang (1997). "Fluorometric and colorimetric detection of caspase activity associated with apoptosis." Anal Biochem **251**: 98-102.

Haass, C., J. Grunberg, A. Capell, C. Wild-Bode, U. Leimer, J. Walter, T. Yamazaki, I. Ihara, I. Zweckbronner, C. Jakubek and R. Baumeister (1998). "Proteolytic processing of Alzheimer's disease associated proteins." J Neural Transm Suppl **53**: 159-67.

Harding, H. P. and D. Ron (2002). "Endoplasmic reticulum stress and the development of diabetes: a review." Diabetes **51 Suppl 3**: S455-61.

Harding, H. P., H. Zeng, Y. Zhang, R. Jungries, P. Chung, H. Plesken, D. D. Sabatini and D. Ron (2001). "Diabetes mellitus and exocrine pancreatic dysfunction in perk-/- mice reveals a role for translational control in secretory cell survival." Mol Cell **7**: 1153-63.

Hardy, C., F. Khanim, R. Torres, M. Scott-Brown, A. Seller, J. Poulton, D. Collier, J. Kirk, M. Polymeropoulos, F. Latif and T. Barrett (1999). "Clinical and molecular genetic analysis of 19 Wolfram syndrome kindreds demonstrating a wide spectrum of mutations in WFS1." Am J Hum Genet **65**: 1279-90.

Hasty, P., J. Rivera-Perez and A. Bradley (1991). "The length of homology required for gene targeting in embryonic stem cells." Mol Cell Biol **11**: 5586-91.

Inoue, H., Y. Tanizawa, J. Wasson, P. Behn, K. Kalidas, E. Bernal-Mizrachi, M. Mueckler, H. Marshall, H. Donis-Keller, P. Crock, D. Rogers, M. Mikuni, H. Kumashiro, K. Higashi, G. Sobue, Y. Oka and M. A. Permutt (1998). "A gene encoding a transmembrane protein is mutated in patients with diabetes mellitus and optic atrophy (Wolfram syndrome)." Nat Genet **20**: 143-8.

Johnson, K., S. Vaingankar, Y. Chen, A. Moffa, M. B. Goldring, K. Sano, P. Jin-Hua, A. Sali, J. Goding and R. Terkeltaub (1999). "Differential mechanisms of inorganic pyrophosphate production by plasma cell membrane glycoprotein-1 and B10 in chondrocytes." Arthritis Rheum **42**: 1986-97.

Kadowaki, T., H. Kadowaki, Y. Mori, K. Tobe, R. Sakuta, Y. Suzuki, Y. Tanabe, H. Sakura, T. Awata, Y. Goto and et al. (1994). "A subtype of diabetes mellitus associated with a mutation of mitochondrial DNA." N Engl J Med **330**: 962-8.

Kapust, R. B. and D. S. Waugh (1999). "Escherichia coli maltose-binding protein is uncommonly effective at promoting the solubility of polypeptides to which it is fused." Protein Sci **8**: 1668-74.

Karasik, A., C. O'Hara, S. Srikanta, M. Swift, J. S. Soeldner, C. R. Kahn and R. D. Herskowitz (1989). "Genetically programmed selective islet beta-cell loss in diabetic subjects with Wolfram's syndrome." Diabetes Care **12**: 135-8.

Katsanis, N., S. Venable, J. R. Smith and J. R. Lupski (2000). "Isolation of a paralog of the Doyne honeycomb retinal dystrophy gene from the multiple retinopathy critical region on 11q13." Hum Genet **106**: 66-72.

Kaufman, R. J. (1999). "Stress signaling from the lumen of the endoplasmic reticulum: coordination of gene transcriptional and translational controls." Genes Dev **13**: 1211-33.

Kinsley, B. T., M. Swift, R. H. Dumont and R. G. Swift (1995). "Morbidity and mortality in the Wolfram syndrome." Diabetes Care **18**: 1566-70.

Laemmli (1970). "Cleavage of structural proteins during the assembly of the head of bacteriophage T4" Nature 681-85.

Labay, V., T. Raz, D. Baron, H. Mandel, H. Williams, T. Barrett, R. Szargel, L. McDonald, A. Shalata, K. Nosaka, S. Gregory and N. Cohen (1999). "Mutations in

SLC19A2 cause thiamine-responsive megaloblastic anaemia associated with diabetes mellitus." Nat Genet **22**: 300-4.

Lamminen, T., K. Huoponen, P. Sistonen, V. Juvonen, P. Lahermo, P. Aula, E. Nikoskelainen and M. L. Savontaus (1997). "mtDNA haplotype analysis in Finnish families with leber hereditary optic neuroretinopathy." Eur J Hum Genet **5**: 271-9.

Lecka-Czernik, B., C. K. Lumpkin, Jr. and S. Goldstein (1995). "An overexpressed gene transcript in senescent and quiescent human fibroblasts encoding a novel protein in the epidermal growth factor-like repeat family stimulates DNA synthesis." Mol Cell Biol **15**: 120-8.

Liu, C. Y., M. Schroder and R. J. Kaufman (2000). "Ligand-independent dimerization activates the stress response kinases IRE1 and PERK in the lumen of the endoplasmic reticulum." J Biol Chem **275**: 24881-5.

Maddux, B. A. and I. D. Goldfine (2000). "Membrane glycoprotein PC-1 inhibition of insulin receptor function occurs via direct interaction with the receptor alpha-subunit." Diabetes **49**: 13-9.

Maddux, B. A., P. Sbraccia, S. Kumakura, S. Sasson, J. Youngren, A. Fisher, S. Spencer, A. Grupe, W. Henzel, T. A. Stewart and et al. (1995). "Membrane glycoprotein PC-1 and insulin resistance in non-insulin-dependent diabetes mellitus." Nature **373**: 448-51.

Manzi, S. V., K. H. Hager, F. R. Murtagh and J. G. Mazalewski (1990). "MR imaging in a patient with Leigh's disease (subacute necrotizing encephalomyelopathy)." Pediatr Radiol **21**: 62-3.

Marmorstein, L. Y., F. L. Munier, Y. Arsenijevic, D. F. Schorderet, P. J. McLaughlin, D. Chung, E. Traboulsi and A. D. Marmorstein (2002). "Aberrant accumulation of EFEMP1 underlies drusen formation in Malattia Leventinese and age-related macular degeneration." Proc Natl Acad Sci U S A **99**: 13067-72.

Martin, B. C., J. H. Warram, A. S. Krolewski, R. N. Bergman, J. S. Soeldner and C. R. Kahn (1992). "Role of glucose and insulin resistance in development of type 2 diabetes mellitus: results of a 25-year follow-up study." Lancet **340**: 925-9.

Milo-Landesman, D., M. Surana, I. Berkovich, A. Compagni, G. Christofori, N. Fleischer and S. Efrat (2001). "Correction of hyperglycemia in diabetic mice transplanted with reversibly immortalized pancreatic beta cells controlled by the tet-on regulatory system." Cell Transplant **10**: 645-50.

Monson, J. P. and B. J. Boucher (1983). "HLA type and islet cell antibody status in family with (diabetes insipidus and mellitus, optic atrophy, and deafness) DIDMOAD syndrome." Lancet **1**: 1286-7.

Nakai, K. and P. Horton (1999). "PSORT: a program for detecting sorting signals in proteins and predicting their subcellular localization." Trends Biochem Sci **24**: 34-6.

Nakano, H., E. Kobayashi, I. Takahashi, T. Tamaoki, Y. Kuzuu and H. Iba (1987). "Staurosporine inhibits tyrosine-specific protein kinase activity of Rous sarcoma virus transforming protein p60." J Antibiot (Tokyo) **40**: 706-8.

Okawa, A., I. Nakamura, S. Goto, H. Moriya, Y. Nakamura and S. Ikegawa (1998). "Mutation in Npps in a mouse model of ossification of the posterior longitudinal ligament of the spine." Nat Genet **19**: 271-3.

Oyadomari, S., E. Araki and M. Mori (2002). "Endoplasmic reticulum stress-mediated apoptosis in pancreatic beta-cells." Apoptosis **7**: 335-45.

Oyadomari, S., A. Koizumi, K. Takeda, T. Gotoh, S. Akira, E. Araki and M. Mori (2002). "Targeted disruption of the Chop gene delays endoplasmic reticulum stress-mediated diabetes." J Clin Invest **109**: 525-32.

Peden, N. R., J. D. Gay, R. T. Jung and K. Kuwayti (1986). "Wolfram (DIDMOAD) syndrome: a complex long-term problem in management." Q J Med **58**: 167-80.

Polymeropoulos, M. H., R. G. Swift and M. Swift (1994). "Linkage of the gene for Wolfram syndrome to markers on the short arm of chromosome 4." Nat Genet **8**: 95-7.

Randall, R. V., B. W. Scheithauer, E. R. Laws, Jr., C. F. Abbound, M. J. Ebersold and P. C. Kao (1985). "Pituitary adenomas associated with hyperprolactinemia: a clinical and immunohistochemical study of 97 patients operated on transsphenoidally." Mayo Clin Proc **60**: 753-62.

Rando, T. A., J. C. Horton and R. B. Layzer (1992). "Wolfram syndrome: evidence of a diffuse neurodegenerative disease by magnetic resonance imaging." Neurology **42**: 1220-4.

Rao, R. V., E. Hermel, S. Castro-Obregon, G. del Rio, L. M. Ellerby, H. M. Ellerby and D. E. Bredesen (2001). "Coupling endoplasmic reticulum stress to the cell death program. Mechanism of caspase activation." J Biol Chem **276**: 33869-74.

Reardon, W., R. J. Ross, M. G. Sweeney, L. M. Luxon, M. E. Pembrey, A. E. Harding and R. C. Trembath (1992). "Diabetes mellitus associated with a pathogenic point mutation in mitochondrial DNA." Lancet **340**: 1376-9.

Richardson, J. E. and W. Hamilton (1977). "Diabetes insipidus, diabetes mellitus, optic atrophy, and deafness. 3 cases of 'DIDMOAD' syndrome." Arch Dis Child **52**: 796-8.

Rindi, G., C. Patrini, U. Laforenza, H. Mandel, M. Berant, M. B. Viana, V. Poggi and A. N. Zarra (1994). "Further studies on erythrocyte thiamin transport and phosphorylation in seven patients with thiamin-responsive megaloblastic anaemia." J Inherit Metab Dis **17**: 667-77.

Rost, B., R. Casadio, P. Fariselli and C. Sander (1995). "Transmembrane helices predicted at 95% accuracy." Protein Sci **4**: 521-33.

Saiz, A., N. Vila, J. E. Munoz, M. J. Marti, F. Graus and E. Tolosa (1995). "[Wolfram's syndrome: correlation of clinical signs and neurological images]." Neurologia **10**: 107-9.

Smith, P. R., S. C. Bain, P. A. Good, A. T. Hattersley, A. H. Barnett, J. M. Gibson and P. M. Dodson (1999). "Pigmentary retinal dystrophy and the syndrome of maternally inherited diabetes and deafness caused by the mitochondrial DNA 3243 tRNA(Leu) A to G mutation." Ophthalmology **106**: 1101-8.

Soeldner, J. S. and D. Slone (1965). "Critical variables in the radioimmunoassay of serum insulin using the double antibody technic." Diabetes **14**: 771-9.

Stoffel, W., M. Duker and K. Hofmann (1993). "Molecular cloning and gene organization of the mouse mitochondrial 3,2-trans-enoyl-CoA isomerase." FEBS Lett **333**: 119-22.

Strom, T. M., K. Hortnagel, S. Hofmann, F. Gekeler, C. Scharfe, W. Rabl, K. D. Gerbitz and T. Meitinger (1998). "Diabetes insipidus, diabetes mellitus, optic atrophy and deafness (DIDMOAD) caused by mutations in a novel gene (wolframin) coding for a predicted transmembrane protein." Hum Mol Genet **7**: 2021-8.

Swift, M. and R. G. Swift (2000). "Psychiatric disorders and mutations at the Wolfram syndrome locus." Biol Psychiatry **47**: 787-93.

Swift, R. G., M. H. Polymeropoulos, R. Torres and M. Swift (1998). "Predisposition of Wolfram syndrome heterozygotes to psychiatric illness." Mol Psychiatry **3**: 86-91.

Swift, R. G., D. B. Sadler and M. Swift (1990). "Psychiatric findings in Wolfram syndrome homozygotes." Lancet **336**: 667-9.

Takaki, R., J. Ono, M. Nakamura, Y. Yokogawa, S. Kumae, T. Hiraoka, K. Yamaguchi, K. Hamaguchi and S. Uchida (1986). "Isolation of glucagon-secreting cell lines by cloning insulinoma cells." In Vitro Cell Dev Biol **22**: 120-6.

Takeda, K., H. Inoue, Y. Tanizawa, Y. Matsuzaki, J. Oba, Y. Watanabe, K. Shinoda and Y. Oka (2001). "WFS1 (Wolfram syndrome 1) gene product: predominant subcellular localization to endoplasmic reticulum in cultured cells and neuronal expression in rat brain." Hum Mol Genet **10**: 477-84.

Thompson, C. J., J. Charlton, S. Walford, J. Baird, J. Hearnshaw, A. McCulloch, W. Kelly and P. H. Baylis (1989). "Vasopressin secretion in the DIDMOAD (Wolfram) syndrome." Q J Med **71**: 333-45.

Thorn, J. A. and S. M. Jarvis (1996). "Adenosine transporters." Gen Pharmacol **27**: 613-20.

Wallace, D. C., G. Singh, M. T. Lott, J. A. Hodge, T. G. Schurr, A. M. Lezza, L. J. Elsas, 2nd and E. K. Nikoskelainen (1988). "Mitochondrial DNA mutation associated with Leber's hereditary optic neuropathy." Science **242**: 1427-30.

Warram, J. H., B. C. Martin, A. S. Krolewski, J. S. Soeldner and C. R. Kahn (1990). "Slow glucose removal rate and hyperinsulinemia precede the development of type II diabetes in the offspring of diabetic parents." Ann Intern Med **113**: 909-15.

Wolcott, C. D. and M. L. Rallison (1972). "Infancy-onset diabetes mellitus and multiple epiphyseal dysplasia." J Pediatr **80**: 292-7.

Wolfram, D. J. and Wagener, H.P. (1938). "Diabetes mellitus and simple optic atrophy among siblings: report of four cases" Mayo Clin. Proc. **13** 715-18.

Wong, A., J. Yang, P. Cavadini, C. Gellera, B. Lonnerdal, F. Taroni and G. Cortopassi (1999). "The Friedreich's ataxia mutation confers cellular sensitivity to oxidant stress which is rescued by chelators of iron and calcium and inhibitors of apoptosis." Hum Mol Genet **8**: 425-30.

Yasunami, R. and J. F. Bach (1988). "Anti-suppressor effect of cyclophosphamide on the development of spontaneous diabetes in NOD mice." Eur J Immunol **18**: 481-4.

Young, T. L., E. Ives, E. Lynch, R. Person, S. Snook, L. MacLaren, T. Cater, A. Griffin, B. Fernandez, M. K. Lee, M. C. King and T. Cator (2001). "Non-syndromic progressive hearing loss DFNA38 is caused by heterozygous missense mutation in the Wolfram syndrome gene WFS1." Hum Mol Genet **10**: 2509-14.

Acknowledgements

I would like to express my gratitude to my supervisors, Hans Weiher and Sibylle Mittnacht for giving me the opportunity to embark on this thesis. Without your support and guidance, this project would never have been possible.

My examiners, Elizabeth Fisher and Vincent O'Connor, were very kind to travel to London for my viva and I want to thank them for this and for their many suggestions for improvement that lead to the final version of this dissertation.

To my colleges and friends...it's been a long journey, but thanks to you, also an enjoyable one. Special thanks goes to Lore Becker for her much appreciated constructive criticism.

I am extremely grateful to my family for their unconditional love and support, no matter how many miles or oceans may lie between us. You have shown me how to be a strong-willed person who does not give up easily.